*Chem. Rev.* 1992, *92*, 1611–1647

# Reactions of the Atomic Oxygen Radical Anion and the Synthesis of Organic Reactive Intermediates

Jeehiun Lee† and Joseph J. Grabowski*,‡

*Departments of Chemistry, Harvard University, Cambridge, Massachusetts 02138, and University of Pittsburgh, Pittsburgh, Pennsylvania 15260*

*Received April 15, 1992 (Revised Manuscript Received July 1, 1992)*

## *Contents*

- I. Introduction 1611
  - A. Importance of the Atomic Oxygen Radical Anion 1611
  - B. Scope of This Review 1612
  - C. Definitions/Nomenclature/Conventions 1613
  - D. Experimental Considerations 1614
- II. Properties of $O^{\bullet -}$, $HO^-$, $HO^\bullet$, and $H_2O$ 1615
  - A. Basicity and Bond Strengths 1615
  - B. Electron Affinity 1615
  - C. p$K_a$ 1615
  - D. Mobilities 1616
  - E. Miscellaneous 1616
- III. Generation of $O^{\bullet -}$ 1616
  - A. From $H_2O$ 1616
  - B. From NO 1616
  - C. From $O_2$ 1617
  - D. From $N_2O$ 1617
  - E. From $CO_2$ 1617
  - F. From Other Compounds 1617
- IV. Reactions with Small Molecules 1617
  - A. Binary Hydrides 1617
    - 1. Dihydrogen 1617
    - 2. Methane and the Alkanes 1619
    - 3. Ammonia 1620
    - 4. Water 1620
    - 5. Hydrogen Halides 1622
  - B. Non-Hydrogen-Containing Diatomics 1622
    - 1. Dinitrogen 1622
    - 2. Carbon Monoxide 1623
    - 3. Nitric Oxide 1623
    - 4. Oxygen 1624
  - C. Non-Hydrogen-Containing Triatomics 1624
    - 1. Carbon Dioxide 1624
    - 2. Nitrous Oxide 1626
    - 3. Nitrogen Dioxide 1626
    - 4. Ozone 1627
    - 5. Sulfur Dioxide 1627
  - D. Non-Hydrogen-Containing Polyatomics 1627
    - 1. Carbon Tetrachloride 1627
    - 2. Other Compounds 1627
- V. Reactive Intermediates from Organic Substrates 1628
  - A. Reactions with Saturated Systems 1628
    - 1. Substituted Methanes (Carbene Radical Anions) 1628
    - 2. Ethers and Epoxides 1631
    - 3. Amines (Nitrene Radical Anions) 1631
    - 4. Alcohols (Ketyl Radical Anions) 1632
    - 5. Thiols (Thioketyl Radical Anions) 1633
  - B. Reactions with Alkenes and Alkynes 1634
    - 1. Ethylene (Vinylidene Radical Anion) 1634
    - 2. Acetylene 1636
    - 3. Allene and Propyne (Propadienylidene and Propargylidene Radical Anions) 1637
    - 4. Other Alkenes and Alkynes 1638
  - C. Aromatic Compounds (Didehydroaromatic Radical Anions) 1639
    - 1. Benzene (*o*-Benzyne Radical Anion) 1639
    - 2. Alkyl Benzenes 1640
    - 3. Other Substituted Benzenes 1640
    - 4. Pyridines 1640
    - 5. 5-Membered Rings 1640
    - 6. Naphthalenes 1641
- VI. A Potpourri of Reactions 1641
  - A. Aldehydes and Ketones 1641
  - B. Esters 1641
  - C. Other Carbonyl Compounds 1643
  - D. Miscellaneous 1643
- VII. Condensed-Phase Reactivity 1643
  - A. In Water 1643
  - B. In Liquid Argon 1644
  - C. On Surfaces 1644
- VIII. Conclusion 1644
- IX. Acknowledgments 1645
- X. References 1645

## *I. Introduction*

### A. Importance of the Atomic Oxygen Radical Anion

The concept of ion–molecule reactions of the atomic oxygen radical anion will elicit a variety of responses from gas-phase chemists, ranging from intense frustration by those attempting analytical applications to unbridled delight by those interested in reactive intermediates. Fundamental studies concerning the chemistry displayed by $O^{\bullet -}$ have existed since the development of negative ion mass spectrometers, and many aspects of $O^{\bullet -}$ chemistry have become commonplace in ion–molecule investigations, such as its utility

---

† Harvard University.

‡ University of Pittsburgh.

0009-2665/92/0792-1611$10.00/0

Jeehiun Lee was born in Endicott, NY, on July 20, 1968. She obtained a B.A. in chemistry from Cornell University (1990) and is currently a National Defense Science and Engineering Graduate Fellow at Harvard University with Prof. Joseph J. Grabowski. She is interested in the application of modern physical–organic techniques to elucidate mechanisms in organic and bioorganic processes; currently she is using gas-phase ion–molecule methodologies to define the intrinsic chemistry of prototypical reactions.

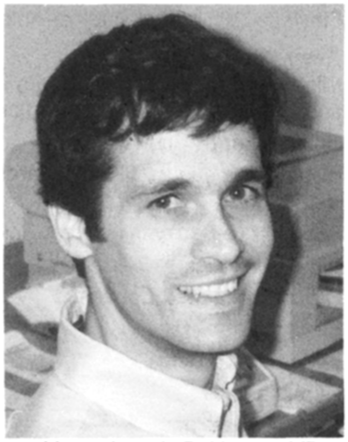

Joseph J. Grabowski was born in Baltimore, MD, on November 4, 1956. He obtained a B.S. in chemistry from the University of Maryland Baltimore County (1978) and a Ph.D. (with Prof. Charles H. DePuy) in chemistry from the University of Colorado (1983). Following his graduate education, he enjoyed a one-year (1983–1984) position as a postdoctoral fellow at Harvard University (with Prof. Kevin S. Peters). In 1984, he was appointed as an Assistant Professor of Chemistry at Harvard University, and in 1991, he accepted his current position as Associate Professor of Chemistry at the University of Pittsburgh. Prof. Grabowski was an NSF Presidential Young Investigator (1986–1991) and was elected a Fellow of the AAAS in 1991. His current research interests are in the area of modern physical–organic chemistry, with emphasis on reactive intermediates and reaction mechanisms, particularly as revealed by gas-phase flow tube techniques and condensed-phase photoacoustic calorimetric methodologies.

for the generation of $HO^-$. One might be tempted, therefore, to assume that the field has long been mature and well-characterized; this is, however, not the case, as is evidenced by the recent numerous papers in this area as well as by the lack of previous reviews.

Because the reactions of $O^{\bullet-}$ are of particular interest in ionospheric chemistry, many of the early investigations dealt with its reactions with known or possible atmospheric species.[1-5] The important role of the atomic oxygen radical anion in flames, and the postulated role of $O^{\bullet-}$ in plasmas of various types, also spawned a number of the studies reported. Other impetuses for the study of $O^{\bullet-}$ include its potential use as a practical reagent ion in negative ion chemical ionization mass spectrometry (NICI-MS) and in atmospheric pressure chemical ionization, as well as its role in the radiolytic chemistry of alkaline aqueous solutions.

While the early studies established many general guidelines, such as the fact that most molecules will react rapidly with $O^{\bullet-}$ and that only a small handful of molecules are unreactive toward $O^{\bullet-}$, conflicting and contradictory data complicated the definition of precise reactivity rules, which in turn diminished the predictive capability necessary for widespread analytical application. The recent surge of interest in $O^{\bullet-}$ chemistry has several sources. New techniques and more careful studies have revealed intriguing aspects of $O^{\bullet-}$ reactions not previously realized. Application of the concepts of reaction mechanisms to apparently conflicting observations have explained some data and suggested experiments to explain others. But perhaps the biggest reason for the widespread resurgence of activity in the field of $O^{\bullet-}$ chemistry has been due to the recognition that it is a source of negative ion versions of many of the classical intermediates of organic chemistry, species such as *o*-benzyne, vinylidene, dichlorocarbene, and small strained molecules. Thus, $O^{\bullet-}$ can be used to synthesize the corresponding molecular anions in the gas phase, and these anions can then be studied to reveal fundamental properties and structures of the neutral intermediates by either ion–molecule reaction methodologies[6-8] or spectroscopic techniques.[9] These advances, the extensive data long in the literature, and the insight provided by new results have made this field ripe for review.

## B. Scope of This Review

While there has not been a comprehensive review dedicated to the chemistry of the atomic oxygen radical anion, bits and pieces of this field have been reviewed within the scope of other topics.[10] Ferguson[11] discusses a number of associative detachment reactions of $O^{\bullet-}$ with both atomic and molecular neutrals in his early review on thermal energy, negative ion–molecule reactions, with special interest in reactions related to the negative ion chemistry of the lower ionosphere. Likewise, Tiernan's[12] (1975) and Viggiano's[10] (1984) chapters, among others,[13] on reactions of negative ions include detailed discussion of several $O^{\bullet-}$ reactions. Harrison's text on chemical ionization mass spectrometry discusses the utility of $O^{\bullet-}$ for ionization and identification of unknown compounds and mixtures of compounds.[14]

Our major goal has been to develop a comprehensive review of the unique chemistry (bond breaking, bond making) displayed by the atomic oxygen radical anion. Although we initially planned to address the $O^{\bullet-}$ reactions of only those compounds containing C–H bonds, it became apparent during the outline stage that the reactivity of the atomic oxygen radical anion should be addressed in terms of the full set of ion–molecule reactions that have been investigated in detail. Therefore, we have chosen to include all peer-reviewed reports of thermal (and near-thermal) energy ion–molecule reactions of $O^{\bullet-}$ in the gas phase. We include all the detailed studies in which the ion-molecule interaction energy is varied in a systematic and controlled fashion, as in variable temperature and drift tube studies. The emphasis in this review is on understanding the bond-making and bond-breaking processes that lead to products in the reactions of $O^{\bullet -}$. Because gas-phase results are being used more frequently to explain observations in the condensed phase, we also touch briefly on the observations and interpretations concerning the reactivity of $O^{\bullet -}$ in condensed phases.

The base of peer-reviewed papers from which this review was written was assembled in the following fashion. An extensive computer search of the Chemical Abstract Service On-Line provided us with a preliminary list of over 850 papers published between 1970 and 1991 (inclusive) that contained a reference to $O^{\bullet -}$ somewhere in the title or abstract. From this set, we culled all those discussing $O^{\bullet -}$ reactions studied in the gas-phase; these in turn led us to additional papers that were not found in the computer search. During this phase of the review writing, we also selected representative or oft-cited papers dealing with the *production* of $O^{\bullet -}$ in the gas-phase or dealing with condensed-phase chemistry of $O^{\bullet -}$; however, we have not attempted to be complete in our review of the literature in these latter two areas. We ultimately ended with about 200 papers dealing explicitly with thermal or near-thermal energy gas-phase reactions of $O^{\bullet -}$ and about 30 allied papers. We have tried to find all peer-reviewed publications that follow the above guidelines; however, the plethora of names and representations used for $O^{\bullet -}$ (vide infra) along with the large variety of journals in which the reports are published have greatly complicated this task.

We have organized the review by the class of molecules undergoing reaction (a functional group approach) after first discussing the physical properties of $O^{\bullet -}$ (and related species) and how it is generated in the gas phase for ion–molecule purposes. The binary hydrides (i.e., those compounds composed of hydrogen and one other element) and the non-hydrogen-containing diatomics and triatomics are among the best-studied $O^{\bullet -}$ reactions and are discussed first since they provide insight into the data obtained for the larger compounds. We discuss in section V a variety of classes of organic molecules that have been studied; since one of our interests in $O^{\bullet -}$ chemistry is the preparation of anionic versions of organic reactive intermediates, we have, where appropriate, identified, as a parenthetical expression in the header, the class of reactive intermediates that might be accessed by reaction with $O^{\bullet -}$. Section VI is a discussion of organic compounds that do not fall within divisions of section V and for which in general far fewer data are available. Finally, a brief discussion of condensed-phase reactions is presented in section VII.

### C. Definitions/Nomenclature/Conventions

Most of the definitions and abbreviations employed in this review are those currently recommended and/or practiced by the gas-phase ion–molecule community; all are explained in this section. We represent the *atomic oxygen radical anion* (the recommended name) as $O^{\bullet -}$ in order to emphasize the radical *and* anionic character of this species; in the literature this species is sometimes represented as $O^-$ or named as oxide, the oxide radical anion, or the atomic oxygen anion. For consistency's sake, then, all open-shell products (and reactants) are clearly noted by the use of the radical symbol ($\bullet$). Adoption of the recommended name and representation for $O^{\bullet -}$ will facilitate future computer-based searches of the literature.

Reaction enthalpies, $\Delta H^\circ_{\rm rxn}$, refer to 298 K and are obtained either from the primary paper referenced, or, more commonly, from the appropriate heats of formation, $\Delta H^\circ_{\rm f\,298}$, in the latest thermochemical compilation.[15] Gas-phase acidities, $\Delta H^\circ_{\rm acid}$, which quantify the enthalpy of gas-phase dissociation of a neutral molecule into an anion and a proton, are obtained from the most recent compilation unless otherwise noted.[15] Energies are listed in units of kilojoule per mole (kJ mol$^{-1}$) with the exception of electron affinities, where the more traditional units of electronvolts (eV) are used. The necessary conversion factors are 4.184 kJ per kcal and 96.48 kJ mol$^{-1}$ per eV. We have tried to list reaction enthalpies for all chemical equations written in this manuscript; some omissions will be found due to lack of appropriate or reliable thermochemical information.

Ion–molecule rate coefficients, $k$, are related to cross sections, $\sigma$, via $k = \sigma\bar{v}$ where $\bar{v}$ is the average ion velocity at that interaction energy. We use $k_{\rm obs}$ to refer to the total rate by which a reactant ion (e.g., $O^{\bullet -}$) disappears upon reaction with some neutral; by definition then, $k_{\rm obs}$ also equals the sum of the rate coefficients for each product channel. Because gas-phase ion–molecule reactions often proceed at or near the maximum rate (this is especially true for $O^{\bullet -}$ reactions) it is more useful to discuss the probability of a reaction occurring per unit collision. A reaction efficiency, EFF, is determined by dividing the observed rate coefficient ($k_{\rm obs}$) by the collision rate coefficient (EFF = $k_{\rm obs}/k_{\rm coll}$); this latter value is calculated according to one of several different theories, such as the average dipole orientation (ADO)[16,17] or the variational transition state theories.[18,19] For those investigations where the ion is accelerated prior to its reaction, the average center-of-mass collision energy is given by $\langle {\rm KE_{CM}} \rangle = E_{\rm LAB}[m/(m + M)]$ where $E_{\rm LAB}$ is the energy of the reactant ion in the laboratory frame, $m$ is the mass of the neutral, and $M$ is the mass of the reactant ion.

When discussing thermochemical or kinetic data for a specific species or reaction, the appropriate process will be noted in square brackets. For example, $\Delta H_{\rm rxn}$[eq 11] = −287 kJ mol$^{-1}$ refers to the 298 K reaction enthalpy for the exact process indicated in eq 11. As another example, $\mu_0[O^{\bullet -}$ in He] refers to the reduced mobility of $O^{\bullet -}$ in a helium buffer gas (see section II.D). When discussing the reactants or products of a reaction we use "M" to refer to the parent neutral. To indicate the chemical identity of a product derived from that neutral, we indicate the atoms that must be removed and/or added to "M" to achieve the correct molecular formula; all of this information is contained within parentheses. Finally, we indicate the overall charge on the species and whether or not it is an odd- or even-electron entity. For example, $(M - H)^-$ refers to the deprotonated neutral (e.g., the phenide ion, $C_6H_5^-$, when the neutral is benzene), $(M - 2H)^{\bullet -}$ refers to the anion formed by removing the equivalent of $H_2^{\bullet +}$ from the neutral (e.g., the *o*-benzyne radical anion, *o*-$C_6H_4^{\bullet -}$, when the neutral is benzene), and $(M - H + O)^-$ refers to the anion formed by adding an oxygen anion to the neutral along with removing a hydrogen atom (e.g., the phenoxide anion, $C_6H_5O^-$, when the neutral is benzene).

We use a variety of other abbreviations throughout this review; PT indicates a proton transfer reaction, ET represents electron transfer, and HAT means a hydrogen-atom transfer. A bimolecular substitution reaction is designated by $S_N2$ while addition–elimination processes occurring at a carbonyl carbon are labeled by the $B_{AC}2$ designator. Base-catalyzed elimination reactions are designated as either E2 (for a 1,2 process) or $\alpha$-elimination (for a 1,1 process). The abstraction of the equivalent of $H_2^{\bullet +}$ from a neutral refers to the formal transfer of a proton and a hydrogen atom from an appropriate neutral to $O^{\bullet -}$; this unique process is designated as $H_2^{\bullet +}$ transfer and is abbreviated $H_2^{\bullet +}$-T.

## D. Experimental Considerations

Examining reactions of ions with neutral molecules in the gas-phase requires specialized apparatus; several different experimental techniques have been employed in the investigations summarized here. Principal among the techniques used are flow tube techniques such as the flowing afterglow (FA)[20] and the selected ion flow tube (SIFT)[21,22] as well as ion cyclotron resonance (ICR)[23] spectrometry and its modern sibling fourier transform ion cyclotron resonance (FT-ICR)[24,25] spectrometry, which is also known as fourier transform mass spectrometry (FT-MS). Many other techniques have been employed as well, especially for the investigations of the effect of added energy on $O^{\bullet -}$ reactions; these include conventional double-focusing mass spectrometers,[26] beam scattering,[27] and drift tube[28] technologies, as well as variable-temperature flowing afterglow (VT-FA).[22] The techniques themselves will not be reviewed nor even briefly discussed here; the interested reader should refer to the papers cited below or to the numerous superb reviews, chapters, and books that are dedicated to reviewing experimental techniques. We will, however, briefly address three issues related to the experimental techniques: which channels of a given reactant pair are probed, complications due to competing and/or subsequent ion–molecule reactions, and the role of interaction energy in observations.

Different experimental techniques may actually probe different product channels or even different aspects of a specified product channel for a given pair of ion and molecule reactants. For example, since $O^{\bullet -}$ is a *radical* anion, associative detachment is a pathway open to it that is not normally available to closed-shell anions (such as $HO^-$, for example). Because most experimental devices employed in the studies reviewed here do not detect free electrons when they are the charged product of an ion–molecule reaction, this channel is often extremely difficult to quantify with any degree of confidence. While many of the original reports neglected consideration of associative detachment channels, we have tried to include them in all discussions where appropriate, even if experimental data are lacking. The two common approaches to experimentally considering the importance of an associative detachment process, ion signal balance throughout the course of a reaction and conversion of free electrons into anions (via attachment reactions), suffer from their own experimental difficulties. Another difference between various experimental approaches is whether the technique or protocol being used investigates all observed reaction channels or just a subset of them. For example, numerous studies discuss data for only one or two of a larger number of competing processes. Unfortunately, it is not always clear from each report whether other channels were simply neglected or were not observed. More than occasionally for reactions of $O^{\bullet -}$, especially with di- and triatomic reagents, one is able to identify *all* reaction channels only with the use of isotopically labeled reagents.

Competing reactions from contaminant ions and further reactions of first formed product ions are two experimental complications that are not unique to $O^{\bullet -}$ reactivity investigations but which are unusually important. Hydroxide ($HO^-$) is often a contaminant ion produced when one makes $O^{\bullet -}$, and complicates $O^{\bullet -}$ reactivity studies in two ways. First, if $HO^-$ (via HAT) is one of several products from the $O^{\bullet -}$ reaction, yield measurements are made difficult by the necessity of distinguishing contaminant $HO^-$ from product $HO^-$. Many of the reports reviewed in this work are limited by this difficulty. Second, the reactions of the "contaminant" $HO^-$ will occur in parallel with the $O^{\bullet -}$ reactions of interest, leading to the potentially erroneous assignment of $HO^-$-induced ion products to the $O^{\bullet -}$ reaction and vice versa. Occasionally, but not always, deuterium labeling studies of the neutral can help distinguish contaminant $HO^-$ coproduced in the ion-source from $DO^-$ produced from the $O^{\bullet -}$ reaction of interest. The amount of $HO^-$ reported by different workers for a given $O^{\bullet -}$ reaction varies widely; there is often much better agreement for the other channels. Another competing reaction that can lead to improper assignment of reaction products is that of metastable neutrals created in the ion source at the time of $O^{\bullet -}$ generation (e.g., *He in the FA) reacting with the neutral of interest to form anionic products by Penning ionization. To overcome these limitations, we have found that it is absolutely imperative to add about 1% argon or dinitrogen to our FA experiments to quench these reactive excited states.[29] Because $O^{\bullet -}$ itself, as well as many of the products it forms from reaction with organic compounds, are reactive with the precursor gas used to form the $O^{\bullet -}$, one must always be aware of and actively investigate how this precursor gas will affect the experimental observations. The latter two complications are especially insidious since many of the standard approaches for determining ion relationships may not correctly identify them. In the chemistry sections that follow, we have tried to point out cases where product ions observed by one technique but not another may be due to the sort of reactions just discussed. Along a similar vein, one must be careful in assigning product ions as primary (i.e., directly formed by the chemical reaction of the reactant ion with reactant neutral) versus secondary (i.e., formed by the chemical reaction of a primary product ion with a second equivalent of the reactant neutral). Such assignments are only correctly achieved by branching ratio measurements made as a function of the extent of the primary reaction. Secondary reactions are unusually important in these $O^{\bullet -}$ studies because of the open-shell (and reactive!) nature of many of these product ions. Numerous examples of secondary reactions are noted in the sections that follow.

Many ion–molecule reactions are known to be dependent upon the energy at which the reaction takes place; reactions of the atomic oxygen radical anion are no exception. One must therefore consider whether the data for a given reaction refers to "thermal" or "nonthermal" conditions. "Thermal" is usually taken to mean that each reaction partner is characterized by a 300 K energy distribution. With the advent of variable-temperature experimental techniques (VT-FA and variable-temperature high-pressure mass spectrometry (VT-HPMS)), thermally equilibrated reactions can be studied from 80 to 600 K and at even higher temperatures while more specialized techniques allow investigations at very low temperatures.[30] Thus the term "thermal" is somewhat ambiguous and is being replaced by the more precise term "thermally equilibrated to 300 K". Since $O^{\bullet-}$ is formed by dissociative electron ionization (vide infra), a process known to impart excess energy to the product species, it will in general be suprathermal. Many authors of papers reporting $O^{\bullet-}$ studies, particularly at low pressures where "thermalizing" collisions are infrequent, have explicitly considered this complication. The reader, however, is urged to bear in mind that data from different techniques may be different simply due to the energy dependence of the common quantifiers of reactions (rate coefficients, cross sections, branching ratios); a number of cases in the data below that appear to be contradictory are apparently due only to the differences in interaction energies. Forming $O^{\bullet-}$ "thermally equilibrated to 300 K" in low-pressure devices is not necessarily trivial; perhaps one of the reactions in this review can be adopted as a "thermometer" for the $O^{\bullet-}$ energy.

## II. Properties of $O^{\bullet-}$, $HO^-$, $HO^\bullet$, and $H_2O$

### A. Basicity and Bond Strengths

The atomic oxygen radical anion is a fairly strong base (eq 1a); another important aspect of $O^{\bullet-}$ is that addition of a hydrogen atom generates hydroxide, which is an even stronger base[15] (eq 1b). The atomic oxygen

$$HO^\bullet \rightarrow O^{\bullet-} + H^+ \qquad \Delta H^\circ_{acid}[HO^\bullet] = 1599\ kJ\ mol^{-1} \tag{1a}$$

$$H_2O \rightarrow HO^- + H^+ \qquad \Delta H^\circ_{acid}[H_2O] = 1635\ kJ\ mol^{-1} \tag{1b}$$

radical anion also possesses a large H-atom affinity[31] (eq 2a), enabling it to have an exothermic H-atom abstraction reaction with most substrates containing an X–H bond; furthermore, the hydroxyl radical, which forms when $O^{\bullet-}$ acts as a base, is an even stronger H-atom abstractor (eq 2b).[31]

$$HO^- \rightarrow O^{\bullet-} + H^\bullet \qquad BDE[^-O\text{–}H] = 463.2\ kJ\ mol^{-1} \tag{2a}$$

$$H_2O \rightarrow HO^\bullet + H^\bullet \qquad BDE[HO\text{–}H] = 498.7\ kJ\ mol^{-1} \tag{2b}$$

For interest, we also consider the thermodynamic properties of $HN^{\bullet-}$ and $S^{\bullet-}$, two ionic species that might be expected to react in a fashion similar to $O^{\bullet-}$. Although $HN^{\bullet-}$ and $H_2N^-$ are stronger bases than $O^{\bullet-}$ and $HO^-$, the X–H bond strengths for the oxygen species are significantly higher than those for the nitrogen species (eq 3).[15] These differences in thermochemistry between

$$H_2N^\bullet \rightarrow HN^{\bullet-} + H^+ \qquad \Delta H^\circ_{acid}[H_2N^\bullet] = 1652\ kJ\ mol^{-1} \tag{3a}$$

$$H_3N \rightarrow H_2N^- + H^+ \qquad \Delta H^\circ_{acid}[H_3N] = 1689\ kJ\ mol^{-1} \tag{3b}$$

$$H_2N^- \rightarrow HN^{\bullet-} + H^\bullet \qquad BDE[^-HN\text{–}H] = 420.1\ kJ\ mol^{-1} \tag{3c}$$

$$H_3N \rightarrow H_2N^\bullet + H^\bullet \qquad BDE[H_2N\text{–}H] = 456.9\ kJ\ mol^{-1} \tag{3d}$$

the water and ammonia systems are likely to account for the preliminary observations[32] that $HN^{\bullet-}$ reacts with organic species primarily by proton abstraction. The sulfur species possess neither the strong basicities nor the large bond strengths of the oxygen species (eq 4).[15] There are many known reactions of $S^{\bullet-}$;[33] however, there are no confirmed reports of an $H_2^{\bullet+}$-transfer pathway (a likely candidate is $^{34}S^{\bullet-} + H_2S$).

$$HS^\bullet \rightarrow S^{\bullet-} + H^+ \qquad \Delta H^\circ_{acid}[HS^\bullet] = 1466\ kJ\ mol^{-1} \tag{4a}$$

$$H_2S \rightarrow HS^- + H^+ \qquad \Delta H^\circ_{acid}[H_2S] = 1469\ kJ\ mol^{-1} \tag{4b}$$

$$HS^- \rightarrow S^{\bullet-} + H^\bullet \qquad BDE[^-S\text{–}H] = 378\ kJ\ mol^{-1} \tag{4c}$$

$$H_2S \rightarrow HS^\bullet + H^\bullet \qquad BDE[HS\text{–}H] = 381\ kJ\ mol^{-1} \tag{4d}$$

### B. Electron Affinity

The electron affinity (EA) of the atomic oxygen radical anion is especially well known; in fact, it has served in many EA measurements for calibration of the energy scale.[34] Lineberger and co-workers[35a] have precisely determined EA[O] = 1.461 122 ± 0.000 003 eV (11 784.645 ± 0.006 $cm^{-1}$) by tunable-laser photodetachment in a coaxial laser-ion-beam spectrometer. For reference, the electron affinity of the hydroxyl radical[35b] is $EA[HO^\bullet]$ = 1.827 670 ± 0.000 021 eV. The $^2P_{3/2}$ and $^2P_{1/2}$ spin-orbit splitting was found to be 177.13 ± 0.05 $cm^{-1}$. Theoretical estimates of the electron affinity of atomic oxygen have also been presented.[36]

### C. p$K_a$

The p$K_a$ of the hydroxyl radical[37,38] is 11.9 ± 0.2 and corresponds to reaction 5a in an aqueous environment. The equilibrium described by reaction 5b is quickly established in alkaline solution[39] with $k_f$[eq 5b] = 1.2 × $10^{10}$ $M^{-1}$ $s^{-1}$ and $k_r$[eq 5b] = 1.7 × $10^6$ $M^{-1}$ $s^{-1}$. Preparation of the hydroxyl radical in strongly basic aqueous solutions leads immediately to formation of the atomic oxygen radical anion in water; this is how many condensed-phase studies of $O^{\bullet -}$ have been carried out.

$$\mathrm{HO^{\bullet}_{(aq)} \rightleftharpoons H^{+}_{(aq)} + O^{\bullet -}_{(aq)}} \qquad (5a)$$

$$\mathrm{HO^{-}_{(aq)} + HO^{\bullet}_{(aq)} \underset{k_r}{\overset{k_f}{\rightleftharpoons}} O^{\bullet -}_{(aq)} + H_2O} \qquad (5b)$$

### D. Mobilities

When ions in a gaseous environment are subjected to an electric field, $E$, they acquire a net velocity in the direction of the field; this *drift velocity*, $\nu_d$, is related to the mobility, $\mu$, of the ion, by eq 6a. The reduced

$$\nu_d = \mu E \qquad (6a)$$

$$\mu_o = \mu \frac{p}{760} \frac{273.16}{T} \qquad (6b)$$

mobility, $\mu_o$ (reduced to 760 Torr and 0 °C), is defined by eq 6b where $p$ is the pressure of the gas and $T$ is the gas temperature in kelvin. Most typically, one considers the reduced mobility (units of $cm^2\ V^{-1}\ s^{-1}$) as a function of $E/N$ ($E$ is the electric field strength and $N$ is the neutral gas number density; $E/N$ is often expressed in units of Townsend [Td] where 1 Td = $10^{-17}$ V $cm^2$). McFarland and co-workers[40] described their flow-drift technique for ion mobility measurements in 1973. The zero-field reduced mobility found by these workers for $O^{\bullet -}$, $\mu_o[O^{\bullet -}$ in He$] = 28.5 \pm 2\ cm^2\ V^{-1}\ s^{-1}$, is 14% greater than that found for $HO^-$, $\mu_o[HO^-$ in He$] = 25 \pm 2\ cm^2\ V^{-1}\ s^{-1}$. The zero-field reduced mobility in carbon dioxide is $\mu_o[O^{\bullet -}$ in $CO_2] = 1.92 \pm 0.14\ cm^2\ V^{-1}\ s^{-1}$ as determined by Moseley and co-workers.[41] The zero-field reduced mobility of $O^{\bullet -}$ in dry air at 300 K is $\mu_o[O^{\bullet -}$ in air$] = 3.32\ cm^2\ V^{-1}\ s^{-1}$ according to flow-drift tube measurements made by Böhringer et al.[42] These authors also discuss the literature reports of the reduced mobility of $O^{\bullet -}$ in pure $O_2$ and note that the effect of an exchange reaction on the mobility still needs to be fully considered. It appears[43] that $\mu_o[O^{\bullet -}$ in $O_2] \approx 3.20\ cm^2\ V^{-1}\ s^{-1}$.

### E. Miscellaneous

Matese has published a theoretical study of doubly excited Feshbach states of $O^{\bullet -}$ and has compared the 12 states located to the six states known experimentally.[44] Lin et al.[45] have calculated the speed distribution for $O^{\bullet -}$ in helium at 300 K and 115 Td (average energy of 2.7 eV in the lab frame or 1.8 eV in the $O^{\bullet -}$, $O_2$ center-of-mass frame); they find that the velocity distribution is substantially different from that calculated for a Maxwellian distribution of the same average energy (the Maxwellian distribution is broader and with a smaller fraction of the population having the maximum velocity).

## III. Generation of $O^{\bullet -}$

Negative ions used as reactants for ion–molecule investigations in the gas-phase are often produced by electron ionization of an appropriate precursor gas. For a species such as the atomic oxygen radical anion, dissociative electron attachment (eq 7) is essentially the only method used. Dissociative electron attachment

$$e^- + ABC \rightarrow A^{\bullet -} + BC \qquad (7)$$

is a significant process for many diatomic and triatomic oxygen-containing compounds at lower pressures and for electron energies up to about 15 eV.[12] In general, the process of dissociative electron attachment involves a vertical transition from the ground state of the neutral molecule to a state of the molecular negative ion; this latter state then decomposes, usually either by autodetachment and/or fragmentation. Ions formed upon dissociation may have a kinetic energy distribution[12] with a peak energy, $E_0$, generally described by eq 8

$$E_0 = \{1 - m_{A^{\bullet -}}/m_{ABC}\}\{E_e - \mathrm{BDE[A{-}BC]} + \mathrm{EA[A]} - E[\mathrm{BC}]\} \qquad (8)$$

where $m_{A^{\bullet -}}$ and $m_{ABC}$ are the masses of the negative ion and precursor respectively, $E_e$ is the electron energy, BDE[A–BC] is the bond dissociation energy of A–BC, EA[A] is the electron affinity of A, and $E$[BC] is the excitation energy of BC. Under many typical mass spectrometer conditions, where ample time for complete collisional deactivation is not available, $A^{\bullet -}$ will have a kinetic energy distribution above and beyond that for an ion thermally equilibrated to the ambient temperature of the experiment (i.e., $A^{\bullet -}$ has an excess kinetic energy and is said to be nonthermal). The excess energy of $O^{\bullet -}$ formed in dissociative electron attachment processes is a function of the identity of the precursor gas, the energy of the ionizing electron, and the number and type of nonreactive collisions experienced by the $O^{\bullet -}$ prior to its chemical reaction.

In the sections that follow, we briefly recount some of what has been experimentally established concerning the formation of $O^{\bullet -}$, via dissociative electron attachment, from di- and triatomic precursors typically employed for ion–molecule investigations of $O^{\bullet -}$ reactivity. In general, dissociative electron attachment is extremely well-characterized for a large number of small molecules; the interested reader will want to consult other material for in-depth reviews and critical comparisons of the literature concerning production of $O^{\bullet -}$.

### A. From $H_2O$

Melton,[46,47] among others,[48] has reported the cross sections for dissociative electron attachment to water by which $H^-$, $O^{\bullet -}$, and $HO^-$ are produced. The cross section for $H^-$ production was found to be the largest and that for $HO^-$ the smallest (by far). For $O^{\bullet -}$ production, three peaks were found (the absolute cross sections are given in parentheses): 6.6 eV ($1.3 \times 10^{-19}\ cm^2$), 8.4 eV ($3.2 \times 10^{-19}\ cm^2$), and 11.2 eV ($5.7 \times 10^{-19}\ cm^2$).[47]

### B. From NO

Gupta and Melton,[49] as well as others,[50–52] examined the ionization efficiency of pure nitric oxide at low pressures and found that the only negative ion formed by dissociative attachment was $O^{\bullet -}$. The maximum in the cross section occurs at 8.0 ± 0.2 eV. Gupta and Melton estimated the threshold of the dissociative attachment process to be 7.0 ± 0.2 eV, a value 2 eV higher than that derived from BDE[NO] = 6.53 eV[53] and EA[O] = 1.461 eV;[35] therefore $O^{\bullet-}$ is likely to possess excess kinetic energy, perhaps on the order of 1 eV, when it is made from dissociative electron attachment to NO.

## C. From $O_2$

When $O^{\bullet-}$ is produced by way of dissociative electron attachment to dioxygen it can have energies in excess of 2.5 eV (depending of course on the energy of the electron).[54] For $O^{\bullet-}$ generated from $O_2$ with 6 eV electrons (which is often typical of certain experimental techniques employed to investigate $O^{\bullet-}$ reactivity[55]), the ion kinetic energy may be as large as 1 eV.[55,56] Krishnakumar and Srivastava[57] have compiled a table of measurements on the cross section for the production of $O^{\bullet-}$ from $O_2$; the peak positions range from 6.2 to 7.0 eV with a peak cross section of $(1.25–2.25) \times 10^{-18}$ $cm^2$. For additional information, the reader is referred to reviews by Christophorou[58] and Itikawa and co-workers.[59]

In a somewhat related study, Moruzzi and Harrison examined the energy distribution of $O^{\bullet-}$ ions produced in a drift tube and found that the distribution is non-Maxwellian with a significant high energy tail, a result of which is that the Wannier expression underestimates the mean energy.[60] The atomic oxygen radical anion can also be formed via ion pair production from the interaction of photons with dioxygen as reported by several groups; the cross section has a peak at about 71 nm and decreases sharply as the wavelength decreases before increasing again at ca. 60 nm and rising to a second peak at 58 nm.[59]

## D. From $N_2O$

Chantry has studied the dissociative electron attachment to nitrous oxide and found that the attachment cross section to produce $O^{\bullet-}$ peaks for 2.2 eV electrons.[61,62] Furthermore, at these energies, the $O^{\bullet-}$ kinetic energy distribution peaks at 0.4 eV; because of this excess kinetic energy, many experimentalists[63] probing the effects of energy on ion–molecule reactions at low pressures have avoided using nitrous oxide to generate $O^{\bullet-}$. Parkes[64] reports a value of $4 \times 10^{-15}$ $cm^3$ $molecule^{-1}$ $s^{-1}$ for eq 9, a value in close agreement to

$$e^- + N_2O \rightarrow O^{\bullet-} + N_2 \qquad \Delta H^\circ_{rxn} = +26\ kJ\ mol^{-1} \qquad (9)$$

that reported by Warman et al.[65] ($6 \times 10^{-15}$ $cm^3$ $molecule^{-1}$ $s^{-1}$). It is clear that with thermal electrons, the process described in eq 9 must involve the high energy tail of the electron energy distribution and ground state $N_2O$ molecules and/or attachment of average-energy electrons to the small number of vibrationally excited $N_2O$ molecules.[66] More recently, Krishnakumar and Srivastava[57] have reexamined the production of $O^{\bullet-}$ from $N_2O$ for electron ionization energies ranging from 0 to 50 eV; their analysis concludes that there is excellent agreement among the various literature values for the cross sections between 1.5 and 4 eV (peak position of 2.2–2.3 eV and peak cross section of $(8.3–9.0) \times 10^{-18}$ $cm^2$) while their study differs considerably above 5-eV electron energies. Electron attachment to nitrous oxide in the gas-phase has also been reviewed by Caledonia.[67]

## E. From $CO_2$

Dissociative electron attachment to carbon dioxide can be represented as a two-step process, the attachment of a free electron with incident energy $E_{in}$ to carbon dioxide to generate a short-lived molecular radical anion followed by dissociation into an anion and a stable neutral (eq 10). Chantry[68] and Orient and Srivastava[69]

$$e^-(E_{in}) + CO_2 \rightarrow [CO_2^{\bullet-}]^* \rightarrow O^{\bullet-}(KE) + CO(\nu,J) \qquad (10)$$

reported on the kinetic energy distribution and the cross section for production of $O^{\bullet-}$ from $CO_2$ by dissociative electron attachment with 0 to 20 eV electron energies; at electron energies of 3.8–5.3 eV, corresponding to energies within the 4.4 eV attachment peak ($\sigma \approx 1.5 \times 10^{-19}$ $cm^2$), very little energy appears as translational kinetic energy of the fragments. In contrast, the ion kinetic energy distributions observed for the 8.2 eV attachment process ($\sigma \approx 4.4 \times 10^{-19}$ $cm^2$), where the maximum allowed $O^{\bullet-}$ kinetic energy is ca. 2.6 eV, has a prominent peak at approximately 0.6 eV, indicative of a uniform distribution between internal and translational modes, as well as a peak at zero kinetic energy indicative of internal excitation only. Other workers have reinvestigated the dissociative electron attachment process for $CO_2$ and have learned a great deal about the specifics of energy partitioning.[70,71] Readers interested in the details of dissociative electron attachment by $CO_2$ will want to consult the original literature including a review by Spence and Schulz.[72]

The atomic oxygen radical anion can also be produced from carbon dioxide by way of ion-pair formation as a result of vacuum ultraviolet photon absorption.[73]

## F. From Other Compounds

It is believed that thermally equilibrated $O^{\bullet-}$ is produced from CO,[61,62,74] $NO_2$,[63,75] and $SO_2$; however, these precursor gases are used only infrequently to generate $O^{\bullet-}$ for ion–molecule investigations.[63] Appearance potentials for $O^{\bullet-}$ production from a variety of acyl derivatives have also been reported.[76] More recently, studies have appeared addressing the mechanism for gas-phase $O^{\bullet-}$ production from electron bombardment of condensed CO monolayers[77] and from other surfaces.[78] $O^{\bullet-}$ can also be produced in flames.[79]

# *IV. Reactions with Small Molecules*

## A. Binary Hydrides

### *1. Dihydrogen*

The associative electron detachment reaction between the atomic oxygen radical anion and the hydrogen atom (eq 11) has been studied theoretically by Acharya and co-workers.[80] Their ab initio theoretical simula-

$$O^{\bullet-} + H^\bullet \rightarrow e^- + HO^\bullet \qquad \Delta H^\circ_{rxn} = -287\ kJ\ mol^{-1} \qquad (11)$$

tions indicate, among other things, that reaction 11 is so slow as to be unmeasurable by current methodologies

**Table I. Room Temperature Rate Coefficients for the Reactions of $O^{\bullet -}$ with Neutral Molecules in the Gas Phase**[a]

| neutral | | rate coefficient | | neutral | | rate coefficient | |
|---|---|---|---|---|---|---|---|
| mass | formula | ($cm^3\ molecule^{-1}\ s^{-1}$) | ref(s) | mass | formula | ($cm^3\ molecule^{-1}\ s^{-1}$) | ref(s) |
| 2 | $H_2$ | $(6.3 \pm 2.1) \times 10^{-10}$ | 81 | 42 | $H_2C{=}CH{-}CH_3$ | $(1.0 \pm 0.3) \times 10^{-9}$ | 184 |
| 2 | $H_2$ | $7.5 \times 10^{-10}$ | 82 | 44 | $CO_2$ | $<1 \times 10^{-13}$ | 11 |
| 2 | $H_2$ | $6.0 \times 10^{-10}$ | 3,118 | 44 | $CO_2$[b] | $(7.5 \pm 0.4) \times 10^{-10}$ | 97 |
| 4 | $D_2$ | $5.9 \times 10^{-10}$ | 82 | 44 | $N_2O$ | $(1.95 \pm 0.06) \times 10^{-10}$ | 64 |
| 14 | N | $2.2 \times 10^{-10}$ | 1 | 44 | $N_2O$ | $2.0 \times 10^{-10}$ | 89 |
| 14 | N | $2.0 \times 10^{-10}$ | 3 | 44 | $N_2O$ | $(2.3 \pm 0.1) \times 10^{-10}$ | 97 |
| 16 | O | $1.4 \times 10^{-10}$ | 3 | 44 | $N_2O$ | $(2.2 \pm 0.4) \times 10^{-10}$ | 74 |
| 17 | $NH_3$ | $1.5 \times 10^{-9}$ | 89 | 44 | $N_2O$ | $(2.5 \pm 0.5) \times 10^{-10}$ | 74 |
| 17 | $NH_3$ | $(1.2 \pm 0.4) \times 10^{-9}$ | 95 | 44 | $N_2O$[b] | $(4.0 \pm 0.2) \times 10^{-10}$ | 97 |
| 18 | $H_2O$ | $<6 \times 10^{-13}$ | 96 | 46 | $NO_2$ | $(1.25 \pm 0.1) \times 10^{-9}$ | 4 |
| 18 | $H_2O$[b] | $(1.4 \pm 0.1) \times 10^{-9}$ | 97 | 46 | $NO_2$ | $1.2 \times 10^{-9}$ | 133 |
| 20 | HF | $\approx 5 \times 10^{-10}$ | 103 | 46 | $NO_2$ | $1.2 \times 10^{-9}$ | 137 |
| 26 | $HC{\equiv}CH$ | $2.0 \times 10^{-9}$ | 183 | 49 | NOF | $(9 \pm 4) \times 10^{-10}$ | 141 |
| 26 | $HC{\equiv}CH$ | $1.9 \times 10^{-9}$ | 123 | 50 | $CH_3Cl$ | $2.4 \times 10^{-9}$ | 147 |
| 27 | HCN | $(3.7 \pm 1.0) \times 10^{-9}$ | 2 | 50 | $CH_3Cl$ | $(1.7 \pm 0.3) \times 10^{-9}$ | 148 |
| 28 | CO | $4.4 \times 10^{-10}$ | 3,118 | 56 | $H_2C{=}CHCH_2CH_3$ | $(1.4 \pm 0.5) \times 10^{-9}$ | 184 |
| 28 | CO | $(5.5 \pm 1.7) \times 10^{-10}$ | 81 | 56 | *cis*-$H_3CCH{=}CHCH_3$ | $(1.2 \pm 0.4) \times 10^{-9}$ | 184 |
| 28 | CO | $6.5 \times 10^{-10}$ | 81 | 56 | *trans*-$H_3CCH{=}CHCH_3$ | $(1.6 \pm 0.5) \times 10^{-9}$ | 184 |
| 28 | CO | $(7.3 \pm 0.7) \times 10^{-10}$ | 108 | 56 | $H_2C{=}C(CH_3)_2$ | $(1.4 \pm 0.5) \times 10^{-9}$ | 184 |
| 28 | CO | $(6.9 \pm 0.3) \times 10^{-10}$ | 97 | 63 | $HNO_3$ | $(3.0 \pm 1.2) \times 10^{-9}$ | 5 |
| 28 | CO[b] | $(7.8 \pm 0.3) \times 10^{-10}$ | 97 | 64 | $SO_2$ | $2.1 \times 10^{-9}$ | 89 |
| 28 | $N_2$ | $<1 \times 10^{-14}$ | 3,118 | 64 | $SO_2$ | $(2.1 \pm 0.1) \times 10^{-9}$ | 97 |
| 28 | $N_2$ | $<1 \times 10^{-12}$ | 89 | 64 | $SO_2$[b] | $(2.2 \pm 0.1) \times 10^{-9}$ | 97 |
| 28 | $H_2C{=}CH_2$ | $(7.7 \pm 2.5) \times 10^{-10}$ | 184 | 65 | $NO_2F$ | $(1.7 \pm 0.8) \times 10^{-9}$ | 141 |
| 28 | $H_2C{=}CH_2$ | $7 \times 10^{-10}$ | 89 | 70 | $Cl_2$ | $(1.0 \pm 0.3) \times 10^{-9}$ | 141 |
| 28 | $H_2C{=}CH_2$ | $(1.02 \pm 0.4) \times 10^{-9}$ | 123 | 71 | $NF_3$ | $(3.7 \pm 1.1) \times 10^{-10}$ | 141 |
| 30 | NO | $1.6 \times 10^{-10}$ | 3,118 | 80 | $SO_2$ | $7 \times 10^{-10}$ | 11 |
| 30 | NO | $(2.8 \pm 0.1) \times 10^{-10}$ | 97 | 80 | HBr | $(1.0 \pm 0.3) \times 10^{-9}$ | 141 |
| 30 | NO | $1.4 \times 10^{-10}$ | 137 | 92 | $CClF_3$[c] | $(1.1 \pm 0.4) \times 10^{-9}$ | 141 |
| 30 | NO | $(2.1 \pm 0.6) \times 10^{-10}$ | 81 | 94 | $CH_3Br$ | $(1.1 \pm 0.2) \times 10^{-9}$ | 148 |
| 30 | NO[b] | $(4.7 \pm 0.2) \times 10^{-10}$ | 97 | 108 | $SF_4$ | $(1.4 \pm 0.4) \times 10^{-9}$ | 142 |
| 30 | $H_2C{=}O$ | $(3.1 \pm 0.8) \times 10^{-9}$ | 194 | 118 | $SOCl_2$ | $(1.8 \pm 0.9) \times 10^{-9}$ | 141 |
| 32 | $O_2$ | $<1 \times 10^{-12}$ | 3a | 134 | $SO_2Cl_2$ | $(1.8 \pm 0.9) \times 10^{-9}$ | 141 |
| 32 | $O_2(a\ ^1\Delta_g)$ | $3 \times 10^{-10}$ | 97 | 148 | $F_3CBr$ | $(1.3 \pm 0.4) \times 10^{-9}$ | 141 |
| 32 | $O_2$[b] | $(1.5 \pm 0.1) \times 10^{-10}$ | 97 | 152 | $CCl_4$ | $(1.0 \pm 0.3) \times 10^{-9}$ | 141 |
| 34 | $CH_3F$ | $(1.1 \pm 0.2) \times 10^{-9}$ | 148 | 152 | $CCl_4$ | $(1.4 \pm 0.4) \times 10^{-9}$ | 138 |
| 36 | HCl | $(1.3 \pm 0.4) \times 10^{-9}$ | 141 | 164 | $F_2CBrCl$ | $(7.2 \pm 2.2) \times 10^{-10}$ | 141 |
| 36 | HCl | $(2.0 \pm 0.6) \times 10^{-9}$ | 138 | 196 | $F_3CI$ | $(1.1 \pm 0.3) \times 10^{-9}$ | 141 |
| 40 | $H_2C{=}C{=}CH_2$ | $(1.1 \pm 0.4) \times 10^{-9}$ | 184 | 198 | $F_3CCF_2Br$ | $(7.2 \pm 2.2) \times 10^{-10}$ | 141 |
| 41 | $CH_3CN$ | $3.5 \times 10^{-9}$ | 10 | 250 | $HCBr_3$ | $(1.4 \pm 0.4) \times 10^{-9}$ | 141 |
| 41 | $CH_3CN$ | $4.6 \times 10^{-9}$ | 146 | | | | |

[a] For saturated hydrocarbons, see Table II. The reactions are listed in order of increasing molecular weight of the neutral reagent. In all cases, for simplicity's sake, the nominal mass of the naturally most abundant isotopomer is listed. [b] This rate coefficient represents the reaction of $^{18}O^{\bullet -}$ with the indicated neutral. [c] The neutral appears in the original citation as "$ClF_3$".

and that there is a propensity for producing $HO^\bullet$ in high vibrational levels.

The interaction of the atomic oxygen radical anion with dihydrogen and various isotopes thereof is perhaps one of the most studied ion–molecule reactions considered in this review (Table I). For this reaction two channels are thermochemically allowed at 300 K (eq 12). In a drift tube at near thermal energies, Parkes

$$O^{\bullet -} + H_2 \rightarrow e^- + H_2O \qquad \Delta H^\circ_{rxn} = -350\ kJ\ mol^{-1} \qquad (12a)$$

$$\rightarrow HO^- + H^\bullet \qquad \Delta H^\circ_{rxn} = -25\ kJ\ mol^{-1} \qquad (12b)$$

$$\nrightarrow H^- + HO^\bullet \qquad \Delta H^\circ_{rxn} = +76.1\ kJ\ mol^{-1} \qquad (12c)$$

found a total rate coefficient of $7.33 \times 10^{-10}$ $cm^3$ $molecule^{-1}$ $s^{-1}$ for $H_2$ and 96% associative detachment with only 4% of the reaction proceeding to give $HO^-$. For $D_2$ the total rate coefficient was found to be $4.9 \times 10^{-10}$ with 98% associative detachment and 2% $DO^-$ formation. (The low yield of HAT product is why $H_2$ is a poor co-reactant in $N_2O$/R–H mixtures for generating $HO^-$ for NICIMS.)

McFarland and co-workers[81] considered the effect of kinetic energy on the reaction of $O^{\bullet -}$ with $H_2$ ($D_2$) in their flow–drift apparatus and found that the rate coefficients are practically independent of energy in the range of thermal to 0.5 (0.8) eV. Viggiano and co-workers,[82] confirming these earlier studies, found that the total rate coefficient of $O^{\bullet -}$ with $H_2$ or $D_2$ depends only weakly on $\langle KE_{cm} \rangle$ (decreasing slightly with increasing energy) but that the distribution between the two exothermic channels (eq 12a,b) is quite sensitive to energy; the $HO^-$ ($DO^-$) channel increases from 5% at 0.022 eV to 13% at 0.18 eV (2% at 0.022 eV to 14% at 0.27 eV). Dotan and Klein,[63] looking only at the $DO^-$ + $D^\bullet$ channel, also found that the rate coefficient increases with both ion energy (to 1 eV) and temperature (to 700 K). There have been reports of a new, formally endothermic channel, giving rise to additional product ions at elevated interaction energies (vide infra); this reaction is that indicated in eq 12c.[83a] Other workers have studied interactions of $O^{\bullet -}$ with $H_2$ and/or $D_2$ in various energy regimes.[83b]

**Scheme I. The Mechanism for the Reaction of the Atomic Oxygen Radical Anion with Dihydrogen**

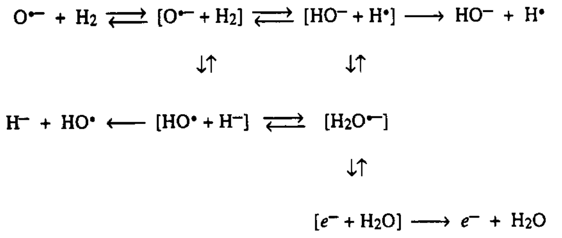

A reaction mechanism that accounts for all the data known is shown in Scheme I, parts of which have been discussed by McFarland and co-workers[81] and Viggiano and co-workers,[82] as well as others.[83] (The nonobservance of the $H^-$ channel by Viggiano and co-workers is most likely explained by the interaction energy not being taken high enough although it may be due in part to the experimental difficulty of detecting $m/z$ 1 by a quadrupole mass filter not explicitly tuned for that ion.) In Scheme I, the first formed *product* complex, [$HO^-$ + $H^\bullet$], partitions at room temperature between separating to distinct products ($HO^-$ + $H^\bullet$), or proceeding farther along the reaction coordinate. As the energy of this complex is raised, for instance, by elevating the kinetic energy of the reactant ion, one should favor direct dissociation of the first formed *product* complex versus further reaction within the complex (i.e., the yield of $HO^-$ will increase with increasing energy at the expense of the associative detachment channel). For the reaction scheme shown in Scheme I to account for all the observations, the associative detachment reaction between $HO^-$ and $H^\bullet$ must be a fast process (i.e., occur on nearly every collision under thermal interaction energies). At even higher interaction energies, a second *product* complex, [$HO^\bullet$ + $H^-$], becomes available, leading to the observed production of $H^-$.

Esaulov and co-workers[84] recently reported their results on reactive scattering measurements of the energy distributions of secondary electrons and $H^-$ ions produced in 0.5 to 10 eV relative energy collisions of $O^{\bullet-}$ with $H_2$. They interpreted their observation, a narrow, unstructured, electron energy distribution, as indicating that the associative detachment reaction (eq 12a) leads to a highly rovibrationally excited $H_2O$ molecule. Esaulov and co-workers also noted that $H^-$ production was small near threshold and that a strong positive increase in signal was observed with increasing collision energy. Furthermore, the $H^-$ energy distributions are structured which indicate that the $HO^\bullet$ product is vibrationally excited. Johnson and co-workers[85] have used a crossed beam machine to measure the angular and energy distribution of the $DO^-$ product in the $O^{\bullet-}$ + $D_2$ reaction in the relative energy range of 1.2–4.7 eV. At lower energies, their data indicate the intermediacy of a long-lived complex; as the energy is increased above 2.5 eV, their data indicate a shortening of the complex lifetime. Furthermore, most of the available energy is released as internal energy in the $DO^-$ product. These workers also noted that they looked for, but did not observe, the endothermic process (eq 12c) monitored by Esaulov and co-workers. Herbst and co-workers[86] also examined the $DO^-$ product channel for the $O^{\bullet-}$ + $D_2$ reaction in a scattering apparatus in the 3.6–13.2 eV energy range. Because they found that $DO^-$ is scattered preferentially in the forward direction, these authors concluded that the reaction channel being investigated could not be considered to proceed via a long-lived intermediate (which would require forward-backward symmetry). Thus, while Scheme I accounts for the thermal (and low-energy) reaction of $O^{\bullet-}$ with $H_2$ ($D_2$), at higher energies a stripping mechanism is believed to play a greater role.

Viggiano and co-workers[82] have measured the total rate coefficients for the reaction of $O^{\bullet-}(H_2O)$ with $H_2$ and $D_2$ at three temperatures (251, 343, and 473 K) and found that they are 50–100 times lower than that for the unsolvated reaction. Addition of a second water molecule to the reactant ion further reduced reactivity to the point that reaction could not be observed in their flow tube apparatus. Determining the product distributions for the monohydrated reaction at all temperatures proved not to be possible "due to the influence of extraneous ions in the flow tube at similar mass numbers".[82] The reaction products that could be anticipated, and their corresponding reaction enthalpies, are shown in eq 13 and should be contrasted to those for the unsolvated system shown in eq 12.

$$O^{\bullet-}(H_2O) + H_2 \rightarrow e^- + H_2O + H_2O \qquad \Delta H^\circ_{rxn} = -245\ \mathrm{kJ\ mol^{-1}} \quad (13a)$$

$$\rightarrow H_2O^{\bullet-} + H_2O \qquad \Delta H^\circ_{rxn} = -37\ \mathrm{kJ\ mol^{-1}} \quad (13b)$$

$$\not\rightarrow HO^- + H^\bullet + H_2O \qquad \Delta H^\circ_{rxn} = +80.3\ \mathrm{kJ\ mol^{-1}} \quad (13c)$$

$$\rightarrow HO^-(H_2O) + H^\bullet \qquad \Delta H^\circ_{rxn} = -22\ \mathrm{kJ\ mol^{-1}} \quad (13d)$$

(Nibbering and co-workers[87] have shown that the $H_2O^{\bullet-}$ product indicated in reaction 13b is best thought of as a hydride ion solvated by a hydroxyl radical, $H^-\cdots HO^\bullet$.) Thus despite the H-atom transfer reactions being equally exothermic for the unsolvated and monosolvated reactions, the monosolvated reaction is substantially slower than the unsolvated one. How exactly hydration reduces the rate of the H-atom transfer remains an intriguing question, but it should also be noted that the reaction of $O^{\bullet-}(H_2O)$ with $H_2$ is one of the few known, exothermic, ion–molecule reactions that exhibits a positive temperature dependence.

### *2. Methane and the Alkanes*

The reaction of the atomic oxygen radical anion with the simple alkanes has been explicitly examined by a few workers both at thermal (300 K, Table II) energy[88,89] and very close to it[90] and has been exploited by many. Lindinger et al., using a flow–drift apparatus, observed that the H-atom transfer from $CH_4$ to $O^{\bullet-}$ (eq 14a) increases with increasing $\langle KE_{cm} \rangle$.[89] These authors also note that in the low interaction energy regime probed by their apparatus for the $O^{\bullet-}$ + $CH_4$ reaction, the ion signals between $O^{\bullet-}$ and $HO^-$ are balanced; since the reactant and product ions have fairly similar mobilities and masses, the observation of detected charge balance is a strong argument for the unimportance of the associative detachment channel (eq 14d). Comer and

**Table II. Room Temperature Rate Coefficients for the Reactions of $O^{\bullet-}$ with Saturated Hydrocarbons in the Gas Phase**

| hydrocarbon | rate coefficient ($cm^3$ $molecule^{-1}$ $s^{-1}$) | efficiency (EFF) | $\Delta H^\circ_{rxn}$[a] ($kJ\ mol^{-1}$) | ref |
|---|---|---|---|---|
| $CH_4$ | $(1.0 \pm 0.3) \times 10^{-10}$ | 0.075 | −26 | 88 |
| $CH_4$ | $(1.1 \pm 0.1) \times 10^{-10}$ | 0.083 | −26 | 90 |
| $CH_4$ | $8 \times 10^{-11}$ [b] | 0.060 | −26 | 89 |
| $CH_4$ | $\sim 9 \times 10^{-11}$ | 0.068 | −26 | 94 |
| $CH_3CH_3$ | $(7.0 \pm 2.1) \times 10^{-10}$ | 0.46 | −44.4 | 88 |
| $CH_3CH_3$ | $7.6 \times 10^{-10}$ | 0.50 | −44.4 | 184 |
| $CH_3CH_2CH_3$ | $(9.3 \pm 2.8) \times 10^{-10}$ | 0.47 | −60.7 | 88 |
| $CH_3CH_2CH_2CH_3$ | $(1.2 \pm 0.4) \times 10^{-9}$ | 0.55 | | 88 |

[a] Assuming BDE[$^-$O–H] = 463 kJ $mol^{-1}$ (see section II.A) and BDE[R-H] as derived from data reported in ref 91. [b] In Table I of ref 89 the rate coefficient for this reaction is said to be in units of $10^{-10}$ $cm^3$ $s^{-1}$ when, based on the associated plot (Figure 4 of ref 89), it must be in units of $10^{-11}$ $cm^3$ $s^{-1}$.

Schulz[92] had previously reported the cross section for eq 14d over the 0.5–2-eV energy range and had found that it fell, as interaction energy increased, by about 50% from a value of $\sim 2 \times 10^{-16}$ $cm^2$. Lindinger et al. noted that the Comer and Schulz cross section corresponds to a $k$[eq 14d] $\approx 7 \times 10^{-11}$ $cm^3$ $molecule^{-1}$ $s^{-1}$ which is clearly at odds with their flow–drift data.

$$O^{\bullet-} + CH_4 \rightarrow HO^- + H_3C^\bullet \qquad \Delta H^\circ_{rxn} = -26\ kJ\ mol^{-1} \tag{14a}$$

$$\nrightarrow H_2C^{\bullet-} + H_2O \qquad \Delta H^\circ_{rxn} = +51.9\ kJ\ mol^{-1} \tag{14b}$$

$$\nrightarrow H_3C^- + HO^\bullet \qquad \Delta H^\circ_{rxn} = +144\ kJ\ mol^{-1} \tag{14c}$$

$$\nrightarrow e^- + CH_3OH \qquad \Delta H^\circ_{rxn} = -235\ kJ\ mol^{-1} \tag{14d}$$

Neither the thermally equilibrated measurements, nor a specific search by Tiernan,[12] nor later flow–drift studies (vide infra) gave any evidence for an associative detachment process between $O^{\bullet-}$ and $CH_4$. Later workers,[93] examining the reaction of $O^{\bullet-}$ with methane as a function of $O^{\bullet-}$ kinetic energy at four temperatures between 93 and 515 K in their variable-temperature SIFT, found the same energy dependence as Lindinger et al. found in their earlier studies.

Viggiano et al.[94] have reported the *total* rate coefficients for several $O^{\bullet-}$ reactions (with CO, NO, $SO_2$, $CH_4$, and $N_2O$) at three temperatures; in each case they observed a slight negative temperature dependence. Of particular interest is why there is a negative temperature dependence for the $O^{\bullet-} + CH_4$ reaction ($T^{-0.3\pm0.15}$) and a positive kinetic energy dependence. In summation, it seems to be the case that under thermal and near-thermal conditions, saturated hydrocarbons react with $O^{\bullet-}$ in the gas-phase exclusively by a facile hydrogen atom transfer and that the reaction efficiency has some correlation with the C–H bond dissociation energy of the alkane (Table II). Many workers have taken advantage of this reaction to prepare "anhydrous" $HO^-$ for gas-phase purposes or have prepared $DO^-$ by allowing $O^{\bullet-}$ to react with perdeuteriocyclohexane, a readily available and relatively inexpensive deuterated NMR solvent.

The effect of hydration of the atomic oxygen radical anion by just one water molecule considerably reduced[94] the rate of its reaction with methane to the point that Viggiano and co-workers could not measure the rate coefficient ($k[O^{\bullet-}(H_2O) + CH_4] \lesssim 5 \times 10^{-12}$ $cm^3$ $molecule^{-1}$ $s^{-1}$). These authors reasoned that the $O^{\bullet-}(H_2O)_n + CH_4$ reactions should be exothermic for both one and two waters of hydration and that the lack of reaction was therefore a kinetic phenomenon rather than simply due to unfavorable thermodynamics.

Chou and Kass have examined the reaction of the atomic oxygen radical anion with a more complicated binary hydride, bicyclo[1.1.0]butane, and observed but a single product corresponding to a $(M-2H)^{\bullet-}$ species.[8]

bicyclo[1.10]butane

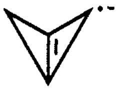

bicyclo[1.10]but-1(3)-ene radical anion

Based on observations of a variety of $C_4H_4^{\bullet-}$ species generated from 1,2-butadiene, 1,3-butadiene, 1-butyne, 2-butyne, and methylene cyclopropane, as well as comparisons of the chemical reactivity of all $C_4H_4^{\bullet-}$ ions with a diverse set of reagents, these authors identified their $(M-2H)^{\bullet-}$ species as the radical anion of bicyclo[1.1.0]but-1(3)-ene, a small strained ring system that heretofore had not been reported experimentally. From thermodynamic measurements of ion properties (EA's and acidities) Chou and Kass were able to determine the heat of formation and the heat of hydrogenation of bicyclo[1.1.0]but-1(3)-ene.[8] This elegant paper by Chou and Kass demonstrates the very strong attributes of the atomic oxygen radical anion and the chemistry of which it is capable, particularly in the elucidation of thermochemical properties of novel, interesting, and especially reactive, organic compounds.

### *3. Ammonia*

The reaction of the atomic oxygen radical anion with ammonia is fast under thermally equilibrated conditions (Table I) and gives only one ion product ($HO^-$); other ion-producing reactions that one might anticipate are considerably endothermic (eq 15).[95] Presumably, the associative detachment reaction to produce hydroxyl amine would be exothermic but it has not been suggested as a viable kinetic product in any reports to date. The rate of the fast H-atom transfer from $NH_3$ to $O^{\bullet-}$ was observed to decrease with increasing $O^{\bullet-}$ kinetic energy ($\langle KE_{cm} \rangle \leq 0.4$) while no new reaction channels were reported.[89]

$$O^{\bullet-} + NH_3 \rightarrow HO^- + H_2N^\bullet \qquad \Delta H^\circ_{rxn} = -14\ kJ\ mol^{-1} \tag{15a}$$

$$\nrightarrow HN^{\bullet-} + H_2O \qquad \Delta H^\circ_{rxn} = +36\ kJ\ mol^{-1} \tag{15b}$$

$$\nrightarrow H_2N^- + HO^\bullet \qquad \Delta H^\circ_{rxn} = +89.5\ kJ\ mol^{-1} \tag{15c}$$

$$\nrightarrow e^- + H_2NOH \tag{15d}$$

### *4. Water*

Fehsenfeld and Ferguson[96] found no binary reaction products for the interaction of the atomic oxygen radical

**Scheme II. The Mechanism for the Reaction of the Atomic Oxygen Radical Anion with Water**

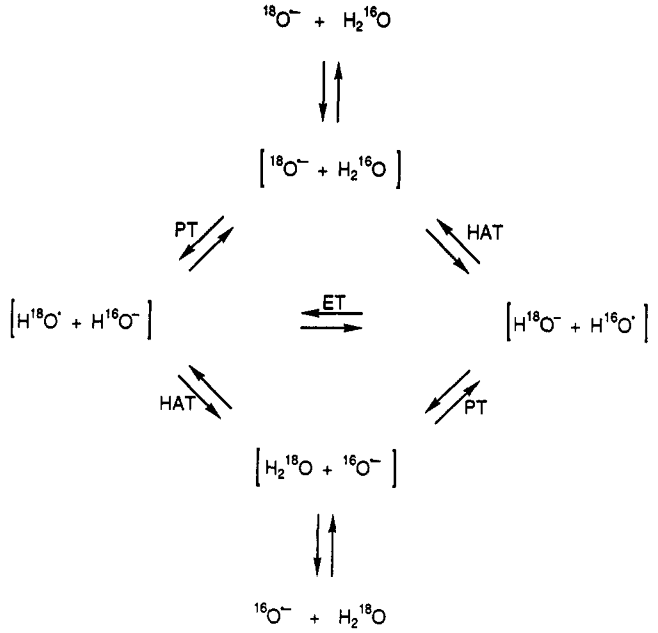

anion and water in a dioxygen buffer gas in their flowing afterglow apparatus. Two binary reactions that might have been expected in their study are shown in eq 16; eq 16a is considerably endothermic and hence should not be observed under their 300 K conditions. Reaction

$$O^{\bullet-} + H_2O \not\rightarrow HO^- + HO^{\bullet} \qquad \Delta H^{\circ}_{rxn} = +36\ \mathrm{kJ\ mol^{-1}} \tag{16a}$$

$$\not\rightarrow e^- + H_2O_2 \qquad \Delta H^{\circ}_{rxn} = -2.1\ \mathrm{kJ\ mol^{-1}} \tag{16b}$$

$$\xrightarrow{O_2} O^{\bullet-}(H_2O) \qquad \Delta H^{\circ}_{rxn} \approx -105\ \mathrm{kJ\ mol^{-1}} \tag{16c}$$

16b, in addition to being essentially thermoneutral, requires that the oxygen insert into an OH bond and hence would be likely to have a significant activation barrier. The only reaction observed was the three-body clustering reaction (eq 16c), calculated to be about 105 kJ mol$^{-1}$ exothermic.[82] When Van Doren and co-workers used $^{18}O^{\bullet-}$ to examine the reaction of the atomic oxygen radical anion with water, they found facile bimolecular isotope exchange (eq 17).[97,98] Since the

$$^{18}O^{\bullet-} + H_2{}^{16}O \xrightarrow{EFF = 41\%} 100\%\ {}^{16}O^{\bullet-} + H_2{}^{18}O \qquad \Delta H^{\circ}_{rxn} \approx 0\ \mathrm{kJ\ mol^{-1}} \tag{17}$$

observed scrambling reaction is near the statistical limit (50% because there are two oxygen atoms in the ion–molecule complex), the oxygen atoms must become essentially equivalent during the estimated 70-ps lifetime of the intermediate complex. The proposed mechanism, in accord with extensive previous work on H/D exchange between carbanions and $D_2O$ and vice versa, is shown in Scheme II. Note that in Scheme II, the ion–molecule complexes drawn in brackets are not observed in this scrambling experiment but are inferred from a variety of data including the previous observation of the $O^{\bullet-}(H_2O)$ cluster ion. Van Doren and co-workers have an extended discussion of this mechanism, in terms of both their data and previous measurements.[98] When van der Wel and Nibbering[99] examined the inverse reaction of that examined by Van Doren and co-workers, namely unlabeled atomic oxygen radical anion with oxygen-18-labeled water, they found the product distribution shown in eq 18; the nonthermal nature of these

$$^{16}O^{\bullet-} + H_2{}^{18}O \xrightarrow{ICR} 60\%\ {}^{18}O^{\bullet-} + H_2{}^{16}O \qquad \Delta H^{\circ}_{rxn} \approx 0\ \mathrm{kJ\ mol^{-1}} \tag{18a}$$

$$\xrightarrow{ICR} 20\%\ H^{16}O^- + H^{18}O^{\bullet} \qquad \Delta H^{\circ}_{rxn} \approx +36\ \mathrm{kJ\ mol^{-1}} \tag{18b}$$

$$\xrightarrow{ICR} 20\%\ H^{18}O^- + H^{16}O^{\bullet} \qquad \Delta H^{\circ}_{rxn} \approx +36\ \mathrm{kJ\ mol^{-1}} \tag{18c}$$

FT-ICR studies is immediately obvious by the high yields of significantly endothermic processes (eq 18b and 18c). Whether the excess energy needed to form the hydroxide products indicated is imparted to the reactant ion $^{16}O^{\bullet-}$ during its formation (from nitrous oxide) or due to the notch–ejection technique employed is not clear. The equivalent yields of labeled and unlabeled hydroxide, however, is completely consistent with the mechanism discussed above and with the expectation that ET between $HO^{\bullet}$ and $HO^-$ should be fast since there is no significant geometry change between these two species.

Futrell and Tiernan[100] observed, in their tandem mass spectrometer, the same endothermic reactions as were observed in the FT-ICR but in considerably lower yields (2% each of $H^{16}O^-$ and 2% $H^{18}O^-$). The principal reaction found in the tandem mass spectrometer was oxygen atom exchange; these data serve to indicate that these latter experiments approached "thermal" conditions. The total rate coefficient found by Futrell and Tiernan is $2.35 \times 10^{-9}$ cm$^3$ molecule$^{-1}$ s$^{-1}$, a value 68% higher than that found by Van Doren et al. Melton and Neece[47] reported that the cross section for $O^{\bullet-} + H_2O \rightarrow HO^- + HO^{\bullet}$ decreases with increasing energy from 0.5 to 5 eV while Karnett and Cross[101] examined the product energy and angular distributions for the endoergic reaction channel $O^{\bullet-} + D_2O \rightarrow DO^- + DO^{\bullet}$ over the relative energy range 3.2–10.5 eV (5.7–18.8 eV lab). These latter workers found that the reaction dynamics are well approximated by the "spectator-stripping" model in which $O^{\bullet-}$ "strips" a D atom from the $D_2O$ leaving the product $DO^{\bullet}$ with the same velocity as the original $D_2O$. Lifshitz[102] carried out ion-beam collision-chamber experiments on $^{16}O^{\bullet-}$ with $H_2{}^{18}O$ in the 0.17–3.5-eV energy range. The branching ratios observed (decreasing $^{18}O^{\bullet-}$ and increasing $HO^-$ yield with increasing energy) were interpreted to indicate the formation of a long-lived ($\tau_d$ = 0.21 ps at 1 eV, 3.6 ps at 0.17 eV, 12 ps at 0.02 eV) collision complex at interaction energies below ca. 1 eV. All new observations as well as those from crossed-beam experiments were elegantly accounted for by Lifshitz in terms of a double-well reaction coordinate diagram of $O^{\bullet-}$ interacting with $H_2O$; the Lifshitz reaction coordinate diagram is for the process shown in Scheme II but in which the oxygen labels have been omitted. Thus most

**Table III. Termolecular Rate Coefficients for the Reactions of $O^{\bullet-}$ with Neutral Molecules in the Gas Phase**[a]

| neutral | | third | rate coefficient | |
|---|---|---|---|---|
| mass | formula | body | ($cm^6$ molecule$^{-2}$ $s^{-1}$) | ref |
| 18 | $H_2O$ | $O_2$ | $1.0 \times 10^{-28}$ | 96 |
| 18 | $H_2O$ | $O_2$ | $1.3 \times 10^{-28}$ | 96 |
| 28 | $N_2$ | He | $\sim 4.0 \times 10^{-32}$ (200 K) | 104 |
| 30 | NO | NO | $6.5 \times 10^{-27}$ | 49 |
| 32 | $O_2$ | $O_2$ | $(1.0 \pm 0.2) \times 10^{-30}$ | 127 |
| 44 | $CO_2$ | He | $2.8 \times 10^{-28}$ (200 K) | 104 |
| 44 | $CO_2$ | He | $1.5 \times 10^{-28}$ | 96 |
| 44 | $CO_2$ | He | $1.5 \times 10^{-28}$ | 131a |
| 44 | $CO_2$ | He | $1.7 \times 10^{-28}$ | 131b |
| 44 | $CO_2$ | $CO_2$ | $(1.1 \pm 0.1) \times 10^{-27}$ | 108 |
| 44 | $CO_2$ | $CO_2$ | $3.1 \times 10^{-28}$ | 96 |
| 44 | $N_2O$ | $N_2O$ | $(4.2 \pm 0.5) \times 10^{-29}$ | 64 |

[a] In all cases, for simplicity's sake, the nominal mass of the naturally most abundant isotopomer is listed. All measurements refer to 300 K unless otherwise noted.

data reported to date has been interpreted in terms of an "ion–molecule complex" mechanism at thermally equilibrated and low interaction energies with a spectator stripping process becoming more important at elevated interaction energies.

Fehsenfeld and Ferguson,[96] while conducting laboratory studies of negative ion reactions with atmospheric trace constituents, examined the clustering reaction of $O^{\bullet-}$ with water in an oxygen buffer gas in their flowing afterglow apparatus. By monitoring the disappearance of the reactant ion signal, these authors were able to obtain the three-body association rate coefficient listed in Table III, despite the lack of observation of the expected $O^{\bullet-}(H_2O)$ product ion. Presumably the initially formed $O^{\bullet-}(H_2O)$ product ion undergoes a facile "switching" reaction with either the added $H_2O$ (eq 19b) or with the $O_2$ present as the buffer gas (eq 19c); the

$$O^{\bullet-} + H_2O \xrightarrow{O_2} O^{\bullet-}(H_2O) \qquad (19a)$$

$$O^{\bullet-}(H_2O) + H_2O \xrightarrow{O_2} HO^{-}(H_2O) + HO^{\bullet} \qquad (19b)$$

$$O^{\bullet-}(H_2O) + O_2 \xrightarrow{O_2} O_3^{\bullet-} + H_2O \qquad (19c)$$

authors hypothesized that these latter reactions would have to be rapid ($k > 10^{-11}$ $cm^3$ molecule$^{-1}$ $s^{-1}$) in order for the initially formed product to be completely quenched by the time the ionic product distribution was analyzed by the quadrupole mass filter on their FA. In a substantially later study, Viggiano and co-workers[94] were able to explicitly examine $O^{\bullet-}(H_2O)_n + H_2O$, for $n = 1$ and 2, and observed no reaction in either case; this latter observation concerning eq 19b is in accord with current thermochemical estimates, BDE[$HO^{-}\cdots H_2O$] = 27, BDE[$O^{\bullet-}\cdots H_2O$] = 25.1 and $\Delta H^{\circ}_{rxn}$[eq 16a] = +36 kJ mol$^{-1}$, which predict reaction 19b to be *endothermic* by 28 kJ mol$^{-1}$ (and therefore would be too slow to be seen under thermally equilibrated conditions). In order for reaction 19b to be thermoneutral, either the bond strength of $HO^{-}\cdots H_2O$ cluster has to be increased by 28 kJ mol$^{-1}$ or that of $O^{\bullet-}\cdots H_2O$ must be decreased by 28 kJ mol$^{-1}$ from those values cited above. In contrast to reaction 19b, reaction 19c is exothermic by 63 kJ mol$^{-1}$ (assuming the $O^{\bullet-} + O_2 \rightarrow O_3^{\bullet-}$ reaction is exothermic by 168 kJ mol$^{-1}$; this reaction was not studied by Viggiano and co-workers). One might wonder whether the ion $O^{\bullet-}(H_2O)$ would be better described as $HO^{-}(HO^{\bullet})$, a postulate raised in the first study.[96] While the 300 K exchange data (vide supra) clearly suggest that these two species interconvert during ion–molecule reactions at low energies, it seems unlikely that $HO^{-}(HO^{\bullet})$ would be lower in energy than $O^{\bullet-}(H_2O)$ since $HO^{-}$ is a strong enough base to readily deprotonate $HO^{\bullet}$ and the solvation ability of the open-shell hydroxyl radical should not be much more than that of the polar closed-shell molecule $H_2O$; the reaction coordinate diagram presented by Lifshitz[102] has these two species separated by about 59 kJ mol$^{-1}$ in energy with $O^{\bullet-}(H_2O)$ being the more stable. Incidentally, it is somewhat surprising that further hydration of $O^{\bullet-}(H_2O)$ is not observed by Viggiano and co-workers given the similarity to the $HO^{-}(H_2O)_n$ system where such further hydration steps are more rapid than the first hydration.[96]

### *5. Hydrogen Halides*

The atomic oxygen radical anion reacts with the hydrogen halides by rapid (see Table I) and exclusive proton transfer; this is not unexpected since all such reactions are considerably exothermic: $\Delta H^{\circ}_{rxn}[O^{\bullet-} + HF]$ = −45.2 kJ mol$^{-1}$; $\Delta H^{\circ}_{rxn}[O^{\bullet-} + HCl]$ = −204 kJ mol$^{-1}$; $\Delta H^{\circ}_{rxn}[O^{\bullet-} + HBr]$ = −245 kJ mol$^{-1}$; $\Delta H^{\circ}_{rxn}[O^{\bullet-} + HI]$ = −284 kJ mol$^{-1}$ (the reaction enthalpies listed are simply the differences in acidity between $HO^{\bullet}$ and HX[15]) and since proton transfer reactions involving such species are known not to have significant kinetic barriers.

Hamilton and co-workers,[103] using laser-induced fluorescence in a flowing afterglow, obtained the product state distributions for the thermally equilibrated ion–molecule proton transfer between HF and $O^{\bullet-}$ (eq 20). The $\nu = 1$ state of $HO^{\bullet}$ lies 3570 cm$^{-1}$ above $\nu = 0$ which corresponds to ca. 95% of the available exothermicity for this latter reaction. The low $HO^{\bullet}(\nu = 1)$ population found is characteristic of product states whose energies are close to the available reaction exothermicity. However, the yield of $HO^{\bullet}(\nu = 1)$ (eq 20b) is substantially higher than that calculated by the authors for a statistical "prior" distribution.

$$O^{\bullet-} + HF \xrightarrow{82\%} F^{-} + HO^{\bullet}\ (\nu = 0) \qquad (20a)$$

$$\xrightarrow{18\%} F^{-} + HO^{\bullet}\ (\nu = 1) \qquad (20b)$$

## B. Non-Hydrogen-Containing Diatomics

### *1. Dinitrogen*

Dinitrogen may be the only chemically unreactive molecule with the atomic oxygen radical anion: Adams and co-workers,[104] using a variable-temperature FA at 200 K, reported a very slow termolecular association rate (Table III) for $O^{\bullet-}$ with $N_2$ with He as the third body. This reaction has been discussed in detail, in light of theoretical and experimental considerations of $N_2O^{\bullet-}$, by Hopper et al.[105] and Rayment and Moruzzi.[106]

Total cross-sections for the production of free electrons in $O^{\bullet-}$ plus $N_2$ collisions have been reported by Lindinger and co-workers[89] for thermal to ca. 2 eV relative kinetic energy and by Compton and Bailey[107] for incident ion energies from 3.5 to 350 eV; each has compared their results to previous measurements. The lower energy measurements, of more pertinence to this review, did not reveal any reaction whatsoever. These later studies were confirmed by Rayment and Moruzzi[106] who measured the rate coefficient for the detachment reaction in a transverse flow–drift apparatus over the $E/p$ range 1–40 V cm$^{-1}$ Torr$^{-1}$ and found that $k$ initially increases rapidly with increasing $E/p$ ($6.8 \times 10^{-15}$ rising to about $10^{-12}$ cm$^3$ molecule$^{-1}$ s$^{-1}$).

### 2. Carbon Monoxide

The reaction of $O^{\bullet-}$ with CO is a process that has been particularly well studied from both experimental[70,81,97,108–113] and theoretical[114–117] points of view. The associative detachment is well known to be fast (Table I).[82,118–120] A substantial fraction of the ejected electrons in the associative detachment process have low translational energy[119] implying that a large fraction of the high reaction exothermicity is taken up in the internal modes of the carbon dioxide product. Bierbaum and co-workers,[112] utilizing the powerful technique of ion–molecule product infrared chemiluminescence, detected a portion of this internal excitation by monitoring the emission from the product $CO_2$ antisymmetric stretch.

Van Doren and co-workers,[97,98] utilizing their tandem flowing afterglow-selected ion flow tube apparatus, have studied a number of thermal energy (300 K) reactions of the isotopically labeled atomic oxygen radical anion, including carbon monoxide. Upon examination of the reaction of $^{18}O^{\bullet-}$ with CO, they uncovered a previously undetected reaction channel that competed with associative detachment, the oxygen atom exchange channel (21a). By comparing their measured efficiencies

$$^{18}O^{\bullet-} + C^{16}O \rightarrow {}^{16}O^{\bullet-} + C^{18}O \quad \Delta H^{\circ}_{rxn} \approx 0 \text{ kJ mol}^{-1} \tag{21a}$$

$$\rightarrow e^- + {}^{16}OC^{18}O \quad \Delta H^{\circ}_{rxn} = -391 \text{ kJ mol}^{-1} \tag{21b}$$

for both $^{18}O^{\bullet-}$ and $^{16}O^{\bullet-}$ reacting with CO (see Table I) they were able to demonstrate that 11% of the *observed* $^{18}O^{\bullet-}$ reaction proceeds by atom exchange and that 90% is the best estimate for the number of $O^{\bullet-}$/CO collisions that should be considered to be "reactive".

McFarland and co-workers[81] examined the reaction of $O^{\bullet-}$ with CO (eq 21b) from thermal energy to ~3 eV; the rate coefficient decreased by 1 order of magnitude with increasing ion kinetic energy over this energy range. Viggiano and co-workers[94,121] have reported the total rate coefficients for $O^{\bullet-}$ with CO at three temperatures; they observed (as with the several other $O^{\bullet-}$ reactions they examined) a slight negative temperature dependence. A comprehensive discussion of the data for this reaction, both at thermal energy and at elevated interaction energies, can be found in the original work by Van Doren et al.[98]

Upon hydration, the reaction of the atomic oxygen radical anion with carbon monoxide is slowed compared to that of the unhydrated version (ca. 30% by one water molecule and a further factor of 7 by a second water molecule).[94] Since no ionic products have been detected for these reactions, it is assumed that they proceed by an exothermic associative detachment process similar to that for the "naked" system (vide supra). However, the role of oxygen atom exchange in the hydrated reactions has yet to be considered.

### 3. Nitric Oxide

Several workers have examined how $O^{\bullet-}$ interacts with NO under a variety of conditions.[49,97,122,123] Under the thermally equilibrated conditions available to their tandem FA-SIFT, Van Doren et al.[97,98] observed a facile (Table I) atom exchange process in addition to the associative detachment process (eq 22); that is, the

$$^{18}O^{\bullet-} + N^{16}O^{\bullet} \rightarrow {}^{16}O^{\bullet-} + N^{18}O^{\bullet} \qquad \Delta H^{\circ}_{rxn} \approx 0 \text{ kJ mol}^{-1} \tag{22a}$$

$$\rightarrow e^- + {}^{16}ON^{18}O \qquad \Delta H^{\circ}_{rxn} = -166 \text{ kJ mol}^{-1} \tag{22b}$$

$$\nrightarrow NO^- + {}^{18}O \qquad \Delta H^{\circ}_{rxn} = +139 \text{ kJ mol}^{-1} \tag{22c}$$

observed reaction efficiency increased from 30% to 50% when the isotopically labeled oxygen anion was used as reactant and thereby "exposed" an exchange channel.

McFarland and co-workers[81] examined the reaction of $O^{\bullet-}$ with NO from thermal to ~1 eV and found the rate coefficient decreases by 1 order of magnitude with increasing ion kinetic energy. For $O^{\bullet-}$ + $NO^{\bullet}$ as a function of temperature as examined in a SIFT, Viggiano and Paulson found that the rate coefficient decreased by a factor of 3–4 as the temperature rose from 88 to 468 K; they fit their data to the form $k(T) = (3.1 \times 10^{-10})(300/T)^{0.83}$ cm$^3$ molecule$^{-1}$ s$^{-1}$. At 88 K, the observed rate coefficient for $O^{\bullet-} + NO \rightarrow e^- + NO_2$ is close to the collision limit; this observation in combination with the net negative temperature dependence led the authors to suggest that the observed temperature dependence is primarily due to a decreasing lifetime of the $O^{\bullet-}$–$NO^{\bullet}$ complex with respect to dissociation back to reactants (and is less a reflection of the temperature dependence of the autodetachment process from the complex). A later publication by Viggiano, Paulson, and co-workers[94] reported, based on measurements at 3 temperatures over a reduced temperature range, a slightly smaller temperature dependence, $k(T) \propto T^{-0.7}$.

Upon hydration, an additional, exothermic reaction channel (eq 23b) becomes available in the $O^{\bullet-}$ + NO system as compared to the solvent free system. Thus

$$O^{\bullet-}(H_2O) + NO^{\bullet} \rightarrow e^- + NO_2 + H_2O \qquad \Delta H^{\circ}_{rxn} = -159 \text{ kJ mol}^{-1} \tag{23a}$$

$$\rightarrow NO_2^- + H_2O \qquad \Delta H^{\circ}_{rxn} \geq -54 \text{ kJ mol}^{-1} \tag{23b}$$

the substantially larger rate coefficients observed by Viggiano and co-workers[94] are not surprising. Experimental complications prevented these workers from obtaining branching ratio data at the three different temperatures that they examined; similar complications restricted their conclusions concerning the doubly hydrated reaction (however, they were able to confirm that it is a factor of 2–3 slower than the monohydrated reaction). The intriguing question of how the oxygen exchange process for the nonhydrated reaction changes upon the addition of one water of hydration has not yet been addressed.

### *4. Oxygen*

Parkes, using a drift-tube device, reported the thermally equilibrated rate coefficient for the association reaction of ${\rm O}^{\bullet-}$ with $O_2$ mediated by $O_2$ (eq 24).[124] When

$${\rm O}^{\bullet-} + {\rm O}_2 \xrightarrow{{\rm O}_2} {\rm O}_3^{\bullet-} \qquad \Delta H^\circ_{\rm rxn} = -168\ {\rm kJ\ mol}^{-1} \quad (24)$$

Van Doren and co-workers used isotopic labels to examine the thermally equilibrated reaction between the atomic oxygen radical anion and dioxygen, they found that bimolecular atom exchange (eq 25) occurs

$${}^{18}{\rm O}^{\bullet-} + {}^{16}{\rm O}{}^{16}{\rm O} \rightarrow {}^{16}{\rm O}^{\bullet-} + {}^{16}{\rm O}{}^{18}{\rm O} \qquad \Delta H^\circ_{\rm rxn} \approx 0\ {\rm kJ\ mol}^{-1} \quad (25)$$

with a 17% efficiency, indicating that the 2-ps lifetime of the intermediate ${\rm O}_3^{\bullet-}$ complex is not long enough for complete oxygen scrambling to occur.[98] Tiernan et al.[125] had first noted the fast atom exchange reaction during their examination of the relative cross sections for ${}^{18}{\rm O}^{\bullet-}$ and ${}^{18}{\rm O}{}^{18}{\rm O}^{\bullet-}$ formation when ${}^{16}{\rm O}^{\bullet-}$ was impacted on ${}^{18}{\rm O}{}^{18}{\rm O}$ at center of mass energies from 0.3 to about 7 eV. This reaction, the atom exchange process, has a cross section that decreases, first rapidly (0.3 to ca. 0.7 eV) and then much more slowly (0.7 to 7 eV), with increasing kinetic energy of the reactant ion. Van Doren and co-workers[98] have an extended discussion of many of the mechanistic details of this atom exchange process with particular emphasis on the role of an ${\rm O}_3^{\bullet-}$ intermediate.

In addition to the atom exchange reaction, two additional channels become possible at elevated interaction energies: associative detachment and charge transfer (eq 26).[83b] Tiernan et al.[125] observed a slow

$${\rm O}^{\bullet-} + {\rm O}_2 \rightarrow {\rm e}^- + {\rm O}_3 \qquad \Delta H^\circ_{\rm rxn} = +35\ {\rm kJ\ mol}^{-1} \quad (26a)$$

$$\rightarrow {\rm O}_2^{\ -} + {\rm O}^\bullet \qquad \Delta H^\circ_{\rm rxn} = +99.6\ {\rm kJ\ mol}^{-1} \quad (26b)$$

electron-transfer reaction which has a cross-section typical of endothermic reactions (it is essentially zero at low energies and then rises sharply at an onset energy that represents, with correct consideration of the Doppler broadening of the effective center-of-mass energy owing to thermal motion of the target molecules, the endothermicity of the reaction). From a series of charge exchange reactions of the ${\rm O}^{\bullet-} + {\rm O}_2$ type (adding kinetic energy to a reactant anion to drive an endothermic electron transfer) Tiernan and co-workers were able to establish a consistent lower limit for the electron affinity of $O_2$ of 0.45 ± 0.1 eV; this value has since been confirmed by precise photodetachment experiments,[126] EA[$O_2$] = 0.451 ± 0.007 eV.

Snuggs et al.[127] reported that the rate coefficient for eq 24 was found to be invariant over the $E/N$ range $(6–29) \times 10^{-17}$ V cm$^2$. They also quantified the rate coefficients of the endothermic charge transfer as a function of $E/N$ (rising from $2.5 \times 10^{-14}$ cm$^3$ molecule$^{-1}$ s$^{-1}$ at 63 Td to $3.4 \times 10^{-12}$ cm$^3$ molecule$^{-1}$ s$^{-1}$ at 140 Td) and have compared and contrasted their data for these two channels with other measurements.

Lin et al.[45] determined the rate coefficient for the charge-transfer reaction of ${\rm O}^{\bullet-}$ with $O_2$ in the relative kinetic energy range from 1 eV (ca. threshold) to about 3 eV using a helium-buffered flow–drift tube. They discussed their data in relation to the literature data on beam studies (5-fold differences in the reported cross-sections at low energies) as well as to the literature data on drift tube studies in dioxygen buffer (10-fold differences in reported rate coefficients). That the rate coefficients for ${\rm O}^{\bullet-}$ in $O_2$ are larger than those for ${\rm O}^{\bullet-}$ in He suggests that the velocity distribution for ${\rm O}^{\bullet-}$ in $O_2$ has a more significant high-energy tail.

Rebentrost has reexamined some prior literature data on the endothermic charge transfer between ${\rm O}^{\bullet-}$ and $O_2$ under nonequilibrium kinetic conditions attainable in a drift tube.[128] In addition to fitting the data to recover an "activation energy" that is approximately the reaction endothermicity, he was able to define an effective temperature scale (in kelvins) as shown in eq 27 where $T_{\rm i}$ is the effective temperature, $T_{\rm g}$ is the gas

$$T_{\rm i} = 0.33\ T_{\rm g} + 50.0\ E/p_{\rm o} \quad (27)$$

temperature, and $E$ and $p_{\rm o}$ define the field and the ambient pressure ($E/p_{\rm o}$ in units of V cm$^{-1}$ Torr$^{-1}$).

As discussed in section IV.A.4, Fehsenfeld and Ferguson[96] hypothesized that the ${\rm O}^{\bullet-}({\rm H_2O})$ product first formed in their studies on the association of ${\rm O}^{\bullet-}$ with $H_2O$ underwent a facile, exothermic, switching reaction with the $O_2$ buffer gas as well as with the added $H_2O$ (eq 19). Viggiano and co-workers have used their variable temperature-selected ion flow tube to explicitly examine reaction 19c and have found that its rate coefficient is about $1 \times 10^{-10}$ cm$^3$ molecule$^{-1}$ s$^{-1}$ near room temperature,[94] confirming the predictions by Fehsenfeld and Ferguson.[96] For the dihydrated atomic oxygen radical anion, Viggiano and co-workers also observed facile switching of a single water (eq 28). That

$${\rm O}^{\bullet-}({\rm H_2O})_2 + {\rm O}_2 \rightarrow {\rm O}_3^{\bullet-}({\rm H_2O}) + {\rm H_2O} \quad (28)$$

the switching rate coefficients for both the mono- and dihydrated atomic oxygen radical anion with oxygen are 1 order of magnitude or so below the collision rate remains an intriguing and unexplained phenomenon since ligand switching reactions usually proceed on approximately every collision.[94] One probable reason for the less than unit efficient reaction is implied in eq 28; i.e., it is not a simple switching reaction but instead requires the rearrangment of ${\rm O}^{\bullet-}$ plus $O_2$ into the molecular radical anion of ozone.

## C. Non-Hydrogen-Containing Triatomics

### *1. Carbon Dioxide*

A large number of workers have examined the interaction of ${\rm O}^{\bullet-}$ with $CO_2$ as a function of ion kinetic energy. Fehsenfeld and Ferguson[96] examined the three-body association of $O^{\bullet-}$ to $CO_2$ in their FA (Table III) and found that oxygen is more effective at stabilizing the $CO_3^{\bullet-}$ product ion than helium. Parkes[108] likewise found that $CO_2$ is about 3.5 times more efficient at stabilizing the $CO_3^{\bullet-}$ product than is $O_2$. Van Doren et al. examined the same reaction in their tandem FA-SIFT, but using an isotopically labeled reactant anion, and found that bimolecular isotope exchange (eq 29) is much more facile than three-body association. The

$$^{18}O^{\bullet-} + CO_2 \xrightarrow{\text{EFF} = 67\%} {}^{16}O^{\bullet-} + {}^{18}OC^{16}O \qquad \Delta H^{\circ}_{\text{rxn}} \approx 0 \text{ kJ mol}^{-1} \quad (29)$$

$^2/_3$ efficiency measured by Van Doren et al. indicates that all three oxygens become equivalent during each $O^{\bullet-}/CO_2$ encounter; the intermediate complex is believed to exist for about 2 ns.[98] van der Wel and Nibbering have also observed this atom exchange reaction in an FT-ICR[99] while Futrell and Tiernan noted both isotopic exchange as well as $CO_3^{\bullet-}$ formation at low interaction energies in a tandem mass spectrometer.[100]

Paulson[129] reported the absolute cross sections for $O_2^{\bullet-}$ (plus CO) and $CO_2^{\bullet-}$ (plus O) production from the interaction of $O^{\bullet-}$ with $CO_2$; the peak values obtained were $0.2 \times 10^{-16}$ and $0.35 \times 10^{-16}$ cm$^2$ respectively and were found in the 8–15-eV (lab) energy region. Fansler and co-workers[130] reported their study of negative ions formed in $CO_2$ as a result of electron ionization and subsequent reactions at various temperatures, pressures, and values of $E/N$ obtained in a drift-tube mass spectrometer. The three body association of $O^{\bullet-}$ with $CO_2$ mediated by $CO_2$ was found to decline only slowly with increasing $E/N$ while the $CO_2$ collision-induced dissociation of $CO_3^{\bullet-}$ was found to be negligible below 300 Td but rises steeply at higher $E/N$ values. These authors also noted that collisional detachment of electrons from $O^{\bullet-}$ by interaction with $CO_2$ becomes important above 200 Td and attains a rate coefficient of $9 \times 10^{-12}$ cm$^3$ molecule$^{-1}$ s$^{-1}$ at 400 Td. Moseley and co-workers have also reported the rate coefficient for the formation of $CO_3^{\bullet-}$ from $O^{\bullet-}$ and $CO_2$ in $CO_2$ gas at 300 K as a function of $E/N$ from 10–120 Td.[41] A comparison of their own thermally equilibrated atom exchange data with the implications of the observations at elevated interaction energies is presented by Van Doren and co-workers.[98]

Viggiano and co-workers[94] and Yang and Castleman[131b] have studied the reactions of the hydrated atomic oxygen radical anion with carbon dioxide. A facile ligand switching process was found for the reactions of $O^{\bullet-}(H_2O)$ with $CO_2$ producing $CO_3^{\bullet-}$. While a fast, reactive loss of $O^{\bullet-}(H_2O)_2$ was noted upon its reaction with $CO_2$, the product was not observed; the lack of observation of $CO_3^{\bullet-}(H_2O)$, which has been assigned as the sole primary product, is presumed to be due to its fast reaction/decomposition under the reaction conditions.[94] The 300 K rate coefficients (Table IV) obtained by both groups are in good agreement. Figure 1 shows how the small $O^{\bullet-}$ hydrates have reaction rate coefficients with $CO_2$ that vary only weakly with temperature. Yang and Castleman also extended their kinetic disappearance studies to large hydrated clusters. In order to make the higher order cluster ions, these workers had to resort to lowering the temperature of their flow-tube apparatus. At 200 K, the measured rate coefficients for $O^{\bullet-}(H_2O)_n$ (for $1 \leq n < 4$) with $CO_2$ are very similar to those measured at room temperature (Figure 1). Lowering the temperature below 140 K permitted even larger cluster anions to be studied. At 130 K, the rate coefficients for $O^{\bullet-}(H_2O)_n$ with $CO_2$ range from $8.9 \times 10^{-10}$ for $n = 1$ to $0.27 \times 10^{-10}$ cm$^3$ molecule$^{-1}$ s$^{-1}$ for $n = 15$ (Figure 2). Yang and Castleman proposed that rather than a simple "switching" reaction, the hydrated $O^{\bullet-}$ clusters produce products with a reduced number of waters of hydration (i.e., some number of $H_2O$ molecules have been "boiled" off, eq 30). They expected that reaction 30 is still very exothermic even when three water ligands are replaced by one $CO_2$ molecule.

$$O^{\bullet-}(H_2O)_n + CO_2 \rightarrow CO_3^{\bullet-}(H_2O)_m + \{n - m\}H_2O \quad (30)$$

**Table IV. Room Temperature Rate Coefficients for Binary Reactions of $O^{\bullet-}(H_2O)_n$ with Neutral Molecules in the Gas Phase**

| reaction | rate coefficient (cm$^3$ molecule$^{-1}$ s$^{-1}$) | ref |
|---|---|---|
| $O^{\bullet-}(H_2O) + CH_4 \rightarrow$ products | $<1 \times 10^{-12\,a}$ | 94 |
| $O^{\bullet-}(H_2O)_2 + CH_4 \rightarrow$ products | $<1 \times 10^{-12\,a}$ | 94 |
| $O^{\bullet-}(H_2O) + H_2O \rightarrow$ products | $<5 \times 10^{-12\,a}$ | 94 |
| $O^{\bullet-}(H_2O)_2 + H_2O \rightarrow$ products | $<5 \times 10^{-12\,a}$ | 94 |
| $O^{\bullet-}(H_2O) + CO \rightarrow e^- +$ products | $4.00 \times 10^{-10\,a}$ | 94 |
| $O^{\bullet-}(H_2O)_2 + CO \rightarrow e^- +$ products | $1.70 \times 10^{-10\,a}$ | 94 |
| $O^{\bullet-}(H_2O) + NO \rightarrow$ products | $3.00 \times 10^{-10\,a}$ | 94 |
| $O^{\bullet-}(H_2O)_2 + NO \rightarrow$ products | $1.90 \times 10^{-10\,a}$ | 94 |
| $O^{\bullet-}(H_2O) + O_2 \rightarrow O_3^{\bullet-} + H_2O$ | $>1 \times 10^{-11}$ | 96 |
| $O^{\bullet-}(H_2O) + O_2 \rightarrow O_3^{\bullet-} + H_2O$ | $1.22 \times 10^{-10\,a}$ | 94 |
| $O^{\bullet-}(H_2O)_2 + O_2 \rightarrow O_3^{\bullet-}(H_2O) + H_2O$ | $7.05 \times 10^{-11\,a}$ | 94 |
| $O^{\bullet-}(H_2O) + CO_2 \rightarrow CO_3^{\bullet-} + H_2O$ | $8.40 \times 10^{-10\,a}$ | 94 |
| $O^{\bullet-}(H_2O) + CO_2 \rightarrow$ products | $8.2 \times 10^{-10}$ | 96 |
| $O^{\bullet-}(H_2O) + CO_2 \rightarrow$ products | $8.5 \times 10^{-10}$ | 131 |
| $O^{\bullet-}(H_2O)_2 + CO_2 \rightarrow$ products | $7.70 \times 10^{-10\,a}$ | 94 |
| $O^{\bullet-}(H_2O)_2 + CO_2 \rightarrow$ products | $7.9 \times 10^{-10}$ | 96 |
| $O^{\bullet-}(H_2O)_2 + CO_2 \rightarrow$ products | $7.8 \times 10^{-10}$ | 131 |
| $O^{\bullet-}(H_2O)_3 + CO_2 \rightarrow$ products | $6.9 \times 10^{-10}$ | 131 |
| $O^{\bullet-}(H_2O) + N_2O \rightarrow$ products | $<1 \times 10^{-12\,a}$ | 94 |
| $O^{\bullet-}(H_2O)_2 + N_2O \rightarrow$ products | $<1 \times 10^{-13\,a}$ | 94 |
| $O^{\bullet-}(H_2O) + CH_3CN \rightarrow$ products | $4.1 \times 10^{-9}$ | 131 |
| $O^{\bullet-}(H_2O)_2 + CH_3CN \rightarrow$ products | $3.7 \times 10^{-9}$ | 96 |
| $O^{\bullet-}(H_2O)_3 + CH_3CN \rightarrow$ products | $3.3 \times 10^{-9}$ | 131 |
| $O^{\bullet-}(H_2O) + SO_2 \rightarrow$ products | $1.50 \times 10^{-9\,a}$ | 94 |
| $O^{\bullet-}(H_2O)_2 + SO_2 \rightarrow$ products | $1.50 \times 10^{-9\,a}$ | 94 |

[a] These values were obtained at 343 K; see the original reference for measurements at either 251 or 473 K.

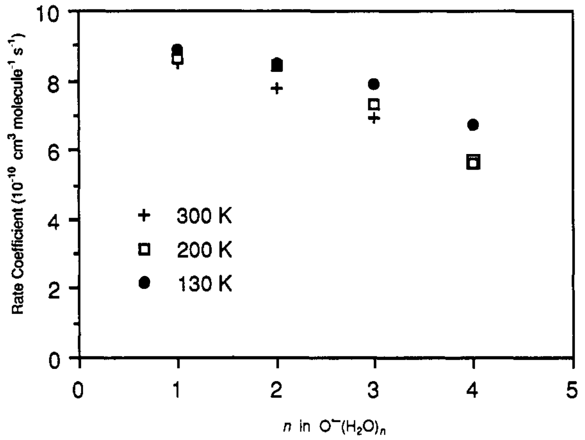

**Figure 1.** Cluster size dependence of the rate coefficient for the reactions of $O^{\bullet-}(H_2O)_n$ with carbon dioxide in helium buffer gas at three different temperatures. Data taken from ref 131.

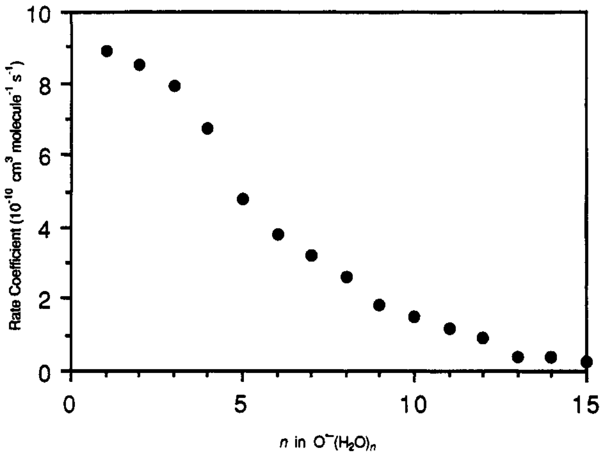

**Figure 2.** Cluster size dependence of the rate coefficient for the reactions of $O^{\bullet-}(H_2O)_n$ with carbon dioxide in helium buffer gas at 130 K. Data taken from ref 131.

### 2. Nitrous Oxide

Parkes[64] examined electron attachment and negative ion–molecule reactions in nitrous oxide in a drift tube fitted with a mass filter. From an extended analysis of ion currents as a function of reduced field, he found a rate coefficient for reaction 31 of $k = (1.95 \pm 0.06) \times 10^{-10}$ cm$^3$ molecule$^{-1}$ s$^{-1}$. At high pressures, a slow three-body reaction (see Table III) is also observed. A joint flowing afterglow-ion cyclotron resonance[74] study showed that the rate coefficient for the reaction of $O^{\bullet-}$ with $N_2O$ decreases with increasing temperature (from $2.2 \times 10^{-10}$ at 278 K to $1.5 \times 10^{-10}$ cm$^3$ molecule$^{-1}$ s$^{-1}$ at 475 K) or with increasing $O^{\bullet-}$ kinetic energy (the cross section drops from 20 Å$^2$ at thermal energy to 4.5 Å$^2$ at 0.4 eV with further decreases up to 2 eV) and that there is but a single product (eq 31). Most importantly, these side-by-side studies indicated that the $O^{\bullet-}$ produced at low pressures from $N_2O$ in the ICR was reacting with suprathermal kinetic energy (ca. 0.4 eV) and that the hot $O^{\bullet-}$ could be cooled by allowing sufficient nonreactive $O^{\bullet-}$/Ar collisions to occur. Dotan and co-workers[132] noted that complex formation with oxygen-atom scrambling is the major channel for this reaction. More recently Van Doren and co-workers[97] have taken advantage of the unique capabilities of their tandem FA-SIFT to contrast the rate coefficients for $^{16}O^{\bullet-}$ and $^{18}O^{\bullet-}$ with $N_2O$. They found that the unlabeled system has a thermally equilibrated rate coefficient which corresponds to a 19% efficiency while the labeled system reveals the atom exchange process and hence possesses an enhanced efficiency of 35%. van der Wel and Nibbering[99] also noted the new atom exchange pathway when they examined the labeled system in an FT-ICR; their results are summarized in eq 32. Dotan and Klein[63] reported the gentle decrease in the rate of $NO^-$ production (and NO) from $O^{\bullet-}$ with $N_2O$ as the temperature was increased to approximately 600 K. In accord with this observation, Viggiano and co-workers[94] have reported a slight negative temperature dependence for this reaction: $k(T) \propto T^{-0.50}$.

$$O^{\bullet-} + N_2O \rightarrow NO^- + NO^\bullet \qquad \Delta H^\circ_{rxn} = -9.6\ \mathrm{kJ\ mol^{-1}} \tag{31}$$

Viggiano and co-workers[94] also found that hydration of the atomic oxygen radical anion by just one water molecule reduced the rate of its reaction with nitrous oxide to below their detection limit ($k < 1 \times 10^{-12}$ cm$^3$ molecule$^{-1}$ s$^{-1}$); at this time it is not clear whether the hydrated reactions remain exothermic and are simply hindered by a kinetic barrier or whether they are limited by a thermochemical barrier.

$$^{18}O^{\bullet-} + N_2{}^{16}O \rightarrow 70\%\ {}^{16}O^{\bullet-} + N_2{}^{18}O \qquad \Delta H^\circ_{rxn} \approx 0\ \mathrm{kJ\ mol^{-1}} \tag{32a}$$

$$\rightarrow 15\%\ N^{16}O^- + N^{18}O^\bullet \qquad \Delta H^\circ_{rxn} = -9.6\ \mathrm{kJ\ mol^{-1}} \tag{32b}$$

$$\rightarrow 15\%\ N^{18}O^- + N^{16}O^\bullet \qquad \Delta H^\circ_{rxn} = -9.6\ \mathrm{kJ\ mol^{-1}} \tag{32c}$$

Dotan and Klein[63] reported the rate coefficient for eq 32 (measurements based on the ratio of product ion to reactant ion intensities) as a function of temperature and excess reactant ion kinetic energy; they were careful to avoid using nitrous oxide as the source gas for $O^{\bullet-}$ because of the known excess energy imparted to the atomic oxygen radical anion. They found a moderate decrease in reaction efficiency over the energy range examined (to 1 eV) in accord with the observations noted by Marx et al. using the ICR.[74] However, Lindinger and co-workers[89] noted a considerably faster falloff in the *total* rate by which $O^{\bullet-}$ reacts with $N_2O$; their rate coefficient versus $\langle KE_{cm} \rangle$ plot shows a decreasing rate up to ca. 0.4 eV and then a rising $k$ as the interaction energy is increased beyond that. Lindinger and co-workers discussed the relationship of their observations to previous measurements at various energies. Viggiano and co-workers[93] have also published their data from a flow tube apparatus for the reaction of $O^{\bullet-}$ with $N_2O$ as a function of energy; their corrected plot shows a shallow decrease in $k$ from ambient energies to about 0.8 eV or so, and then a shallow increase in the rate as one goes to even higher energies.

### 3. Nitrogen Dioxide

Dotan and co-workers[132] examined the reaction of $O^{\bullet-}$ with $NO_2^\bullet$ in their ICR instrument; while it was unclear which precursor gas was used to create the reactant ion, they report that the only reaction noted was a charge transfer process (eq 33a). Earlier reports by Vogt[133] and Futrell and Tiernan[100] both indicated that an oxygen atom exchange process was a minor channel. However, a different report indicated that no isotopic scrambling occurs for this ion–molecule reaction[63] and thus that the reaction proceeds only by charge transfer. The rate coefficient of the fast, highly exothermic, charge transfer between $O^{\bullet-}$ and $NO_2^\bullet$ was found to decrease with increasing ion kinetic energy[63,100,133-135] as well as with increasing temperature.[63]

$$^{18}O^{\bullet-} + N^{16}O_2^\bullet \xrightarrow{\text{major}} N^{16}O_2^- + {}^{18}O \qquad \Delta H^\circ_{rxn} = -80.8\ \mathrm{kJ\ mol^{-1}} \tag{33a}$$

$$\xrightarrow{\text{minor}} {}^{16}O^{\bullet-} + {}^{18}ON^{16}O^\bullet \qquad \Delta H^\circ_{rxn} \approx 0\ \mathrm{kJ\ mol^{-1}} \tag{33b}$$

### 4. Ozone

The cross section for the charge transfer reaction of $O^{\bullet -}$ with $O_3$ has been examined in the 1–500-eV range[136] and decreases slowly with increasing energy. For this reaction, Lifshitz and co-workers[137] noted that at ca. 0.3 eV (LAB), the total rate coefficient is $5.1 \times 10^{-10}$ cm$^3$ molecule$^{-1}$ s$^{-1}$ with the major process being associative detachment (59%) followed by charge transfer (39%) with a minor amount of $O_2^{\bullet -}$ production (2%) (eq 34).

$$O^{\bullet -} + O_3 \rightarrow e^- + O_2 + O_2 \qquad \Delta H^{\circ}_{rxn} = -250 \text{ kJ mol}^{-1} \qquad (34a)$$

$$\rightarrow O_3^{\bullet -} + O \qquad \Delta H^{\circ}_{rxn} = -61.1 \text{ kJ mol}^{-1} \qquad (34b)$$

$$\rightarrow O_2^{\bullet -} + O_2 \qquad \Delta H^{\circ}_{rxn} = -293 \text{ kJ mol}^{-1} \qquad (34c)$$

### 5. Sulfur Dioxide

Van Doren et al.[97] found that $^{18}O^{\bullet -}$ reacts 7% more efficiently with $SO_2$ than does $^{16}O^{\bullet -}$; therefore, although the associative detachment reaction between the atomic oxygen radical anion and sulfur dioxide is a very facile process, a small amount of atom exchange does take place (eq 35). The electron transfer channel (eq 35c) is thermochemically not accessible under thermally equilibrated conditions.

$$^{18}O^{\bullet -} + SO_2 \rightarrow e^- + {}^{18}OSO_2 \qquad \Delta H^{\circ}_{rxn} = -207 \text{ kJ mol}^{-1} \qquad (35a)$$

$$\rightarrow {}^{16}O^{\bullet -} + {}^{18}OSO \qquad \Delta H^{\circ}_{rxn} \approx 0 \text{ kJ mol}^{-1} \qquad (35b)$$

$$\nrightarrow SO_2^{\bullet -} + {}^{18}O \qquad \Delta H^{\circ}_{rxn} = +35 \text{ kJ mol}^{-1} \qquad (35c)$$

At low $\langle KE_{cm} \rangle$, Lindinger and co-workers[89] observed only the associative detachment reaction between $O^{\bullet -}$ and $SO_2$. As the interaction energy increases, the endothermic charge transfer channel becomes the dominant process. The decline in total rate at low energies is said to be typical of associative detachment reactions while the leveling off of the rate at higher energies is probably accounted for by a charge transfer process whose rate is relatively insensitive to energy (0.6–3 eV). Dotan and Klein[63] found that this reaction has a rate coefficient which decreases with both energy and temperature on the basis of their pulsed mass spectrometer measurements. Viggiano and co-workers[94,121] have reported the rate coefficient for the associative detachment channel (by using unlabeled reagents) at three temperatures; the rate coefficient has a slight negative temperature dependence, $k(T) \propto T^{-0.3}$. The close similarity in the temperature dependences of the experimental and collision limiting rate coefficients indicates that the reaction efficiency is not changing in the 200–500 K regime over which they made their measurements, in accord with the earlier explanation by Lindinger and co-workers. Viggiano and co-workers have also examined the dependence of the total rate coefficient on $\langle KE_{cm} \rangle$ (negative dependence found) at three different helium bath gas temperatures; all data are in excellent agreement with one another, suggesting that the rate coefficient depends only upon total energy and not on the type of energy, again in accord with all previous observations. These authors found that the fractional contribution of the charge transfer channel increased with increasing $\langle KE_{cm} \rangle$, as had been reported earlier by Lindinger and co-workers;[89] analysis of their data led to a threshold activation energy of 0.3 eV for the charge transfer, in agreement with the known electron affinities.

The mono- and dihydrated atomic oxygen radical anion reactions with sulfur dioxide proceed with nearly identical rate coefficients (however, the reaction efficiencies actually increase slightly with increased hydration). As for many of the other reactions examined by these authors,[94] the product distributions for the hydrated $O^{\bullet -}(H_2O)_n$ $\{n = 1 \text{ or } 2\}$ plus $SO_2$ reactions were unable to be obtained.

## D. Non-Hydrogen-Containing Polyatomics

### 1. Carbon Tetrachloride

Dotan and co-workers[138] found that $ClO^-$ is the major, and perhaps exclusive, channel for the rapid reaction of $O^{\bullet -}$ with $CCl_4$ (the authors could not exclude the possibility that the observed minor ions $Cl^-$ and $Cl_2^-$ were reaction products). From the observation that reaction 36 is fast, these authors were able to place a

$$O^{\bullet -} + CCl_4 \rightarrow ClO^- + {}^{\bullet}CCl_3 \qquad \Delta H^{\circ}_{rxn} = -39 \text{ kJ mol}^{-1} \qquad (36)$$

limit on the electron affinity of ClO: EA[ClO] ≥ 1.70 eV (164 kJ mol$^{-1}$). Lineberger and co-workers[139] have since precisely measured EA[ClO] = 2.276 ± 0.006 eV by negative ion photoelectron spectroscopy, confirming the limit established by the earlier kinetic measurements. Hence reaction 36 should readily serve as a convenient source of the reactive species $ClO^-$ for further investigations. Estimates for a similar reaction with $CBr_4$ indicate that $BrO^-$ is a thermochemically allowed reaction product (eq 37).

$$O^{\bullet -} + CBr_4 \rightarrow BrO^- + {}^{\bullet}CBr_3 \qquad \Delta H^{\circ}_{rxn} \leq -4.6 \text{ kJ mol}^{-1} \qquad (37)$$

### 2. Other Compounds

Dawson and co-workers[140] have examined the negative ion chemistry of mixtures of nitrous oxide/propene/carbonyl fluoride and assigned the substitution process noted in eq 38. This type of addition–elimination is

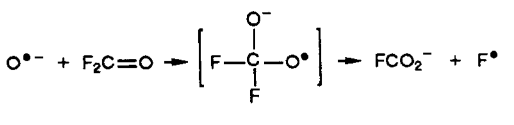

$$O^{\bullet -} + F_2C{=}O \rightarrow \left[ F{-}\overset{O^-}{\underset{F}{C}}{-}O^{\bullet} \right] \rightarrow FCO_2^- + F^{\bullet} \qquad (38)$$

discussed in greater detail in sections VI.A–C. Streit and co-workers have reported rate coefficients for $O^{\bullet -}$ reacting with several halogenated compounds (Table I); for example, they found fast charge transfer between $O^{\bullet -}$ and $SF_4$;[141,142] other values that they measured can be found in Table I.

**Scheme III. The Chemical Processes Occurring When the Atomic Oxygen Radical Anion Reacts with Acetonitrile**

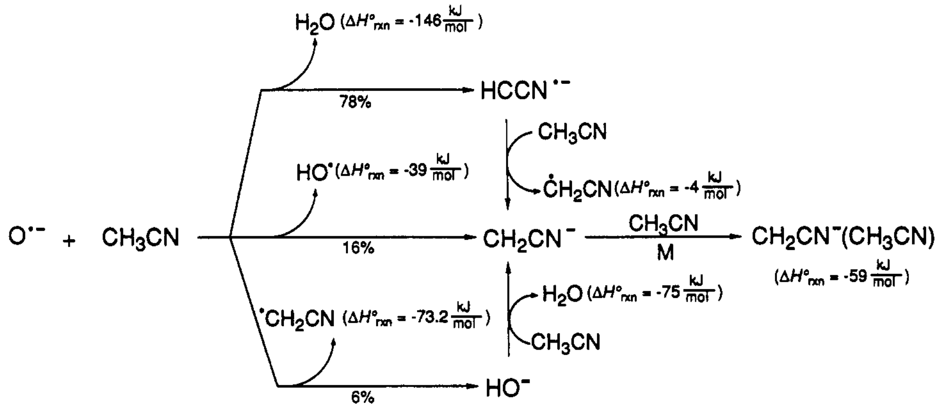

## V. Reactive Intermediates from Organic Substrates

### A. Reactions with Saturated Systems

#### 1. Substituted Methanes (Carbene Radical Anions)

When the atomic oxygen radical anion is allowed to react with substituted methanes, three reaction channels are typically observed: $H^+$ transfer, $H_2^{\bullet+}$ transfer, and H-atom transfer. Other channels may also be seen; for example, if the substituted methane contains a good leaving group, then nucleophilic substitution is usually noted. Because of its unique character, the carbene radical anion (e.g., $XYC^{\bullet-}$), which results from $H_2^{\bullet+}$ transfer (e.g., from $XYCH_2$), is perhaps the most interesting product. Large O–H bond strengths, coupled with the atomic oxygen radical anion's open-shell nature and high proton affinity, make the gas-phase synthesis of these novel anions possible. While carbene radical anions are important reactive intermediates in their own right,[143] their ready availability in the gas-phase permits experiments which provide valuable information on the structures, energies, and properties of the corresponding neutral carbene.

*a. Acetonitrile.* One of the best understood reactions of the atomic oxygen radical anion with an organic neutral is that of $O^{\bullet-}$ with acetonitrile. Dawson and Jennings[144] were among the first to study the reaction of $O^{\bullet-}$ with $CH_3CN$ in an ICR spectrometer. They observed three products, corresponding to $H_2^{\bullet+}$ transfer, H-atom transfer, and proton transfer (eq 39); the

$$O^{\bullet-} + CH_3CN \rightarrow HCCN^{\bullet-} + H_2O \quad (39a)$$

$$\rightarrow HO^- + {}^{\bullet}CH_2CN \quad (39b)$$

$$\rightarrow H_2CCN^- + HO^{\bullet} \quad (39c)$$

approximate relative rate coefficients for these reactions were found to be 6:1:3, respectively. Later examination of this reaction[10] using the SIFT technique indicated that the reaction of $O^{\bullet-}$ with $CH_3CN$ was extremely rapid ($k_{obs} = 3.5 \times 10^{-9}$ cm$^3$ molecule$^{-1}$ s$^{-1}$; EFF = 0.65) and that the sole product was that from proton transfer (eq 39c). Subsequent investigation of this reaction and its secondary reactions by Grabowski and Melly[145] using the flowing afterglow yielded product distributions indicated in reaction 40. Note that the reaction enthalpies listed in eq 40 are actually those for the all-protio compounds.

$$O^{\bullet-} + CD_3CN \rightarrow 78\%\ DCCN^{\bullet-} + D_2O \qquad \Delta H^{\circ}_{rxn} = -146\ \text{kJ mol}^{-1} \quad (40a)$$

$$\rightarrow 16\%\ D_2CCN^- + DO^{\bullet} \qquad \Delta H^{\circ}_{rxn} = -39\ \text{kJ mol}^{-1} \quad (40b)$$

$$\rightarrow 6\%\ DO^- + CD_2CN^{\bullet} \qquad \Delta H^{\circ}_{rxn} = -73.2\ \text{kJ mol}^{-1} \quad (40c)$$

$$\rightarrow 0\%\ CN^- + CD_3O^{\bullet} \qquad \Delta H^{\circ}_{rxn} = -93.7\ \text{kJ mol}^{-1} \quad (40d)$$

In their ICR experiments, Dawson and Jennings[144] observed that as the pressure of the $N_2O/CH_3CN$ mixture was increased, the $HCCN^{\bullet-}$ peak diminished until at some pressure it disappeared completely. On the basis of the change in the $[HCCN^{\bullet-}]/[H_2CCN^-]$ ratio as well as on the results from electron ejection experiments, the authors concluded that $HCCN^{\bullet-}$ reacted with another molecule of acetonitrile by an associative detachment reaction (eq 41). Grabowski

$$HCCN^{\bullet-} + CH_3CN \rightarrow e^- + \text{neutral products} \quad (41)$$

and Melly[145] also observed a fast secondary reaction between $DCCN^{\bullet-}$ and $CD_3CN$, but saw no decrease in total ion intensity as this reaction was allowed to progress. Cross-labeling studies were conducted wherein the reaction of $O^{\bullet-}$ and $CH_3CN$ was allowed to proceed until all the reactant ion and the $HO^-$ product ion were quenched. At this point, $CD_3CN$ was added to the product ion mixture with the result that rapid decay of the $HCCN^{\bullet-}$ signal was observed concomitant with the appearance of a $D_2CCN^-$ signal. These authors concluded that the reaction of the carbene radical anion of acetonitrile with acetonitrile proceeds primarily via a proton transfer pathway. Yang et al. interpreted their later data in the same manner.[146] All reactions, both primary and secondary, are summarized in Scheme III. Of all the substituted carbene radical anions synthesized to date via reaction with atomic oxygen radical anion, acetonitrile yields the largest amount of $XYC^{\bullet-}$.

At 300 K, it is found[146] that $O^{\bullet -}(H_2O)_n$ reacts with $CH_3CN$ at the same efficiency for 0–3 waters of hydration. This latter result is in contrast with those data found for $HO^-(H_2O)_n$ with $CH_3CN$, in which it is found that the reaction efficiency drops off dramatically with each additional water of hydration ($n$ = 0–3). At low temperature (130 K), very large hydrated clusters of $O^{\bullet -}$ can be formed in the fast flow apparatus employed by Yang et al.; for clusters up to $n$ = 20, the rate coefficients are near the collision limit and hence the efficiency remains independent of the number of waters of hydration. (The plot of rate coefficient versus cluster size for $O^{\bullet -}(H_2O)_n$ with $CH_3CN$ is essentially of the shape and form of that for $O^{\bullet -}(H_2O)_n$ with $CO_2$ (Figure 2) with $k$ for the present reaction dropping from ca. $6.2 \times 10^{-9}$ to ca. $3.6 \times 10^{-9}$ cm$^3$ molecule$^{-1}$ s$^{-1}$ as $n$ varies from 0 to 20 at 130 K.) Although they were unable to quantify the rates of the larger $O^{\bullet -}$ hydrates ($20 < n \leq 59$), Yang et al. noted that the trend of a fast reaction with acetonitrile continues in this hydration range. While the products are not unambiguously clear, these authors concluded that hydrated $O^{\bullet -}$ (at all levels of hydration) reacts with acetonitrile by an H-atom transfer (eq 42); "boil-off" of waters of hydration, however, is unknown for this reaction. As noted for the smaller hydrates, $O^{\bullet -}(H_2O)_n$ remains considerably more reactive than $HO^-(H_2O)_n$, especially for large $n$.

$$O^{\bullet -}(H_2O)_n + CH_3CN \rightarrow HO^-(H_2O)_n + {}^{\bullet}CH_2CN \quad (42)$$

*b. $H_2CXY$ (X = Halogen, Y = Halogen or Hydrogen).* The atomic oxygen radical anion is found to react rapidly with methyl chloride by three reaction pathways: $H_2^{\bullet +}$ transfer, H-atom transfer, and nucleophilic displacement (eq 43);[145,147,148] the proton-transfer pathway is thermodynamically prohibited. Bohme et al. have reported two different values for the rate coefficients for this reaction ($k_{obs}$ = $1.7 \pm 0.3 \times 10^{-9}$ cm$^3$ molecule$^{-1}$ s$^{-1}$; EFF = 0.56 and $2.4 \times 10^{-9}$; EFF = 0.79).[147,148] Not only does $O^{\bullet -}$ react rapidly with methyl chloride, but two of the initial product ions, $HO^-$ and $HCCl^{\bullet -}$, react equally rapidly in secondary processes: $HO^-$ is known to undergo a displacement reaction with $CH_3Cl$ to produce $Cl^-$,[145,147,148] and evidently $HCCl^{\bullet -}$ reacts with $CH_3Cl$ by the same process.[145] All reactions, both primary and secondary, are summarized in Scheme IV.

$$O^{\bullet -} + CH_3Cl \rightarrow 66\%\ HCCl^{\bullet -} + H_2O \qquad \Delta H^{\circ}_{rxn} = -87.4\ \mathrm{kJ\ mol^{-1}} \quad (43a)$$

$$\rightarrow 19\%\ Cl^- + CH_3O^{\bullet} \qquad \Delta H^{\circ}_{rxn} = -238\ \mathrm{kJ\ mol^{-1}} \quad (43b)$$

$$\rightarrow 15\%\ HO^- + {}^{\bullet}CH_2Cl \qquad \Delta H^{\circ}_{rxn} = -33\ \mathrm{kJ\ mol^{-1}} \quad (43c)$$

$$\rightarrow 0\%\ CH_2Cl^- + HO^{\bullet} \qquad \Delta H^{\circ}_{rxn} = +58.2\ \mathrm{kJ\ mol^{-1}} \quad (43d)$$

Methylene chloride reacts with the atomic oxygen radical anion to yield the radical anion of dichlorocarbene as the major primary product ion; the primary product distribution found under the thermally equilibrated (300 K) conditions of the flowing afterglow, as well as the fast secondary reactions that occur, are summarized in Scheme V. Other halogenated methanes have been studied to a lesser extent;[144,148] many of these results are summarized in Tables V and VI. It should be noted that due to the extremely high reactivity displayed by many of the carbene radical anions either with their parent compounds and/or with the compound used to form $O^{\bullet -}$, any results from experimental approaches that did not explicitly consider such reactions must be treated with caution.

*c. Aliphatic Nitriles.* In addition to acetonitrile (discussed above), a variety of other saturated nitriles

**Scheme IV. The Chemical Processes Occurring When the Atomic Oxygen Radical Anion Reacts with Methyl Chloride**

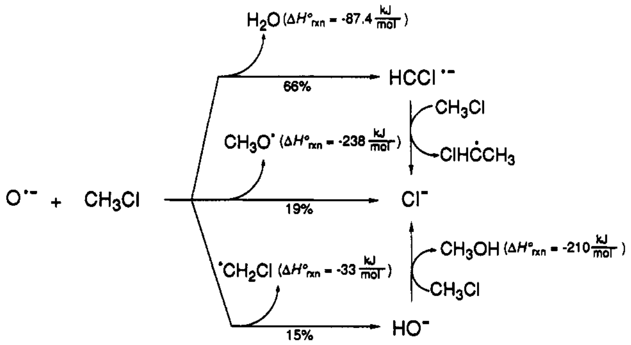

**Scheme V. The Chemical Processes Occurring When the Atomic Oxygen Radical Anion Reacts with Methylene Chloride**

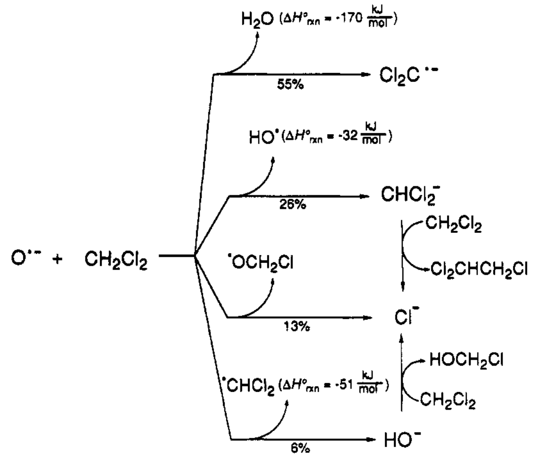

**Table V. Substituted Methanes Which Have Been Reported To Yield (M – 2H)$^{\bullet -}$ Radical Ions upon Reaction with O$^{\bullet -}$**

| neutral | | |
|---|---|---|
| $(XYCH_2)$ | ref(s) | EA[XYC] (eV), ref |
| $CH_3F$ | 144,148 | 0.542 ± 0.005, 150 |
| $CH_3Br$ | 148 | 1.454 ± 0.008, 150 |
| $CH_3Cl$ | 145,148 | 1.210 ± 0.005, 150 |
| $CH_2N_2$ | 140,151 | |
| $CH_2F_2$ | 144 | 0.179 ± 0.005, 149 |
| $CH_2Cl_2$ | 145 | 1.603 ± 0.008, 149 |
| $CH_3CN$ | 144,145,151 | |
| $CH_3CH_2CN$ | 151 | |
| $CH_3CH_2CH_2CN$ | 144,151 | |
| $HCO_2CH_3$ | 56 | |
| $CH_3OCH_2CN$ | 151 | |
| $CH_3OCH_2CH_2CN$ | 151 | |
| $CH_3CH_2OCH_2CH_2CN$ | 151 | |
| $(CH_3)_3P$ | 152 | |

**Table VI. Products and Bimolecular Rate Coefficients for the Reaction of $O^{\bullet-}$ with Halogenated Methanes and Ethanes**[a]

| neutral |  | $k_{obs}$ ($cm^3$ molecule$^{-1}$ $s^{-1}$) | ion product observed [and corresponding neutral] | ref |
|---|---|---|---|---|
| mass | formula |  |  |  |
| 34 | $CH_3F$ | $1.7 \times 10^{-10}$ | 82% $HO^- + {}^{\bullet}CH_2F$<br>18% $HCF^{\bullet-} + H_2O$ | 100 |
| 34 | $CH_3F$ | $1.1 \times 10^{-10}$ | $HO^- + {}^{\bullet}CH_2F$<br>$F^- + CH_3O^{\bullet}$<br>$HCF^{\bullet-} + H_2O$ | 148 |
| 48 | $C_2H_5F$ | $3.1 \times 10^{-10}$ | 87% $HO^- + {}^{\bullet}C_2H_4F$<br>10% $F^- + C_2H_5O^{\bullet}$<br>3% $C_2H_3F^{\bullet-} + H_2O$ | 100 |
| 50 | $CH_3Cl$ | $2.4 \times 10^{-9}$ | 50% $Cl^- + CH_3O^{\bullet}$<br>40% $HO^- + {}^{\bullet}CH_2Cl$<br>10% $HCCl^{\bullet-} + H_2O$ | 147 |
| 50 | $CH_3Cl$ | $(1.7 \pm 0.3) \times 10^{-9}$ | $Cl^- + CH_3O^{\bullet}$<br>$HO^- + {}^{\bullet}CH_2Cl$<br>$HCCl^{\bullet-} + H_2O$ | 148 |
| 50 | $CH_3Cl$ | $7.3 \times 10^{-10}$ | 53% $HO^- + {}^{\bullet}CH_2Cl$<br>10% $Cl^- + CH_3O^{\bullet}$<br>37% $HCCl^{\bullet-} + H_2O$ | 100 |
| 50 | $CH_3Cl$ |  | 66% $HCCl^{\bullet-} + H_2O$<br>19% $Cl^- + CH_3O^{\bullet}$<br>15% $HO^- + {}^{\bullet}CH_2Cl$ | 145 |
| 84 | $CH_2Cl_2$ |  | 55% $Cl_2C^{\bullet-} + H_2O$<br>26% $HCCl_2^- + HO^{\bullet}$<br>13% $Cl^- + CH_2ClO^{\bullet}$<br>6% $HO^- + {}^{\bullet}CHCl_2$ | 145 |
| 95 | $CH_3Br$ | $(1.1 \pm 0.1) \times 10^{-9}$ | $Br^- + CH_3O^{\bullet}$<br>$HO^- + {}^{\bullet}CH_2Br$<br>$HCBr^{\bullet-} + H_2O$ | 148 |
| 95 | $CH_3Br$ | $2.1 \times 10^{-10}$ | 52% $HO^- + {}^{\bullet}CH_2Br$<br>14% $Br^- + CH_3O^{\bullet}$<br>33% $HCBr^{\bullet-} + H_2O$ | 100 |
| 109 | $C_2H_5Br$ | $3.6 \times 10^{-10}$ | 39% $HO^- + {}^{\bullet}C_2H_4Br$<br>61% $Br^- + C_2H_5O^{\bullet}$ | 100 |
| 142 | $CH_3I$ | $4.7 \times 10^{-10}$ | 43% $HO^- + {}^{\bullet}CH_2I$<br>30% $I^- + CH_3O^{\bullet}$<br>28% $HCI^{\bullet-} + H_2O$ | 100 |
| 156 | $C_2H_5I$ | $3.1 \times 10^{-10}$ | 42% $HO^- + {}^{\bullet}C_2H_4I$<br>52% $I^- + C_2H_5O^{\bullet}$<br>3% $C_2H_3I^{\bullet-} + H_2O$<br>3% $C_2H_4I^- + HO^{\bullet}$ [b] | 100 |

[a] In all cases, for simplicity's sake, the nominal mass of the naturally most abundant isotopomer is listed. [b] This product is written as $CH_4I^-$ in the original citation.

have been found to yield carbene radical anions upon reaction with the atomic oxygen radical anion (Table V).[144,151] Dawson and Nibbering[151] investigated the reaction of $O^{\bullet-}$ with propionitrile and butyronitrile and showed that the $(M - 2H)^{\bullet-}$ ions formed are carbene radical anions (that is, $O^{\bullet-}$ abstracts an $\alpha$-proton and an $\alpha$-hydrogen of the nitrile) by studying appropriately deuterated analogues. The authors also found that when the atomic oxygen radical anion is allowed to react with cyclopropanecarbonitrile (c-$C_3H_5CN$, 1), the for-

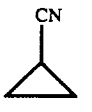

1

mation of an $(M - 2H)^{\bullet-}$ ion represented about half of the total reaction cross section. However, reaction of the $\alpha$-deuterium-labeled cyclopropanecarbonitrile with $O^{\bullet-}$ showed that the acidic hydrogen (the hydrogen on the carbon $\alpha$ to the cyano group) was retained in the ion product. Although subsequent studies of 2,2-dideuteriocyclopropanecarbonitrile were clouded by the difficulty of successfully eliminating contributions from incompletely labeled substrate molecules, the authors were able to conclude that for the most part (>90%), these stable $(M - 2H)^{\bullet-}$ ions are formed with high specificity, involving abstraction of the $H_2^{\bullet+}$ from the same corner of the ring (eq 44). In this same study, 1,2-dicyanoethane was found to yield $(M - 2H)^{\bullet-}$ as the major product ion from reaction with $O^{\bullet-}$.

**Scheme VI. The Chemical Processes Occurring When the Atomic Oxygen Radical Anion Reacts with Nitromethane**

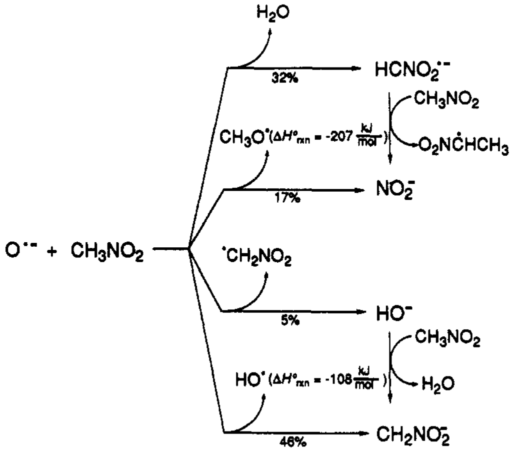

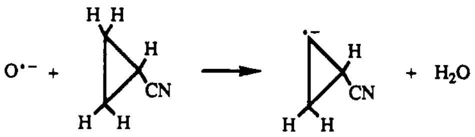

(44)

*d. Other.* The atomic oxygen radical anion reacts with trimethylphosphine rapidly ($k_{obs} = \sim 2 \times 10^{-9}$ $cm^3$ molecule$^{-1}$ $s^{-1}$, EFF = 0.7); in this case, however, the $(M - 2H)^{\bullet-}$ ion (eq 45c) is but a minor product. A novel pathway, that of alkyl radical displacement, is observed as a minor channel (eq 45d).[152]

$$O^{\bullet-} + Me_3P \rightarrow 55\%\ Me_2PCH_2^- + HO^{\bullet} \quad (45a)$$

$$\rightarrow 25\%\ HO^- + Me_2PCH_2^{\bullet} \quad (45b)$$

$$\rightarrow 10\%\ C_3H_7P^{\bullet-} + H_2O \quad (45c)$$

$$\rightarrow 10\%\ Me_2PO^- + Me^{\bullet} \quad (45d)$$

When $O^{\bullet-}$ is allowed to react with nitromethane,[145] the expected products corresponding to $H^+$ transfer, $H_2^{\bullet+}$ transfer, nucleophilic substitution, and $H^{\bullet}$ transfer are observed. Two of the primary product ions, $HO^-$ and $HCNO_2^{\bullet-}$, react in secondary processes (by proton abstraction and by displacement, respectively) with additional molecules of $CH_3NO_2$ (Scheme VI).

Noest and Nibbering examined the reaction of $O^{\bullet-}$ with a variety of aliphatic nitrites and found that with the exception of neopentyl nitrite ($(CH_3)_3CCH_2ONO$), the $NO_2^-$ ion was the major reaction product for all systems studied ($CH_3ONO$, $CH_3CH_2ONO$, $CH_3CH_2CH_2CH_2ONO$, $(CH_3)_3CONO$, $CH_3CH_2CH_2CH_2CH_2ONO$, and $(CH_3)_2CHCH_2CH_2ONO$). They concluded that for each nitrite, $NO_2^-$ formation resulted

**Scheme VII. The Pathways by Which the Atomic Oxygen Radical Anion Reacts with Alkyl Nitrites**

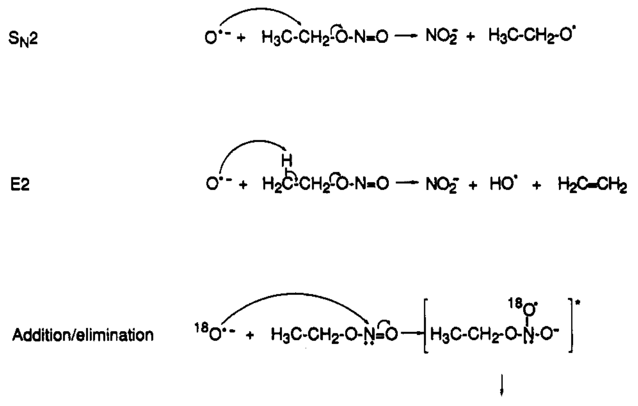

from one or all of the following three pathways: $S_N2$ displacement, E2 elimination, and/or addition–elimination (Scheme VII).[153] The reaction of $O^{\bullet-}$ with *tert*-butyl nitrite to produce the $NO_2^-$ ion probably proceeds primarily by E2 and/or $S_N2$, since labeling studies with $H^{18}O^-$ (which also produces $NO_2^-$ as a major product from this compound) show only 10% incorporation of the label into the $NO_2^-$. The labeling studies also indicate that $NO_2^-$ is produced from the reaction of $O^{\bullet-}$ with neopentyl nitrite, primarily through the addition–elimination reaction channel (pathway c, Scheme VII). These authors concentrated on $NO_2^-$ formation and did not discuss the presence (or lack) of an $H_2^{\bullet+}$ transfer pathway.

### 2. Ethers and Epoxides

Only a small number of ethers have been examined as to how they react with the atomic oxygen radical anion (Table VII). Dimethyl ether (300 K, flowing afterglow),[145] diethyl ether, and *p*-dioxane (low interaction energy, tandem mass spectrometer)[100] react with $O^{\bullet-}$ to give $HO^-$ as the exclusive product. The mechanistically reasonable reaction products for the $O^{\bullet-}/CH_3OCH_3$ process are shown in eq 46; the lack of

$$O^{\bullet-} + CH_3OCH_3 \rightarrow 0\%\ CH_3OCH^{\bullet-} + H_2O \qquad (46a)$$

$$\rightarrow 0\%\ CH_3OCH_2^- + HO^\bullet \qquad \Delta H^\circ_{rxn} = +104\ \mathrm{kJ\ mol^{-1}} \qquad (46b)$$

$$\rightarrow 100\%\ HO^- + CH_3OCH_2^\bullet \qquad \Delta H^\circ_{rxn} = -73.2\ \mathrm{kJ\ mol^{-1}} \qquad (46c)$$

$$\rightarrow 0\%\ CH_3O^- + CH_3O^\bullet \qquad \Delta H^\circ_{rxn} = -54.0\ \mathrm{kJ\ mol^{-1}} \qquad (46d)$$

an $S_N2$ process, even though it is substantially exothermic, is in accord with the extremely poor leaving group ability of alkoxides for displacements at saturated centers in the gas phase. As far as we are aware, the methoxy-substituted methylene radical anion is unknown in the gas phase; it might be anticipated that this species will have a very low (possibly negative) electron affinity.

**Table VII. Data for the Reaction of $O^{\bullet-}$ with Amines and Ethers**[a]

| neutral | $k_{obs}$ (cm$^3$ molecule$^{-1}$ s$^{-1}$) | ion product observed [and corresponding neutral] |
|---|---|---|
| | Amines | |
| $(CH_3)_2NH$ | $5.5 \times 10^{-10}$ | $HO^- + [M - H]^\bullet$ |
| $CH_3CH_2NH_2$ | $5.9 \times 10^{-10}$ | $HO^- + [M - H]^\bullet$ |
| $(CH_3)_3NH$ | $6.0 \times 10^{-10}$ | $HO^- + [M - H]^\bullet$ |
| $(CH_3)_2CHNH_2$ | $3.6 \times 10^{-10}$ | $HO^- + [M - H]^\bullet$ |
| | Ethers | |
| $CH_3CH_2OCH_2CH_3$ | $7.1 \times 10^{-10}$ | $HO^- + [M - H]^\bullet$ |
| $OCH_2CH_2OCH_2CH_2$ | $5.7 \times 10^{-10}$ | $HO^- + [M - H]^\bullet$ |

[a] See ref 100.

Dawson and Nibbering[155] have examined, in an ICR, the reactions of $O^{\bullet-}$ (formed from nitrous oxide) with ethylene and propylene oxides. Using $^{18}O^{\bullet-}$, these authors showed that carbon-containing ionic products result exclusively from proton abstraction followed by either ring opening or ring opening with $H_2$ loss. In contrast to the products shown in eq 47, $HO^-$ reacts with ethylene oxide[156] to yield a single ion, $O{=}CH{-}CH_2{-}O^-$ (nucleophilic ring opening followed by $H_2$ loss). The major product in the ICR mass spectrum of the nitrous oxide/propylene oxide system is *m/z* 57 ($(M - H)^-$), the same species observed for the $HO^-$ reaction.[156] Lesser amounts of *m/z* 41 ($HC{\equiv}CO^- + HO^\bullet + CH_4$) and *m/z* 55 ($CH_3C{\equiv}CO^- + HO^\bullet + H_2$) are formed, presumably in processes analogous to eq 47c for ethylene oxide. The additional fragmentation pathways observed for the $O^{\bullet-}$ reactions, compared to the $HO^-$ reactions, despite the fact that $O^{\bullet-}$ is a weaker base, might not necessarily indicate a new chemical pathway for the atomic oxygen reactions since the $HO^-$ and $O^{\bullet-}$ reactions were run under different interaction energies. If the differences between the $O^{\bullet-}$ and $HO^-$ with a common epoxide persist under identical interaction conditions, then one must reconsider the proposed common mechanism involving initial proton abstraction. A likely alternative is initial H-atom abstraction for the atomic oxygen radical anion reaction; a consequence of this latter mechanism would be that the *m/z* 41 ion found in the propylene oxide reaction (for example) would correspond to $H_2O$ and $CH_3^\bullet$ neutral products rather than $HO^\bullet$ and $CH_4$.

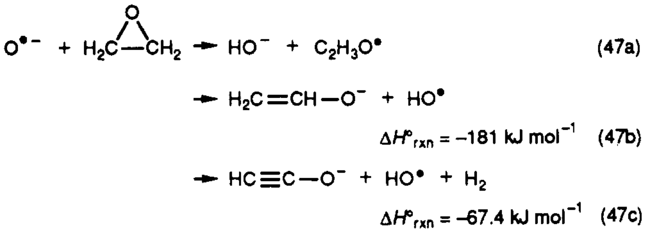

### 3. Amines (Nitrene Radical Anions)

Only a small amount of work has been reported concerning the reaction of the atomic oxygen radical anion with amines (Table VII); ammonia has been discussed in the binary hydride section above. Futrell and Tiernan[100] reported $HO^-$ as the exclusive product from several simple aliphatic amines in a tandem mass spectrometer. de Koning and Nibbering[87] found 19 times as much $HO^-$ as $DO^-$ in the reaction of $O^{\bullet-}$ with $CD_3NH_2$ in an ICR; thus it appears that preferential abstraction of an amino hydrogen occurs rather than that of a carbon-bound hydrogen $\alpha$ to the amino group despite the thermochemical preference for the latter result. There are no reports of nitrene radical anions being formed from the atomic oxygen radical anion reacting with simple aliphatic amines. de Koning and Nibbering, however, did note an intriguing trace (6%) product ion from the reaction of $O^{\bullet-}$ with methylamine, ethylamine, and dimethylamine: $H_2O^{\bullet-}$, which they describe as "a hydroxide ion to which a hydrogen atom is attached". Observation of $HDO^{\bullet-}$ from $O^{\bullet-}$ and $CD_3NH_2$ proves that a hydrogen atom is lost from both the amino group and the methyl group.

Several preliminary experiments carried out on a flowing afterglow indicate that a fragmentation pathway analogous to that suggested by Houriet et al. for the alcohols (vide infra) is at best a trace pathway for the room temperature reaction of $O^{\bullet-}$ with $(CH_3)_2CHNH_2$: $HO^-$ is the major product ion while $H_2C{=}CH{-}NH^-$ and $H_2C{=}C(CH_3){-}NH^-$ are but minor product ions.

In contrast to the aliphatic amines, anilines provide sizeable yields of $(M - 2H)^{\bullet-}$ products upon reaction with $O^{\bullet-}$. For example, Lin,[157] using a flowing afterglow, found that $O^{\bullet-}$ reacts rapidly with aniline itself, giving the yields indicated in eq 48 while 4-fluoroaniline yields

$$O^{\bullet-} + \text{Ph-NH}_2 \rightarrow 65\%\ \text{Ph-N}^{\bullet-} + H_2O \qquad \Delta H^\circ_{\text{rxn}} = -187\ \text{kJ mol}^{-1} \quad (48a)$$

$$\rightarrow 35\%\ \text{Ph-NH}^- + HO^\bullet \qquad \Delta H^\circ_{\text{rxn}} = -70.7\ \text{kJ mol}^{-1} \quad (48b)$$

$$\rightarrow 0\%\ HO^- + \text{PhNH}^\bullet \qquad \Delta H^\circ_{\text{rxn}} = -103\ \text{kJ mol}^{-1} \quad (48c)$$

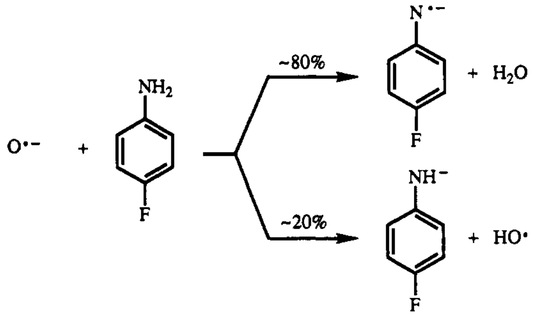

(49a)

(49b)

the data summarized in eq 49. It remains to be shown that the $(M - 2H)^{\bullet-}$ species detected for the anilines are in fact the corresponding nitrene radical anions as indicated or if they are isomeric species such as amino-substituted benzyne radical anion. If in fact the $(M - 2H)^{\bullet-}$ ions are aromatic nitrene radical anions, then the $O^{\bullet-}$ synthetic route is a good one because the yields are quite high. The gas-phase chemistry[158-160] and properties[161] of phenyl nitrene radical anion have been extensively studied; in all cases, however, the nitrene radical anion has been generated by dissociative electron ionization of phenyl azide.

### 4. Alcohols (Ketyl Radical Anions)

**Table VIII. Product Distributions and Bimolecular Rate Coefficients for the Reaction of $O^{\bullet-}$ with Alcohols[a]**

| neutral | | $k_{obs}$ (cm$^3$ molecule$^{-1}$ s$^{-1}$) | ion product observed [and corresponding neutral] | ref |
|---|---|---|---|---|
| mass | formula | | | |
| 32 | $CH_3OH$ | $2.5 \times 10^{-10}$ | 67% $HO^- + CH_3O^\bullet$<br>33% $CH_3O^- + HO^\bullet$ | 100 |
| 32 | $CH_3OH$ | | 75% $HO^- + CH_3O^\bullet$<br>25% $CH_3O^- + HO^\bullet$ | 154 |
| 33 | $CH_3OD$ | $2.0 \times 10^{-10}$ | 7% $HO^- + {}^\bullet CH_2OD$<br>61% $DO^- + CH_3O^\bullet$<br>32% $CH_3O^- + DO^\bullet$ | 100 |
| 33 | $CH_3OD$ | | 24% $HO^- + {}^\bullet CH_2OD$<br>52% $DO^- + CH_3O^\bullet$<br>25% $CH_3O^- + DO^\bullet$ | 154 |
| 35 | $CD_3OH$ | $2.0 \times 10^{-10}$ | 65% $HO^- + CD_3O^\bullet$<br>5% $DO^- + {}^\bullet CH_2OH$<br>30% $CD_3O^- + HO^\bullet$ | 100 |
| 36 | $CD_3OD$ | $1.7 \times 10^{-10}$ | 69% $DO^- + CD_3O^\bullet$<br>31% $CD_3O^- + DO^\bullet$ | 100 |
| 46 | $CH_3CH_2OH$ | $3.1 \times 10^{-10}$ | 41% $HO^- + CH_3CH_2O^\bullet$<br>23% $H_2C{=}CH{-}O^- + [H_3O]$<br>36% $CH_3CH_2O^- + HO^\bullet$ | 100 |
| 46 | $CH_3CH_2OH$ | | 53% $HO^- + CH_3CH_2O^\bullet$<br>11% $H_2C{=}CH{-}O^- + [H_3O]$<br>35% $CH_3CH_2O^- + HO^\bullet$ | 154 |
| 48 | $CH_3CD_2OH$ | $3.2 \times 10^{-10}$ | 37% $HO^- + CH_3CD_2O^\bullet$<br>2% $DO^- + CH_3C^\bullet DOH$<br>25% $H_2C{=}CD{-}O^- + [H_2OD]$<br>35% $CH_3CD_2O^- + HO^\bullet$ | 100 |
| 51 | $CD_3CD_2OH$ | $2.4 \times 10^{-10}$ | 29% $HO^- + CD_3CD_2O^\bullet$<br>10% $DO^- + CD_3C^\bullet DOH$<br>22% $D_2C{=}CD{-}O^- + [D_2OH]$<br>39% $CD_3CD_2O^- + HO^\bullet$ | 100 |

[a] In all cases, for simplicity's sake, the nominal mass of the naturally most abundant isotopomer is listed.

The interaction of the atomic oxygen radical anion with various alcohols has been examined by several workers, at differing, but not always clearly specified, interaction energies; some of these reactions, those in which all products have been clearly identified and yields measured, are tabulated in Table VIII. The data of Futrell and Tiernan[100] seem to suggest that for methanol (eq 50), ca. 90% of the H atoms that are transferred originate from the hydroxyl group (approximately 70% of the product forming interactions proceed by HAT). Houriet and co-workers[162,163] find that proton transfer (eq 50c) is the predominant process

$$O^{\bullet-} + CH_3OH \rightarrow HO^- + CH_3O^\bullet \qquad \Delta H^\circ_{\text{rxn}} = -28\ \text{kJ mol}^{-1} \quad (50a)$$

$$\rightarrow HO^- + {}^\bullet CH_2OH \qquad \Delta H^\circ_{\text{rxn}} = -69.5\ \text{kJ mol}^{-1} \quad (50b)$$

$$\rightarrow CH_3O^- + HO^\bullet \qquad \Delta H^\circ_{\text{rxn}} = -6.7\ \text{kJ mol}^{-1} \quad (50c)$$

$$\rightarrow e^- + H_2O + H_2C{=}O \qquad \Delta H^\circ_{\text{rxn}} = -257\ \text{kJ mol}^{-1} \quad (50d)$$

for *all* primary alcohols reacting with $O^{\bullet-}$ in an ICR, in contrast with the data shown in Table VIII. Furthermore, they report an $(M - D)^-$ species as the exclusive product from $O^{\bullet-}$ with $CH_3OD$. It is interesting that the HAT process is found by Futrell and Tiernan to be more important than proton transfer for methanol, since hydrogen atom transfers are often believed to have considerably higher activation barriers than proton transfers. Less surprising is the observation that the HAT process prefers the thermodynamically less favorable but kinetically more mobile hydroxyl hydrogen over the $\alpha$-carbon hydrogen. For ethanol, Futrell and Tiernan found that about 75% of the H atoms that are transferred originate from the hydroxyl group. One must be cautious in interpreting the apparent contradictions between the data in Table VIII and that reported by Houriet and co-workers since the branching fractions and rate coefficients for these $O^{\bullet-}/ROH$ reactions are likely to be extremely sensitive to the conditions under which the data were obtained. Some of the issues that must be explicitly addressed in resolving the apparent contradictions are as follows: (i) $HO^-$ undergoes extremely rapid proton abstraction reaction with alcohols so one must ensure that any possible opportunity for a first-formed $HO^-$ product ion to react with a second alcohol molecule is correctly considered when assigning product yields. (ii) The acidic hydrogen (deuterium) of alcohols exchanges rapidly with the walls of the apparatus adding additional uncertainty to branching fractions obtained from ROD compounds. (iii) The $O^{\bullet-}$ rate coefficients, and most likely the product yields as well, are a sensitive function of the temperature at which the reaction is run as well as the kinetic energy of the reactant ion; these values must be known precisely in order to compare data from different experiments. Further complicating this last issue is the excess kinetic energy imparted to the reactant $O^{\bullet-}$ during its formation by dissociative electron attachment (see section III) and the number of nonreactive collisions the $O^{\bullet-}$ experiences prior to reaction. It seems likely that an in-depth study of $O^{\bullet-}$ with methanol, under both thermally equilibrated (300 K) conditions and as a function of increased interaction energy ($T$ or $O^{\bullet-}$(KE)) would be particularly useful.

Houriet and co-workers[162] examined the reactions of $O^{\bullet-}$ with secondary and tertiary alcohols, as well as the primary alcohols, under conditions in an ICR where the $O^{\bullet-}$ formed from dissociative electron attachment to pure $N_2O$ is known to possess an average 0.4 eV of kinetic energy. They report that $HO^-$ is formed by a hydrogen atom transfer from the hydroxylic position, but give no yields of this product from the various alcohols examined. Simple proton transfer from the hydroxyl group is the major process observed for all primary and secondary alcohols. A third anionic product, $[ROH - 3H]^-$, is formed from all alcohols containing an $\alpha$-proton except methanol. This latter product, from the labeling studies, corresponds to loss of an $\alpha$- and a $\beta$-hydrogen atom from the alkoxide anion. For secondary and tertiary alcohols, a series of lower mass anions is also observed which correspond to loss of an $\alpha$-alkyl group and a $\beta$-hydrogen from the alkoxide anion.

The rather disparate observations concerning the products formed from the various alcohols are nicely explained by the reaction mechanism proposed by Houriet et al.; this mechanism is shown in generic form in Scheme VIII and for one specific molecule in Scheme IX. This mechanism predicts that a water molecule is formed from the reactant $O^{\bullet-}$, the hydroxylic proton, and a hydrogen $\beta$ to the hydroxyl oxygen. An $\alpha$-hydrogen atom or, more generally, an $\alpha$-radical is also lost, leading to the enolate ions observed.

In general, the atomic oxygen radical anion reacts rapidly with the alcohols, often giving proton transfer as the major product, but also yielding "fragment" ions that can be used to clearly identify all groups attached to the carbon bearing the hydroxyl group. There have been no reports of an $H_2^{\bullet+}$ transfer channel for the simple aliphatic alcohols; this lack is undoubtedly due to the fact that the ketyl radical anions that would be formed would be unbound anions. Thus while atomic oxygen radical ion negative ion chemical ionization can be used to generate mixtures of alkoxides and enolate anions as reactive intermediates, it is unfortunately not a source for the simple ketyl radical anions. For comparison purposes, the reaction exothermicities of the important channels available to the $O^{\bullet-}/CH_3CH_2OH$ system are shown in eq 51.

**Scheme VIII. A Generic Mechanism for the Reactions of the Atomic Oxygen Radical Anion with Alcohols**

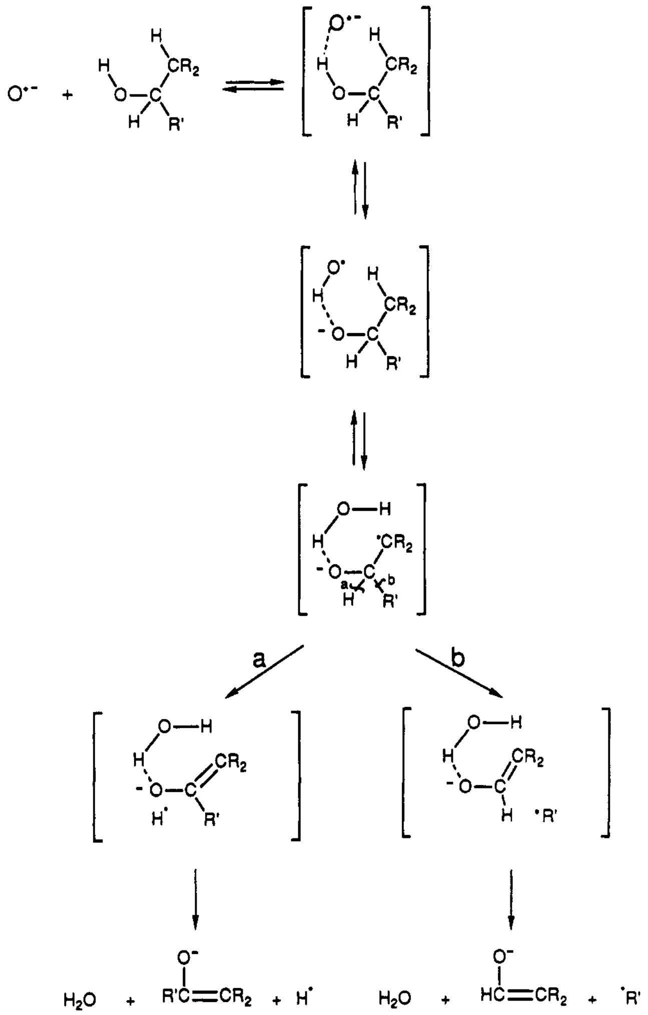

$$O^{\bullet-} + CH_3CH_2OH \rightarrow CH_3CH_2O^- + HO^\bullet \qquad \Delta H^\circ_{rxn} = -21\ \mathrm{kJ\ mol^{-1}} \quad (51a)$$

$$\rightarrow HO^- + CH_3CH_2O^\bullet \qquad \Delta H^\circ_{rxn} = -27\ \mathrm{kJ\ mol^{-1}} \quad (51b)$$

$$\rightarrow HO^- + CH_3H_2C^\bullet OH \qquad \Delta H^\circ_{rxn} = -77.0\ \mathrm{kJ\ mol^{-1}} \quad (51c)$$

$$\rightarrow H_2C{=}CH{-}O^- + H_2O + H^\bullet \qquad \Delta H^\circ_{rxn} = -61.5\ \mathrm{kJ\ mol^{-1}} \quad (51d)$$

### *5. Thiols (Thioketyl Radical Anions)*

The literature search we conducted found no published ion–molecule studies concerning the atomic

**Scheme IX. The Mechanism for the Reaction of the Atomic Oxygen Radical Anion with 2-Butanol**

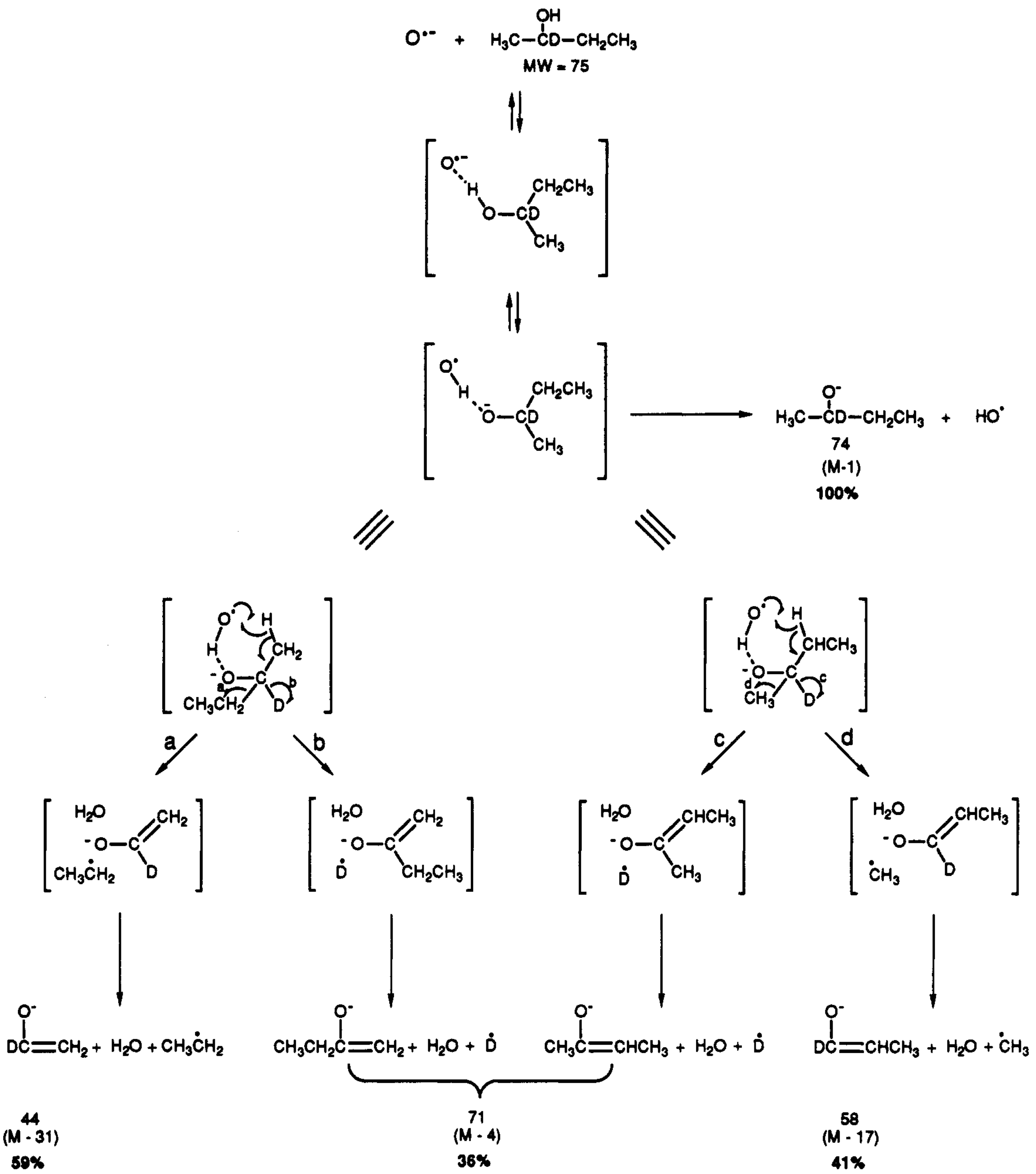

oxygen radical anion reacting with thiols; some information, however, is available from preliminary unpublished work from our laboratory. In a flowing afterglow, the atomic oxygen radical anion reacts with methanethiol to give $(M - H)^-$ and $(M - 2H)^{\bullet -}$ anions as the only product ions in nearly equal intensity.[164] Labeling studies using $CD_3SH$ lead to a 1:1 mixture of $m/z$ 50 $[(M - H)^-]$ and $m/z$ 48 $[(M - HD)^{\bullet -}]$. Unlike formaldehyde, thioformaldehyde is known to have a bound molecular anion ($EA[H_2C{=}S] = 0.465 \pm 0.023$ eV),[165] and thus both proton transfer and $H_2^{\bullet +}$ transfer channels generate stable anions, and both channels turn out to be highly exothermic (eq 52).

$$O^{\bullet -} + CH_3SH \rightarrow H_2C^{\bullet}S^- + H_2O \qquad \Delta H^{\circ}_{rxn} = -271 \text{ kJ mol}^{-1} \quad (52a)$$

$$\rightarrow CH_3S^- + HO^{\bullet} \qquad \Delta H^{\circ}_{rxn} = -106 \text{ kJ mol}^{-1} \quad (52b)$$

By far and away, the predominant product ion detected from the reaction of $O^{\bullet -}$ with ethanethiol in the flowing afterglow is that from simple proton transfer; only a trace amount (ca. 5%) of $(M - 2H)^{\bullet -}$ is observed. For $(CH_3)_2CHSH$, no $(M - 2H)^{\bullet -}$ is detected. One explanation for these results is that the electron affinities of the simple thioaldehydes decrease with increasing degree of alkyl substitution; weakly bound anions may undergo collisionally induced attachment in the flowing afterglow due to the large number of collisions experienced.

## B. Reactions with Alkenes and Alkynes

### 1. Ethylene (Vinylidene Radical Anion)

Vinylidene, $H_2C{=}C$, is the simplest member of a class of unsaturated carbenes which are postulated to be key reactive intermediates in some organic transformations.[166-171] Although this prototypical alkylidenecarbene is thought to be short-lived in the gas

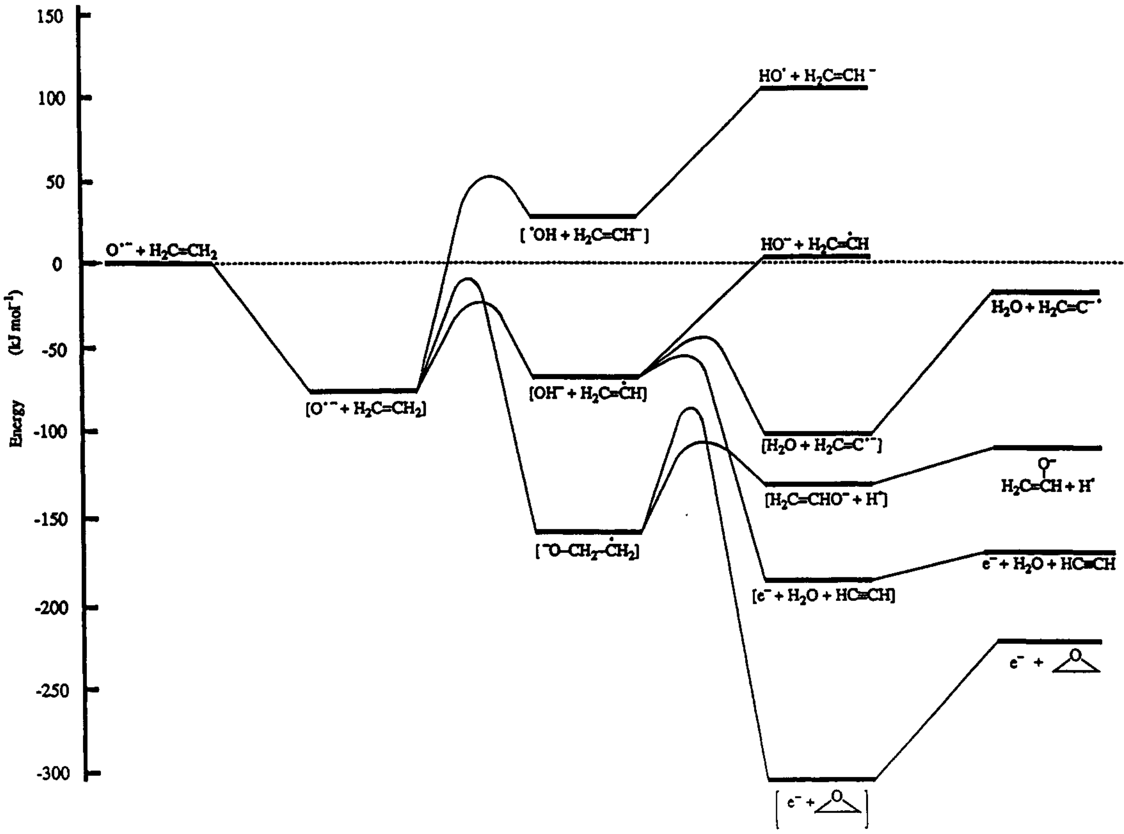

**Figure 3.** Energy level diagram showing relative energies of intermediates/products in the reaction of $O^{\bullet -}$ with $H_2C{=}CH_2$. Note that the formation the vinylidene radical anion, $H_2C{=}C^{\bullet -}$, probably forms via H-atom abstraction followed by proton abstraction, rather than the reverse, since the first step in the former pathway is ~2 kJ $mol^{-1}$ endothermic versus 100 kJ $mol^{-1}$ endothermic for proton transfer as the first step.

phase,[172,173] its anion, $H_2C{=}C^{\bullet -}$, is a stable gas-phase species.[144] The vinylidene radical anion is the major ion product formed when $O^{\bullet -}$ reacts with ethylene (eq 53, $k_{obs}$ = 1.0 × $10^{-9}$ $cm^3$ $molecule^{-1}$ $s^{-1}$; EFF = 0.66).[6,75,89,90,100,123,144,174]

$$O^{\bullet -} + H_2C{=}CH_2 \rightarrow 68\%\ e^- + c\text{-}C_2H_4O \qquad \Delta H^\circ_{rxn} = -213\ \mathrm{kJ\ mol^{-1}} \quad (53a)$$

$$\rightarrow 29\%\ H_2C{=}C^{\bullet -} + H_2O \qquad \Delta H^\circ_{rxn} = -38\ \mathrm{kJ\ mol^{-1}} \quad (53b)$$

$$\rightarrow 3\%\ H_2C{=}CHO^- + H^\bullet \qquad \Delta H^\circ_{rxn} = -109\ \mathrm{kJ\ mol^{-1}} \quad (53c)$$

$$\rightarrow 0\%\ HO^- + H_2C{=}CH^\bullet \qquad \Delta H^\circ_{rxn} = -13\ \mathrm{kJ\ mol^{-1}} \quad (53d)$$

Goode and Jennings[174] found that the reaction of $O^{\bullet -}$ with $H_2C{=}CD_2$ yielded ions at m/z 26 and 28, corresponding to $H_2C{=}C^{\bullet -}$ and $D_2C{=}C^{\bullet -}$, but yielded no products at m/z 27, which would correspond to $C_2HD^{\bullet -}$. These results clearly show that in reaction 53b, the two hydrogen atoms are removed from the same carbon atom of the ethylene molecule. Further evidence that both hydrogen atoms are removed from the same carbon is provided by the observation that the reaction of $O^{\bullet -}$ with $H_2C{=}CF_2$ yields a peak at m/z 62, corresponding to $F_2C{=}C^{\bullet -}$.[144,174-176] $H_2^{\bullet +}$ abstraction leading to the formation of $H_2C{=}C^{\bullet -}$ from ethylene probably proceeds in a stepwise fashion in which thermodynamics dictate that the hydrogen atom abstraction must occur before the proton abstraction since initial proton abstraction from ethylene is 100 kJ $mol^{-1}$ endothermic, whereas initial hydrogen atom abstraction from ethylene is only 2 kJ $mol^{-1}$ endothermic. A reaction coordinate diagram that presents all the chemically reasonable processes is shown in Figure 3.[13] While the barrier heights in Figure 3 are qualitative estimates only, they rationalize a large amount of experimental data, including that obtained from examining the reaction of the products.

Study of the chemical reactivity of the vinylidene radical anion has provided various important thermochemical values. Guo and Grabowski, via flowing afterglow acidity bracketing studies, concluded that $\Delta H^\circ_{acid}[H_2C{=}CH^\bullet]$ = 1611 ± 13 kJ $mol^{-1}$.[6] From this experimental acidity of the vinyl radical and appropriate thermochemical data from the literature, they were also able to derive an estimate of the heat of formation of the vinyl radical, of the C–H bond dissociation energy in ethylene, and of the C–H bond dissociation energy in the vinyl radical. Lineberger and co-workers subsequently confirmed these values as part of their study of the bond strengths of ethylene and acetylene using data derived from negative ion photoelectron spectroscopy and gas-phase proton transfer experiments.[171]

The reactivity of the vinylidene radical anion with several molecules has been reported (e.g., with $N_2O$, the conjugate base of acetonitrile is formed;[6,177] with CO, rapid associative detachment occurs[6]); these reactions can be studied because of the ease of gas-phase synthesis of $H_2C{=}C^{\bullet -}$ via the reaction of $O^{\bullet -}$ with

$H_2C{=}CH_2$. One particularly interesting reaction is that of $H_2C{=}C^{\bullet-}$ and dioxygen. This reaction was first studied in 1975 by Lindinger et al.,[89] who found that the vinylidene radical anion undergoes charge transfer with $O_2$ ($k_{obs} = 3.0 \times 10^{-10}$ cm$^3$ molecule$^{-1}$ s$^{-1}$; EFF = 0.33). The rate coefficient increased when the relative kinetic energy of the reactants was increased, suggesting that the reaction is slightly endothermic, or that EA[$H_2C{=}C$] ≥ EA[$O_2$]. The electron affinity of vinylidene was subsequently determined to be 0.490 ± 0.006 eV,[171,178] and in fact is slightly greater than that of $O_2$ (0.451 ± 0.007 eV).[126,179] Studies by Guo and Grabowski[6] showed that the reaction of $H_2C{=}C^{\bullet-}$ and $O_2$ yielded $O_2^{\bullet-}$ (major channel), $HC{\equiv}C^-$, and an ion with a mass-to-charge ratio of 41, which the authors proposed to be the conjugate base of ketene[180] (see Scheme X). SIFT experiments carried out by Viggiano et al.[181] in which $D_2CC^{\bullet-}$ was injected and allowed to react with $O_2$ were interpreted to indicate that the products are $O_2^{\bullet-}$ (~50%), $e^-$ (~25%), $O^{\bullet-}$ (19%), $DC{\equiv}C^-$ (3%), $DC{\equiv}CO^-$ (1%), and $DO^-$ (trace) as products of the reaction. The lack of detection of the $O^{\bullet-}$-producing channel in the flowing afterglow studies is presumably due to the high concentration of ethylene present (i.e., the product $O^{\bullet-}$ is instantly quenched as depicted in eq 54).

**Scheme X. The Mechanism for the Reaction of the Vinylidene Radical Anion with Dioxygen** (reprinted from ref 6; copyright 1990 Elsevier Science Publishers, B.V.)

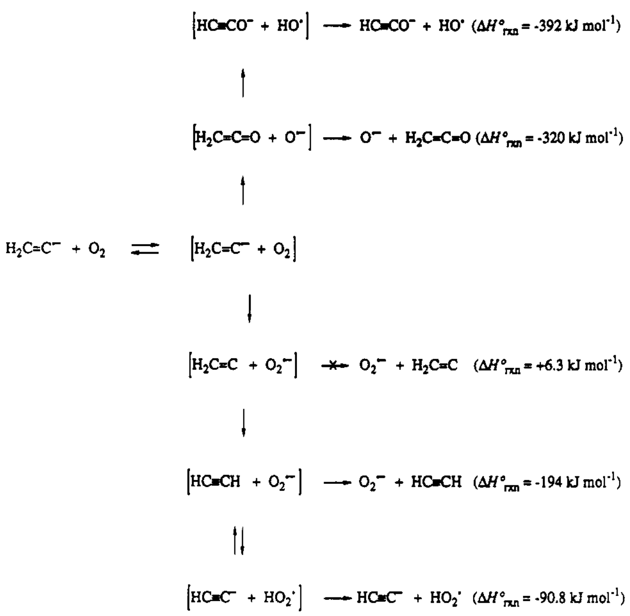

Viggiano and Paulson[123] have examined how temperature affects the total rate coefficient for the $O^{\bullet-}$ + $H_2C{=}CH_2$ reaction as well as the product distribution. Unlike the reaction of $O^{\bullet-}$ with $HC{\equiv}CH$ (vide infra), which has a $k_{obs}$ independent of $T$, the total rate coefficient for ethylene shows a negative temperature dependence, $k_{obs}(T) = (9.0 \times 10^{-10})(300/T)^{0.43}$ cm$^3$ molecule$^{-1}$ s$^{-1}$. Also, in contrast to the acetylene reaction, where the product distribution changed significantly with temperature, the ethylene reaction gave the same product distribution at all temperatures (eq 54; the data to the right of the chemical reactions in eq 54 are the product yields at interaction energies defined by 140, 294, and 494 K).[123]

$$\begin{array}{llllll} & & 140\text{ K} & 294\text{ K} & 494\text{ K} & \\ O^{\bullet-} + H_2C{=}CH_2 & \rightarrow e^- + C_2H_4O & 65\% & 68\% & 57\% & (54a) \\ & \rightarrow H_2C{=}C^{\bullet-} + H_2O & 34\% & 29\% & 40\% & (54b) \\ & \rightarrow H_2C{=}CH{-}O^- + H^\bullet & 1\% & 3\% & 3\% & (54c) \end{array}$$

### 2. Acetylene

Parkes,[90] using a drift tube under near thermal energy conditions, found three product channels for the interaction of $O^{\bullet-}$ with $HC{\equiv}CH$ (eq 55) and a total reaction rate coefficient of $2.18 \times 10^{-9}$ cm$^3$ molecule$^{-1}$ s$^{-1}$. The dominance of the direct proton transfer

$$O^{\bullet-} + HC{\equiv}CH \rightarrow 59\%\ e^- + C_2H_2O \qquad (55a)$$

$$\rightarrow 37\%\ HC{\equiv}C^- + HO^\bullet \quad \Delta H^\circ_{rxn} = -23\ \text{kJ mol}^{-1} \qquad (55b)$$

$$\rightarrow 4\%\ HC{\equiv}C{-}O^- + H^\bullet \quad \Delta H^\circ_{rxn} = -169\ \text{kJ mol}^{-1} \qquad (55c)$$

pathway 55b over the substitution pathway 55c is in accord with many other reactions reported herein; however, the most abundant pathway, associative detachment, is perhaps somewhat surprising since the obvious neutral product, ketene, would require a 1,2-H-atom transfer within the ion formed from the addition of $O^{\bullet-}$ to $HC{\equiv}CH$. Futrell and Tiernan[100] reported that $O^{\bullet-}$ reacts with acetylene with a total rate coefficient of $1.23 \times 10^{-9}$ cm$^3$ molecule$^{-1}$ s$^{-1}$ and that the products are 87% proton transfer (eq 55b), 9% H-atom replacement (eq 55c), 3% $H_2^+$ transfer (forming $C_2^{\bullet-}$ + $H_2O$), and 1% H-atom abstraction (forming $HO^-$ + $HC{\equiv}C^\bullet$). Goode and Jennings, using an ICR, found a relative rate ratio of ~17 for reactions 55b–c and a total rate coefficient of $9.1 \times 10^{-10}$ cm$^3$ molecule$^{-1}$ s$^{-1}$, but note that in their studies, the reactant ion is probably best characterized as having 0.4 eV excess kinetic energy due to its being formed from dissociative electron detachment to nitrous oxide under low-pressure conditions.[174,182]

Stockdale and co-workers have investigated the products and rates of reaction of $O^{\bullet-}$ with acetylene in the $O^{\bullet-}$ energy range of 0–2 eV.[75] In part, these authors report rate coefficients for a large number of reactions in which the source of $O^{\bullet-}$ *and therefore its energy* was varied. Substantial variation in measured rate coefficients were found for the relatively small energy changes considered (0–2 eV). For example, a plot of $k_{obs}$ for the production of acetylide from $O^{\bullet-}$ and $HC{\equiv}CH$ versus the most probable energy of the $O^{\bullet-}$ reactant ion (formed from $N_2O$, NO, and $O_2$) shows a positive energy dependence; their data for this reaction is reproduced in Table IX. Note that the energy dependence observed by Stockdale and co-workers of increasing rate of proton transfer as the interaction energy increases has since been confirmed by variable temperature studies of the $O^{\bullet-}$ + $HC{\equiv}CH$ reaction by Viggiano and Paulson (vide infra).

Bohme[183] and Viggiano and Paulson[123] have both measured the rate coefficient and branching ratio for reaction 56 in flow tube devices at room temperature (296 and 294 K, respectively) and obtained essentially

**Table IX. Data on the Reaction $O^{\bullet-}$ + HC≡CH → HC≡$C^-$ + $HO^\bullet$ in the Energy Region between 0 and 2 eV**[a]

| source of $O^{\bullet-}$ | $O^{\bullet-}$ energy (eV) | rate coefficient ($cm^3$ $molecule^{-1}$ $s^{-1}$) |
|---|---|---|
| Using Protio Acetylene (HC≡CH) | | |
| $O^{\bullet-}/NO_2$, 1st peak | ≤0.3 | $(1.4 \pm 0.3) \times 10^{-9}$ |
| $O^{\bullet-}/NO_2$, 2nd peak | | $(2.4 \pm 0.7) \times 10^{-9}$ |
| $O^{\bullet-}/NO_2$, 3rd peak | | $(1.3 \pm 0.4) \times 10^{-9}$ |
| $O^{\bullet-}/N_2O$ | 0.39 | $(2.6 \pm 0.8) \times 10^{-9}$ |
| $O^{\bullet-}/NO$ | 0.8 | $(1.9 \pm 0.6) \times 10^{-9}$ |
| $O^{\bullet-}/O_2$ | 1.6 | $(4.2 \pm 1.3) \times 10^{-9}$ |
| Using Deuterio Acetylene (DC≡CD) | | |
| $O^{\bullet-}/NO_2$, 1st peak | ≤0.3 | $(7.8 \pm 2.0) \times 10^{-10}$ |
| $O^{\bullet-}/NO_2$, 2nd peak | | $(1.0 \pm 0.3) \times 10^{-9}$ |
| $O^{\bullet-}/NO_2$, 3rd peak | | $(8.6 \pm 3.0) \times 10^{-10}$ |
| $O^{\bullet-}/N_2O$ | 0.39 | $(1.8 \pm 0.6) \times 10^{-9}$ |
| $O^{\bullet-}/NO$ | 0.8 | $(2.5 \pm 0.8) \times 10^{-9}$ |
| $O^{\bullet-}/O_2$ | 1.6 | $(3.2 \pm 1.0) \times 10^{-9}$ |

[a] Reference 75.

identical results (their combined results are summarized in eq 56) which are fairly similar to those reported by Parkes (eq 55).[90]

$$O^{\bullet-} + HC{\equiv}CH \rightarrow 59\%\ e^- + C_2H_2O \qquad (56a)$$

$$\rightarrow 33\%\ HC{\equiv}C^- + HO^\bullet \qquad \Delta H^\circ_{rxn} = -23\ kJ\ mol^{-1} \qquad (56b)$$

$$\rightarrow 4\%\ HC{\equiv}C{-}O^- + H^\bullet \qquad \Delta H^\circ_{rxn} = -169\ kJ\ mol^{-1} \qquad (56c)$$

$$\rightarrow 4\%\ C_2^{\bullet-} + H_2O \qquad \Delta H^\circ_{rxn} = -72.8\ kJ\ mol^{-1} \qquad (56d)$$

Viggiano and Paulson have also reported the temperature dependence of the total rate coefficient and the branching ratio of the reaction of the atomic oxygen radical anion with acetylene.[123] The total rate coefficient remains essentially unchanged over the three temperatures examined ($1.85 \times 10^{-9}$, $1.90 \times 10^{-9}$, and $2.07 \times 10^{-9}$ $cm^3$ $molecule^{-1}$ $s^{-1}$ at 140, 294, and 494 K, respectively). The product distribution (eq 57) shows that the associative detachment channel decreases with increasing temperature and is exactly compensated for by an increase in the proton transfer process; the other two channels (eq 57c,d) display no temperature sensitivity.

| | 140 K | 294 K | 494 K | |
|---|---|---|---|---|
| $O^{\bullet-}$ + HC≡CH → $e^-$ + $C_2H_2O$ | 82% | 59% | 45% | (57a) |
| → HC≡$C^-$ + $HO^\bullet$ | 12% | 33% | 46% | (57b) |
| → HC≡C—$O^-$ + $H^\bullet$ | 5% | 4% | 6% | (57c) |
| → $C_2^{\bullet-}$ + $H_2O$ | 1% | 4% | 3% | (57d) |

### *3. Allene and Propyne (Propadienylidene and Propargylidene Radical Anions)*

Dawson et al. found that when $O^{\bullet-}$ was allowed to react with allene in an ICR spectrometer the major ionic product was that from $H_2^{\bullet+}$ transfer.[144] Subsequent studies by Grabowski et al.[175] revealed that in the flowing afterglow, the reaction of $O^{\bullet-}$ with allene resulted in two distinct ions, corresponding to $H^+$ transfer (25%) and $H_2^{\bullet+}$ transfer (75%); furthermore, the concentrations of these two products changed as a function of the extent of the initial reaction. The product distribution corrected to zero secondary reaction is that noted above; as the reaction was allowed to proceed, however, and the product ions were given ample time to react with a second equivalent of allene, the yield of the *m/z* 38 ion dropped while a simultaneous, proportionate increase in *m/z* 39 was observed. The yields leveled out to approximately 65% $C_3H_2^{\bullet-}$ and 35% $C_3H_3^-$; the workers proposed that two isomeric $C_3H_2^{\bullet-}$ ions were being formed in the initial reaction between $O^{\bullet-}$ and allene, and that the minor $C_3H_2^{\bullet-}$ ion product was basic enough to deprotonate allene, but that the major $C_3H_2^{\bullet-}$ ion product was not (eq 58). They suggested that one product ion is the propargylidene radical anion (HC≡C—$CH^{\bullet-}$) and that the other is the propadienylidene radical anion ($H_2C$=C=$C^{\bullet-}$). Interestingly, a very early flowing afterglow study of $O^{\bullet-}$ with allene indicated that only two product ions are formed: those corresponding to proton abstraction (HC≡C—$CH_2^-$) and to H-atom abstraction ($HO^-$).[184] Although no signal corresponding to $H_2^{\bullet+}$ abstraction was observed in this early study, the authors did see an ion at *m/z* 41, $HC_2O^-$, which they attributed to the reaction of $C_3H_3^-$ with $O_2$ (eq 59); the dioxygen was present since it was the precursor gas used to generate the atomic oxygen radical anion. The lack of observation of $C_3H_2^{\bullet-}$ in this early study may be due to its fast reaction with the dioxygen in the system. Fast reaction with dioxygen has been observed for both the vinylidene radical anion[6] as well as the *o*-benzyne radical anion (see sections V.B and C).[7] Such complications of product ions reacting with the neutral used to produce the initial reacting ion are not unknown in ion–molecule studies; although they cause problems infrequently, they are of particularly serious concern in $O^{\bullet-}$ studies.

$$O^{\bullet-} + H_2C{=}C{=}CH_2 \rightarrow 65\%\ C_3H_2^{\bullet-}\ (\text{isomer one}) + H_2O \qquad (58a)$$

$$\rightarrow 10\%\ C_3H_2^{\bullet-}\ (\text{isomer two}) + H_2O \qquad (58b)$$

$$\rightarrow 25\%\ HC{\equiv}C{-}CH_2^- + HO^\bullet \qquad (58c)$$

$$C_3H_3^- + O_2 \rightarrow H{-}C{\equiv}C{-}O^- + H_2C{=}O \qquad (59)$$

In their studies of $O^{\bullet-}$ with propyne-$d_3$ [(trideuteriomethyl)acetylene], Dawson et al.[185] observed four major, distinct ionic products with *m/z* 39–42 as well as two minor products with *m/z* 25 and 41. They concluded that two of the major ions corresponded to $H_2^{\bullet+}$ or $HD^{\bullet+}$ transfer (eq 60a,b) and that the other two major ions corresponded to $H^+$ or $D^+$ transfer (eq 60c,d). Note that the heats of reaction in eq 60 are for the all-protio compounds. Thus, when the atomic oxygen radical anion is allowed to react with propyne, two isomeric $C_3H_2^{\bullet-}$ ions are formed from $H_2^{\bullet+}$ transfer; these are the same ions proposed as products in the allene reaction. Likewise, two isomeric $C_3H_3^-$ ions are formed from $H^+$ transfer, as has been previously reported for closed-shell bases deprotonating propyne.[186] The minor

$$\mathrm{O^{\bullet-} + D_3C{-}C{\equiv}C{-}H \rightarrow DC{\equiv}C{-}CH^{\bullet-} + D_2O} \quad (60a)$$

$$\mathrm{\rightarrow D_2C{=}C{=}C^{\bullet-} + HOD} \quad (60b)$$

$$\mathrm{\rightarrow HC{\equiv}C{-}CD_2^{-} + DO^{\bullet}} \quad (60c)$$

$$\mathrm{\rightarrow D_3C{-}C{\equiv}C^{-} + HO^{\bullet}} \quad \Delta H^{\circ}_{\mathrm{rxn}} = -4.6\ \mathrm{kJ\ mol^{-1}} \quad (60d)$$

$$\mathrm{\rightarrow H{-}C{\equiv}C{-}O^{-} + D_3C^{\bullet}} \quad \Delta H^{\circ}_{\mathrm{rxn}} = -200\ \mathrm{kJ\ mol^{-1}} \quad (60e)$$

$$\mathrm{\rightarrow H{-}C{\equiv}C^{-} + CD_3O^{\bullet}} \quad \Delta H^{\circ}_{\mathrm{rxn}} = -5.0\ \mathrm{kJ\ mol^{-1}} \quad (60f)$$

products in the reaction of $O^{\bullet-}$ with propyne were attributed to $O^{\bullet-}$-addition/radical loss (eq 60e,f).

Karnett and Cross have reported on their crossed-beam studies of the reaction of $O^{\bullet-}$ with allene over the relative energy range of 4.6–10.8 eV in which the reaction mechanism is best described as a spectator-stripping process; in contrast with the thermally equilibrated reactions, they found no evidence of carbanionic products in this energy region.[187]

### *4. Other Alkenes and Alkynes*

Bohme and Young, who were perhaps the first to study the reaction of $O^{\bullet-}$ with propene, reported two major reaction pathways, corresponding to proton transfer (yielding $H_2C{=}CH{-}CH_2^- + HO^{\bullet}$) and H atom transfer (yielding $HO^- + H_2C{=}CH{-}CH_2^{\bullet}$).[184] Since the proton transfer is 35 kJ mol$^{-1}$ *endothermic*, the observed allyl anion could not have been formed from the thermally equilibrated $O^{\bullet-}$ reaction to which Bohme and Young attributed it. Jennings and co-workers reported the same products in their ICR studies of $O^{\bullet-}$ with propene;[144,174] they also investigated the $NO_2/D_3C{-}CH{=}CH_2$ and the $NO_2/H_3C{-}CH{=}CD_2$ labeled systems and found that the proton is removed exclusively from the methyl group in the proton transfer channel, but that hydrogen atom abstraction is a more random process. In later studies, Dawson et al.[140] found that additional ions were produced in the $O^{\bullet-}$/propene system in very small proportions: $C_3H_4^{\bullet-}$, $CH_3C(O^-){=}CH_2$, and $CH_3CH{=}CHO^-$. Recently, Grabowski et al. reexamined the reaction in their flowing afterglow[175] and observed two primary reaction pathways, corresponding to H-atom transfer and $H_2^{\bullet+}$ transfer (eq 61). It should be kept in mind that these

$$\mathrm{O^{\bullet-} + H_2C{=}CH{-}CH_3 \rightarrow 89\%\ HO^- + C_3H_5^{\bullet}} \quad \Delta H^{\circ}_{\mathrm{rxn}} = -100\ \mathrm{kJ\ mol^{-1}} \quad (61a)$$

$$\mathrm{\rightarrow 11\%\ C_3H_4^{\bullet-} + H_2O} \quad (61b)$$

$$\mathrm{\rightarrow 0\%\ H_2C{=}CH{-}CH_2^- + HO^{\bullet}} \quad \Delta H^{\circ}_{\mathrm{rxn}} = +35\ \mathrm{kJ\ mol^{-1}} \quad (61c)$$

are not necessarily conflicting data: the oxygen anions used in the flowing afterglow experiment are thermally equilibrated to 300 K, making pathway 61c inaccessible. The anions generated in the ICR may be at somewhat higher, unspecified energies, thus making the direct generation of allyl anion a distinct possibility. Furthermore, it is well known that any hydroxide produced from reaction of $O^{\bullet-}$ with $H_2C{=}CH{-}CH_3$ reacts rapidly in a secondary reaction with another molecule of propene, resulting in the production of allyl anion (this was observed in the recent FA studies). Some or all of the allyl anion product observed in the early studies could therefore be from this secondary reaction.

**Table X. Alkenes Which Yield $(M - 2H)^{\bullet-}$ Ions upon Reaction with $O^{\bullet-}$** [a]

| neutral | | |
|---|---|---|
| mass | formula | ref(s) |
| 28 | $H_2C{=}CH_2$ | 89,90,100,123,144,174 |
| 40 | $H_2C{=}C{=}CH_2$ | 144,175,185 |
| 42 | $H_2C{=}CH{-}CH_3$ | 140,175 |
| 46 | $CHF{=}CH_2$ | 144 |
| 53 | $NCCH{=}CH_2$ | 144,151,175 |
| 54 | $H_2C{=}CH{-}CH{=}CH_2$ | 144 |
| 56 | $H_2C{=}CH{-}CHO$ | 175 |
| 58 | $CH_3OCH{=}CH_2$ | 144 |
| 60 | $CH_3CF{=}CH_2$ | 144 |
| 62 | $H_2C{=}CHCl$ | 175 |
| 64 | $F_2C{=}CH_2$ | 144,174,175 |
| 67 | $H_2C{=}CHCH_2CN$ | 151 |
| 67 | $CH_3CH{=}CHCN$ | 151 |
| 67 | $H_2C{=}C(CH_3)CN$ | 151 |
| 69 | $CH_3CH{=}C(CH_3)CN$ | 151 |
| 81 | $(CH_3)_2C{=}CHCN$ | 151 |
| 81 | $H_2C{=}C(CH_3)CH_2CN$ | 151 |
| 95 | $(CH_3)_2C{=}C(CH_3)CN$ | 151 |
| 96 | $CF_3CH{=}CH_2$ | 144 |
| 110 | $CF_3CH_2C{=}CH_2$ | 144 |

[a] In all cases, for simplicity's sake, the nominal mass of the naturally most abundant isotopomer is listed.

The reactions of various other alkenes with $O^{\bullet-}$ have been studied[8,144,174,175,184] (Table X). Alkenes such as 1-butene, 2-butene, and isobutene have been found to undergo H-atom transfer and proton transfer, but not $H_2^{\bullet+}$ transfer.[144,184] Acrolein and vinyl chloride react rapidly with the atomic oxygen radical anion, but in neither case is the $H_2^{\bullet+}$ transfer pathway the major process.[175] Dawson and Jennings[144] found that when $O^{\bullet-}$ is allowed to react with methyl vinyl ether, $H_2^{\bullet+}$ transfer is the major reaction pathway. Work with $D_3COCH{=}CH_2$ showed that no deuterium atoms are lost, revealing that the product ion is most likely a vinylidene radical anion. In the reaction of $O^{\bullet-}$ with acrylonitrile, $H_2^{\bullet+}$ transfer is not the major process;[175] however, some $(M - 2H)^{\bullet-}$ ion *is* formed, and reaction of the atomic oxygen radical anion with $H_2C{=}CD{-}CN$ reveals that the two hydrogens are in fact abstracted from the terminal methylene group, thus forming a vinylidene-type radical anion.[151] While investigating the formation of $C_4H_4$ negative ions, Chou and Kass[8] found that methylenecyclopropane reacts with $O^{\bullet-}$ to form not only the vinylidene-type radical anion, but also the $(M - 2H)^{\bullet-}$ ions corresponding to $H_2^{\bullet+}$ abstraction from one corner of the ring (eq 62). These authors also found that reaction of $O^{\bullet-}$ with 1,2-butadiene, 1,3-butadiene, 1-butyne and 2-butyne all yield the $(M - 2H)^{\bullet-}$ ion as one of the products. Dawson and Nibbering[151] studied a variety of unsaturated nitriles and found that all yielded $(M - 2H)^{\bullet -}$ ions upon reaction with $O^{\bullet -}$, although that ion was not always the major product (Table X).

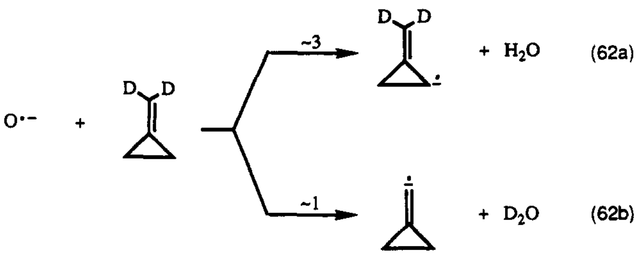

(62a)

(62b)

## C. Aromatic Compounds (Didehydroaromatic Radical Anions)

### 1. Benzene (o-Benzyne Radical Anion)

The benzyne radical anion, $o\text{-}C_6H_4^{\bullet -}$, is the major ion product formed when $O^{\bullet -}$ reacts with benzene.[29,75,100,188,189] Guo and Grabowski found that the overall reaction proceeds extremely rapidly ($k_{obs}$ = 2.0 × $10^{-9}$ cm$^3$ molecule$^{-1}$ s$^{-1}$; EFF = 0.96).[29] Of the anticipated reaction products, only two, $o\text{-}C_6H_4^{\bullet -}$ and $C_6H_5O^-$, have been directly observed (eq 63). Upon deuteration of

$$O^{\bullet -} + C_6H_6 \rightarrow 66\%\ C_6H_4^{\bullet -} + H_2O \qquad \Delta H^{\circ}_{rxn} = -40\ \text{kJ mol}^{-1} \quad (63a)$$

$$\rightarrow 34\%\ C_6H_5O^- + H^{\bullet} \qquad \Delta H^{\circ}_{rxn} = -138\ \text{kJ mol}^{-1} \quad (63b)$$

$$\rightarrow 0\%\ H^- + C_6H_5O^{\bullet} \qquad \Delta H^{\circ}_{rxn} = +4\ \text{kJ mol}^{-1} \quad (63c)$$

$$\rightarrow 0\%\ HO^- + C_6H_5^{\bullet} \qquad \Delta H^{\circ}_{rxn} = +0.8\ \text{kJ mol}^{-1} \quad (63d)$$

$$\rightarrow 0\%\ C_6H_5^- + HO^{\bullet} \qquad \Delta H^{\circ}_{rxn} = +77.4\ \text{kJ mol}^{-1} \quad (63e)$$

$$\rightarrow 0\%\ e^- + C_6H_5OH \qquad \Delta H^{\circ}_{rxn} = -287\ \text{kJ mol}^{-1} \quad (63f)$$

the benzene, the distribution of products change slightly: one observes 59% of the $D_2^{\bullet +}$-transfer product and 41% oxide ion formation (i.e., channels 63a,b respectively). Jennings and co-workers found that the reaction of $O^{\bullet -}$ with 1,3,5-trideuteriobenzene gave predominantly $HD^{\bullet +}$ transfer, indicating that the benzyne radical anion produced is almost entirely the ortho and/or para isomers.[188] Leopold et al. subsequently conducted photoelectron spectroscopic studies of the $C_6H_4^{\bullet -}$ and $C_6D_4^{\bullet -}$ ions produced in a flowing afterglow by the reaction of $O^{\bullet -}$ and benzene and perdeuteriobenzene.[9] Their results provided strong spectroscopic evidence that the main signal carrier (>98%) is in fact the o-benzyne isomer; in particular, both the electron affinity (EA[$o\text{-}C_6H_4$] = 0.560 ± 0.010 eV; EA[$o\text{-}C_6D_4$] = 0.551 ± 0.010 eV) and the o-benzyne singlet–triplet splitting (158 ± 2.5 kJ mol$^{-1}$) measured by the authors agreed with theoretical predictions.

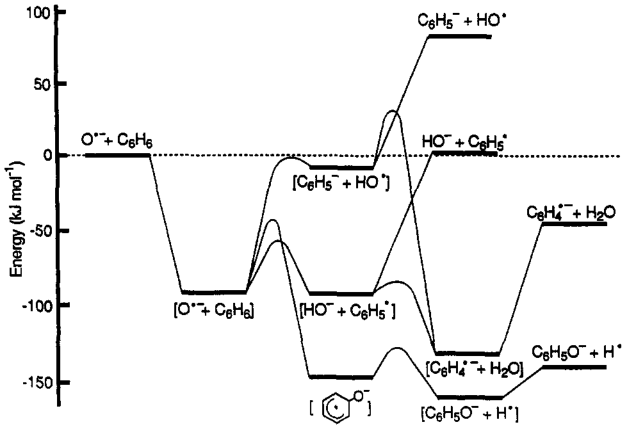

**Figure 4.** Schematic reaction energy diagram for the interaction of $O^{\bullet -}$ with $C_6H_6$. The horizontal dotted line marks the thermoneutral point while the dashed lines connecting starting materials, intermediates, and products are purely hypothetical but account for all the observations (reprinted from ref 29; copyright 1992 Elsevier Science Publishers B.V.).

Extensive studies on the reaction of $O^{\bullet -}$ with benzene (and related simple aromatic compounds), along with ion–molecule and physical studies of the products of this reaction, have enabled researchers to devise a reaction coordinate diagram (Figure 4) which explains the products observed and not observed in the $O^{\bullet -}$ plus $C_6H_6$ system.[29] Guo and Grabowski,[7] using flowing-afterglow bracketing studies, established the gas-phase acidity of the phenyl radical as $\Delta G^{\circ}_{acid}[C_6H_5^{\bullet}] = 1552^{+25}_{-13}$ kJ mol$^{-1}$, which yields $\Delta H^{\circ}_{acid}[C_6H_5^{\bullet}]$ = 1586 kJ mol$^{-1}$ (via $\Delta S^{\circ}_{acid}[C_6H_5^{\bullet}]$ = 25.7 cal mol$^{-1}$ K$^{-1}$), a value in accord with an FT-ICR study by Matimba et al. on the acidity of the phenyl radical and other substituted phenyl radicals.[190] Combination of this value with appropriate thermochemical data from the literature yields the important $\Delta H^{\circ}_{f\,298}[o\text{-}C_6H_4]$ = 439 kJ mol$^{-1}$. Guo and Grabowski also studied the reaction of $C_6H_4^{\bullet -}$ with $D_2O$, which underwent efficient and exclusive H/D exchange ($k_{obs}$ = (3.69 ± 0.27) × $10^{-10}$ cm$^3$ molecule$^{-1}$ s$^{-1}$; EFF = 0.166), which appeared to proceed predominantly via a single H-for-D exchange per benzyne radical anion–$D_2O$ collision.[7] With all this information in hand, the authors were able to compose the reaction coordinate diagram shown in Figure 4.[29] Each chemical conversion is initiated by formation of a long-lived ion–neutral complex between the $O^{\bullet -}$ and benzene, [$O^{\bullet -}$ + $C_6H_6$]. This complex can then react via four different chemical pathways. The first pathway is back-dissociation to reactants; return to separated products is deemed insignificant due to the high efficiency of the title reaction (EFF = 0.96). The three remaining pathways are (i) H-atom transfer to form [$HO^-$ + $C_6H_5^{\bullet}$], (ii) addition of $O^{\bullet -}$ to the aromatic ring to form the oxycyclohexadienyl radical anion, and (iii) proton transfer to form [$C_6H_5^-$ + $HO^{\bullet}$]. The reaction coordinate diagram (Figure 4) shows the pathways available to each of these complexes, with corresponding relative barrier heights, which account for all the observations in the $O^{\bullet -}$ plus benzene system. Further discussion of this reaction coordinate diagram can be found in the original citation.[29]

The reactivity of the o-benzyne radical anion (prepared by the reaction of $O^{\bullet -}$ with benzene) has been studied;[7] it is a highly reactive ion that not only undergoes rapid H/D exchange with water, but also displays a diverse set of reactions including electron transfer, $H_2^{\bullet+}$ abstraction, and direct addition. One particularly interesting direct addition reaction is that of the *o*-benzyne radical anion and carbon dioxide. The benzyne radical anion adds readily to $CO_2$ to give the addition complex $C_7H_4O_2^{\bullet-}$ ($k_{obs}$ = 3.5 × $10^{-10}$ $cm^3$ $molecule^{-1}$ $s^{-1}$ at a helium buffer gas pressure of 0.3–0.7 Torr, EFF = 0.47). This adduct is found to be unreactive toward additional equivalents of $CO_2$ or toward $D_2O$, but displays a variety of atom and group abstraction reactions; the $C_7H_4O_2^{\bullet-}$ product is most likely a distonic radical anion consisting of a phenyl radical and a carboxylate anion (eq 64).

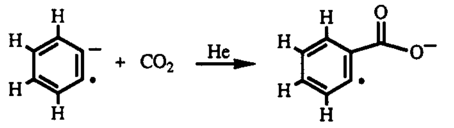

(64)

Stockdale et al.[75] investigated the nonthermal reaction of the atomic oxygen radical anion with benzene and perdeuteriobenzene using a pulsed source mass spectrometer. When $O^{\bullet-}$ was generated from $NO_2$ and was allowed to react with benzene, two major reaction pathways corresponding to $H_2^{\bullet+}$ transfer (57%) and oxide formation (43%) were observed (eq 63a,b; $k_{obs}$ = 1.9 × $10^{-10}$ $cm^3$ $molecule^{-1}$ $s^{-1}$; EFF = 0.09). These authors also saw minor $HO^-$ production, for which no rate coefficient was obtained. The reaction of $O^{\bullet-}$ generated from $NO_2$ with perdeuteriobenzene yielded the same ion products (60% $C_6D_4^{\bullet-}$, 40% $C_6D_5O^-$), but with a larger rate coefficient, $k_{obs}$ = 4.3 × $10^{-10}$ $cm^3$ $molecule^{-1}$ $s^{-1}$; EFF = 0.21. Studies by VanOrden et al.[189] on the $O^{\bullet-}$ with $C_6H_6$ reaction in an ICR spectrometer yielded a product distribution (13% $HO^-$, 48% $C_6H_4^{\bullet-}$, 39% $C_6H_5O^-$) similar to those found by Stockdale et al. but a rate coefficient ($k_{obs}$ = (1.5 ± 0.5) × $10^{-9}$ $cm^3$ $molecule^{-1}$ $s^{-1}$; EFF = 0.72) similar to that found by Guo and Grabowski. There is some discrepancy between the FA studies under thermally equilibrated conditions and those using other techniques. Two of the observations from the latter studies suggest that they are suprathermal in nature: the inverse isotope effect and the sizeable yield of the thermoneutral hydrogen atom transfer pathway.[29]

### 2. Alkyl Benzenes

Bruins et al.[188] looked at the reaction of $O^{\bullet-}$ and xylenes using an MS50 double-focusing mass spectrometer modified for negative ion operation. For the ortho and para isomers the major product was found to be the $(M - H)^-$ ion, with no other peak exceeding 10% of the intensity of this peak except the $(M - H + O)^-$ peak in the *p*-xylene reaction (16%). The meta isomer, however, gave $(M - 2H)^{\bullet-}$ as the base peak, with the $(M - H)^-$ peak being the second most major peak (81%). Deuterium labeling studies showed that the $(M - 2H)^{\bullet-}$ is formed by removal of a hydrogen atom or a proton from each of the methyl groups, thus forming a distonic radical anion. In accord with these observations, it was also found that the reaction of $O^{\bullet-}$ with 1,3,5-trimethylbenzene yields $(M - 2H)^{\bullet-}$ as the base peak with the only other peak of significant intensity being the $(M - H)^-$ peak (58%).

### 3. Other Substituted Benzenes

The reaction of $O^{\bullet-}$ with *o*-, *m*-, and *p*-fluorotoluenes was examined by Bruins et al.,[188] who noted that introduction of the fluorine atom into the toluene promoted the formation of an $(M - 2H)^{\bullet-}$ ion. Ingemann et al.[191] studied the reaction of $O^{\bullet-}$ with alkyl pentafluorophenyl ethers and found that in the reaction of $C_6F_5OCH_3$, one observes *ipso* substitution (on the carbon atom bearing the methoxy substituent), $S_N2$ on the methyl group, and "possible charge transfer"; an unambiguous assignment of mechanism, however, was not possible. Matimba et al.[190] conducted gas-phase ICR studies of the atomic oxygen radical anion with $C_6H_6$ as well as various $C_6H_6X$ compounds (X = F, Cl, CN). Their goal was to find the gas-phase acidities of the corresponding radicals, $C_6H_4X^{\bullet}$. They found that the reaction between $O^{\bullet-}$ and their $C_6H_5X$ compounds proceeded to some extent by $H_2^{\bullet+}$ transfer, which allowed them to estimate acidities of the radicals; their data revealed that the $C_6H_4X^{\bullet}$ radicals are much more acidic than their corresponding closed-shell parent compounds, as has been noted for many organic radicals previously.[143] However, the effect of the radical center on the acidity is less pronounced for these substituted compounds than for benzene. Furthermore, it was found that isomeric radical anions are formed from several of the $C_6H_5X$ compounds, since $H_2^{\bullet+}$ as well as $HD^{\bullet+}$ abstraction was observed for the reaction of $O^{\bullet-}$ with *p*-deuteriofluorobenzene, *p*-deuteriochlorobenzene, and *p*-deuteriobenzonitrile.

### 4. Pyridines

Bruins et al.[188] also studied the reaction of $O^{\bullet-}$ with 2-, 3-, and 4-methylpyridines. The three compounds showed "striking differences" in their spectra, yielding a wide range of products in different ratios. 2-Methylpyridine gives $(M - H + O)^-$ as the base peak; the 3-methyl and 4-methyl isomers both give $(M - H)^-$ as the major product. From study of the spectra produced by $O^{\bullet-}$ with (trideuteriomethyl)pyridines, the authors found that the $(M - H)^-$ ion is formed predominantly by proton transfer from the methyl groups, whereas the $H_2^{\bullet+}$ abstraction is less selective. Guo and Grabowski[29] studied the reaction of pyridine and pyridine-$d_5$ with $O^{\bullet-}$ and observed: (i) for pyridine, 46% $(M - 2H)^{\bullet-}$ and 54% $(M - H + O)^{\bullet-}$; (ii) for pyridine-$d_5$, 38% $(M - 2H)^{\bullet-}$ and 62% $(M - H + O)^{\bullet-}$, results consistent with their observations for the reaction of $O^{\bullet-}$ with benzene and the reaction coordinate diagram derived for it (Figure 4, vide supra).

### 5. 5-Membered Rings

Guo and Grabowski[29] allowed $O^{\bullet-}$ to react with furan, thiophene, pyrrole, and 1,3-cyclopentadiene. For furan, they observed 100% $(M - 2H)^{\bullet-}$; for thiophene, they observed 27% $(M - 2H)^{\bullet-}$, 4% $(M - H + O)^-$, and 69% $(M - H)^-$; for pyrrole, they observed 16% $(M - 2H)^{\bullet-}$, 3% $HO^-$, and 81% $(M - H)^-$; for cyclopentadiene, they observed 52% $(M - 2H)^{\bullet-}$, 8% $HO^-$, and 40% $(M - H)^-$. The furan system was the most novel since it was found that $(M - 2H)^{\bullet-}$ anions underwent detachment before the majority of them could be detected in the authors' flowing afterglow.

### *6. Naphthalenes*

VanOrden et al. examined the reactions (see section V.C.1) of the atomic oxygen radical anion with naphthalene and 2-methyl-, 1-chloro-, 2-chloro-, and 1-bromonaphthalene in an ICR spectrometer.[189] For the reaction of $O^{\bullet-}$ (generated from $N_2O$) with naphthalene ($k_{obs}$ = (2.1 ± 0.7) × $10^{-10}$ $cm^3$ $molecule^{-1}$ $s^{-1}$; EFF = 0.08), three pathways were observed, corresponding to H-atom transfer, $H_2^{\bullet+}$ transfer, and oxide formation (eq 65). 2-Methylnaphthalene was found to react by the same pathways, with an additional product resulting from proton transfer. The halogenated naphthalenes were found to react by similar pathways, with some additional products due to nucleophilic attack of $O^{\bullet-}$ at the halogen-bearing carbon.

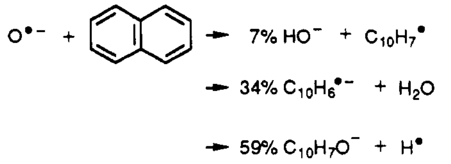

(65a)

(65b)

(65c)

## *VI. A Potpourri of Reactions*

### A. Aldehydes and Ketones

The reaction of $O^{\bullet-}$ with a variety of aldehydes and ketones has been studied by several groups.[13,99,100,145,155,192-196] One can envision four main pathways by which aldehydes can react with the atomic oxygen radical anion: $H_2^{\bullet+}$ transfer, $H^+$ transfer, H-atom transfer, and a carbonyl-addition/radical-displacement pathway. These pathways are demonstrated in Scheme XI for the reaction of $O^{\bullet-}$ with acetaldehyde, in which only the primary reactions are indicated.[145] When other aldehydes are allowed to react with the atomic oxygen radical anion, some or all of the above channels are observed (Table XI).[99,195] For example, when formaldehyde reacts with $O^{\bullet-}$, the two major product ions observed correspond to nucleophilic-addition/radical-displacement (eq 66a) and to H-atom abstraction (eq 66b).[99,194] For formaldehyde, proton transfer to $O^{\bullet-}$ is endothermic ($\Delta H^\circ_{acid}[H_2C{=}O]$ = 1646 kJ $mol^{-1}$) and $H_2^{\bullet+}$ transfer would lead to a species that would promptly autodetach (and hence if $H^{\bullet+}$ transfer occurs, it will not lead to any observable product).

$$O^{\bullet-} + H_2C{=}O \rightarrow HCO_2^- + H^\bullet \qquad \Delta H^\circ_{rxn} = -245 \text{ kJ mol}^{-1} \quad (66a)$$

$$\rightarrow HO^- + H{-}C^\bullet{=}O \qquad \Delta H^\circ_{rxn} = -91.2 \text{ kJ mol}^{-1} \quad (66b)$$

A similar set of reaction channels can be envisioned for the reaction of $O^{\bullet-}$ with ketones; these pathways are illustrated for acetone in Scheme XII. When Jennings et al. studied the reaction of $O^{\bullet-}$ with acetone in their ICR, they observed all the products shown in Scheme XII.[192] van der Wel and Nibbering also investigated the reaction of $O^{\bullet-}$ with acetone using their FT-ICR; although products corresponding to proton transfer, hydrogen atom transfer, and $H_2^{\bullet+}$ transfer were observed, the addition/elimination ($B_{AC}2$) product was not.[99] Perhaps the most interesting aspect of the $O^{\bullet-}$/acetone system is the competition between the two possible $H_2^{\bullet+}$ transfer pathways (1,1 versus 1,3). Dawson et al.[193] conducted a study of the reaction of $O^{\bullet-}$ with 1,1,1-trideuterioacetone in order to elucidate which hydrogens are involved in the $H_2^{\bullet+}$ abstraction. These workers found that the 1,1-$H_2^{\bullet+}$ abstraction accounted for 44 ± 2%, while 1,3-$H_2^{\bullet+}$ abstraction accounted for the remainder of the $H_2^{\bullet+}$-transfer channel. Furthermore, they found that the primary product ion ($C_3H_4O^{\bullet-}$) of the 1,1-$H_2^{\bullet+}$ transfer subsequently fragments to $HC{\equiv}CO^-$ + $CH_3^\bullet$; whether this process is collisionally induced in the ICR, or whether the initial product has enough energy to fragment, is unclear from their study. The FA investigation of $O^{\bullet-}$ with $CH_3CHO$ discussed above did not report $HC{\equiv}CO^-$ + $H^\bullet$ + $H_2O$ as a product channel, although one-third of the reaction proceeded by 1,1-$H_2^{\bullet+}$ abstraction; hence it may be the case that the ICR fragment observed in the acetone system is collisionally induced. Other ketones have been investigated to a lesser extent (Table XII).[13,99,100,155,192,196]

**Scheme XI. The Primary Chemical Processes Occurring When the Atomic Oxygen Radical Anion Reacts with Acetaldehyde**

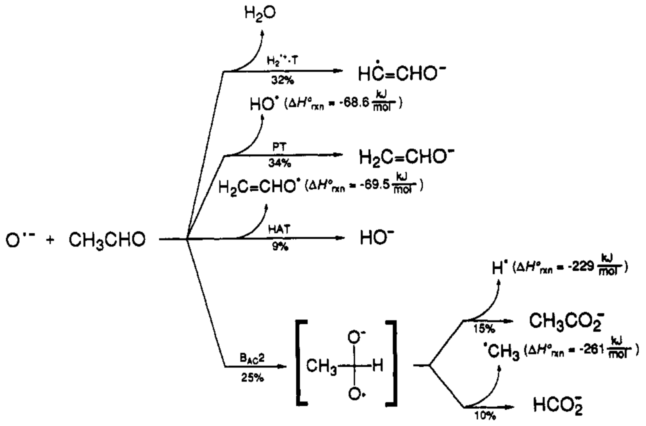

**Table XI. Aldehydes Whose Chemical Ionization Reactions with $O^{\bullet-}$ Have Been Investigated**[a]

| neutral | | |
|---|---|---|
| mass | formula | ref(s) |
| 30 | $H_2C{=}O$ | 99,194 |
| 44 | $CH_3CHO$ | 145 |
| 72 | $CH_3CH_2CH_2CHO$ | 196 |
| 72 | $(CH_3)_2CHCHO$ | 196 |
| 86 | $CH_3CH_2CH_2CH_2CHO$ | 144 |
| 86 | $CH_3CH_2CH(CH_3)CHO$ | 196 |
| 86 | $(CH_3)_2CHCH_2CHO$ | 196 |
| 86 | $(CH_3)_3CCHO$ | 196 |
| 100 | $CH_3CH_2CH_2CH_2CH_2CHO$ | 196 |
| 100 | $CH_3CH_2CH(CH_3)CHO$ | 196 |
| 100 | $(CH_3CH_2)_2CHCHO$ | 196 |
| 106 | $C_6H_5CHO$ | 99,195 |

[a] In all cases, for simplicity's sake, the nominal mass of the naturally most abundant isotopomer is listed.

### B. Esters

When the atomic oxygen radical anion is allowed to react with esters, a wealth of reactions has been observed to occur. These are exemplified in the well-studied reaction of the atomic oxygen radical anion with methyl formate.[55,56,99,155,197,198] When $^{18}O^{\bullet-}$ (from $N_2{}^{18}O$) is allowed to react with methyl formate in an FT-ICR,[56]

**Scheme XII. The Primary Chemical Processes Occurring When the Atomic Oxygen Radical Anion Reacts with Acetone**

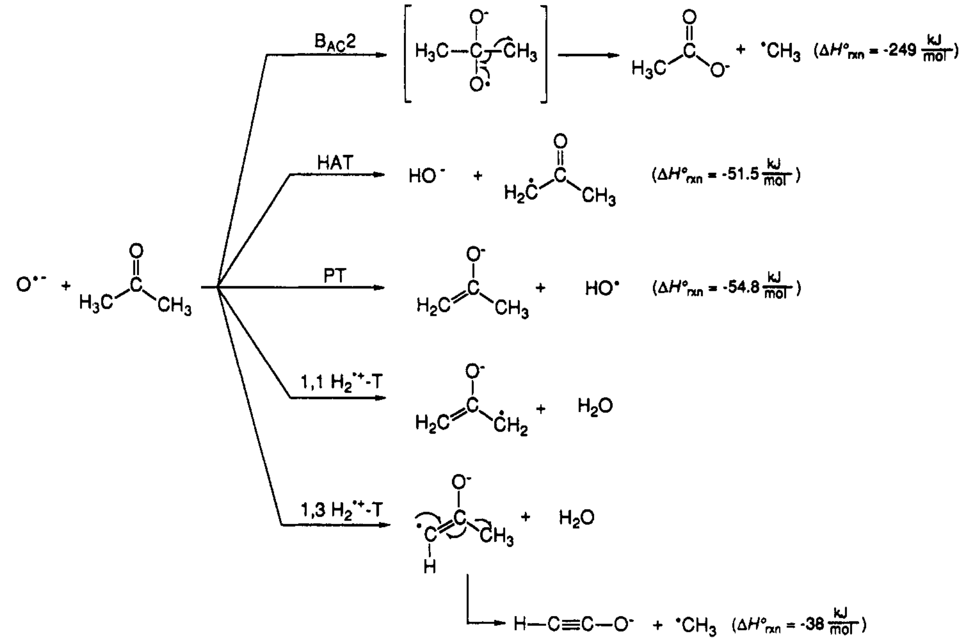

**Table XII. Ketones Whose Chemical Ionization Reactions with O•⁻ Have Been Investigated**[a]

| neutral | | |
|---|---|---|
| mass | formula | ref(s) |
| 58 | $CH_3C(O)CH_3$ | 99,100,155,192,193 |
| 72 | $CH_3CH_2C(O)CH_3$ | 196 |
| 72 | $CH_3C(O)CH_2CH_3$ | 192 |
| 84 | c-$C_5H_8O$ (cyclopentanone) | 192 |
| 86 | $CH_3C(O)CH_2CH_2CH_3$ | 144 |
| 86 | $CH_3C(O)CH(CH_3)_2$ | 196 |
| 86 | $CH_3CH_2C(O)CH_2CH_3$ | 196 |
| 86 | $CH_3C(O)CH_2CH_2CH_3$ | 192 |
| 86 | $CH_3C(O)CH(CH_3)_2$ | 192 |
| 86 | $CH_3CH_2C(O)CH_2CH_3$ | 192 |
| 98 | c-$C_6H_{10}O$ (cyclohexanone) | 192 |
| 100 | $CH_3C(O)CH_2CH_2CH_2CH_3$ | 196 |
| 100 | $CH_3C(O)CH(CH_3)CH_2CH_3$ | 196 |
| 100 | $CH_3C(O)CH_2CH(CH_3)_2$ | 196 |
| 100 | $CH_3C(O)C(CH_3)_3$ | 196 |
| 100 | $CH_3CH_2C(O)CH_2CH_2CH_3$ | 196 |
| 100 | $CH_3CH_2C(O)CH(CH_3)_2$ | 196 |
| 100 | $CH_3C(O)C(CH_3)_3$ | 192 |
| 114 | $CH_3C(O)CH_2CH_2CH_2CH_2CH_3$ | 196 |
| 114 | $CH_3C(O)CH(CH_3)CH_2CH_2CH_3$ | 196 |
| 114 | $CH_3C(O)CH_2CH(CH_3)CH_2CH_3$ | 196 |
| 114 | $CH_3C(O)CH_2CH_2CH(CH_3)_2$ | 196 |
| 114 | $CH_3C(O)CH_2C(CH_3)_3$ | 196 |
| 114 | $CH_3CH_2C(O)CH_2CH_2CH_2CH_3$ | 196 |
| 114 | $(CH_3)_2CHC(O)CH(CH_3)_2$ | 196 |
| 114 | $(CH_3)_2CHC(O)CH_2CH_2CH_3$ | 196 |
| 114 | $CH_3CH_2CH_2C(O)CH_2CH_2CH_3$ | 196 |
| 114 | $(CH_3)_3CC(O)CH_2CH_3$ | 196 |
| 114 | $CH_3CH_2CH_2C(O)CH_2CH_2CH_3$ | 192 |
| 114 | $(CH_3)_2CHC(O)CH(CH_3)_2$ | 192 |

[a] In all cases, for simplicity's sake, the nominal mass of the naturally most abundant isotopomer is listed.

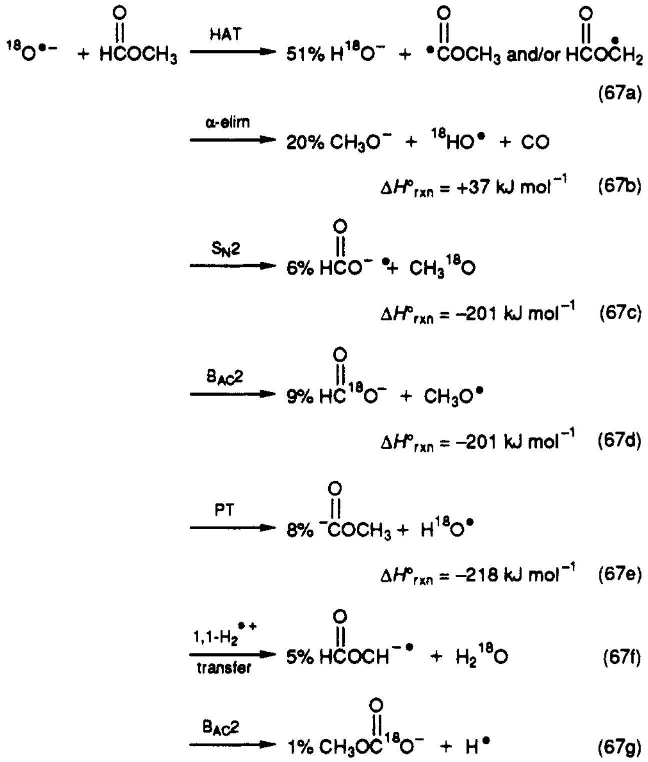

$$^{18}O^{\bullet-} + HC(O)OCH_3 \xrightarrow{HAT} 51\%\ H^{18}O^- + {}^\bullet C(O)OCH_3 \text{ and/or } HC(O)OCH_2^\bullet \quad (67a)$$

$$\xrightarrow{\alpha\text{-elim}} 20\%\ CH_3O^- + {}^{18}HO^\bullet + CO \qquad \Delta H^\circ_{rxn} = +37\ kJ\ mol^{-1} \quad (67b)$$

$$\xrightarrow{S_N2} 6\%\ HC(O)O^- {}^\bullet\!+ CH_3{}^{18}O \qquad \Delta H^\circ_{rxn} = -201\ kJ\ mol^{-1} \quad (67c)$$

$$\xrightarrow{B_{AC}2} 9\%\ HC(O){}^{18}O^- + CH_3O^\bullet \qquad \Delta H^\circ_{rxn} = -201\ kJ\ mol^{-1} \quad (67d)$$

$$\xrightarrow{PT} 8\%\ {}^-C(O)OCH_3 + H^{18}O^\bullet \qquad \Delta H^\circ_{rxn} = -218\ kJ\ mol^{-1} \quad (67e)$$

$$\xrightarrow[transfer]{1,1\text{-}H_2^{\bullet+}} 5\%\ HC(O)OCH^{-\bullet} + H_2{}^{18}O \quad (67f)$$

$$\xrightarrow{B_{AC}2} 1\%\ CH_3OC(O){}^{18}O^- + H^\bullet \quad (67g)$$

products corresponding to H-atom transfer, α-elimination, $S_N2$, $B_{AC}2$, proton transfer, and $H_2^{\bullet+}$ transfer are observed (eq 67). Note that the heats of reaction in eq 67 are for the all-protio compounds. van der Wel et al. also conducted studies with $DCO_2CH_3$ and $HCO_2CD_3$ to elucidate the origin of the hydrogens abstracted during the formation of the $HO^-$, $(M - H)^-$, and $(M - 2H)^{\bullet-}$ ions.[56] They found that while hydrogen-atom transfer occurs from both the formyl and the methyl positions, $H_2^{\bullet+}$ transfer occurs only from the methyl position, and $H^+$ transfer occurs only from the formyl position. These authors[56] have also demonstrated how product distributions from $O^{\bullet-}$ and $HCO_2CH_3$ are sensitive to the kinetic energy of the reactant ion where its excess energy is simply a result of its method of formation. For example, the higher the translational energy of $O^{\bullet-}$, the more favorable the simple proton transfer processes (leading to both $(M - H)^-$ and $CH_3O^-$ products) compared to the $B_{AC}2$ and $S_N2$ processes.

Reaction of $^{18}O^{\bullet-}$ with methyl pivalate has been reported to yield only two anionic products, corre-

**Table XIII. Esters Whose Chemical Ionization Reactions with $O^{\bullet -}$ Have Been Investigated**[a]

| neutral | | |
|---|---|---|
| mass | formula | ref(s) |
| 60 | $HCO_2CH_3$ | 55,56,64,99,155,198 |
| 86 | $H_2C{=}CHCO_2CH_3$ | 99 |
| 116 | $(CH_3)_3CCO_2CH_3$ | 55 |
| 128 | $CF_3CO_2CH_3$ | 99 |
| 136 | $C_6H_5CO_2CH_3$ | 99 |

[a] In all cases, for simplicity's sake, the nominal mass of the naturally most abundant isotopomer is listed.

sponding to the $B_{AC}2$ and the $S_N2$ pathways (eq 68).[55] The lack of observation of the $\alpha$-elimination and proton-transfer channels (i.e., eqs 67b and 67e) is due to lack of the requisite proton. The lack of observation of the HAT (eq 67a), the 1,1-$H_2^{\bullet +}$ transfer (eq 67f), and the alternate $B_{AC}2$ (eq 67g) channels for methyl pivalate, all of which were found for methyl formate, is unexplained at this time. A variety of other esters have also been studied (Table XIII).[99]

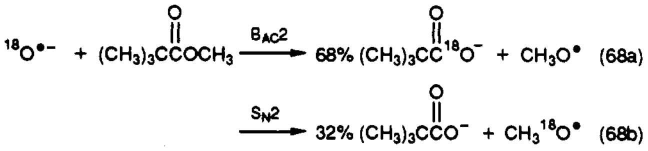

$$ {}^{18}O^{\bullet -} + (CH_3)_3C\overset{\overset{O}{\|}}{C}OCH_3 \xrightarrow{B_{AC}2} 68\%\ (CH_3)_3C\overset{\overset{O}{\|}}{C}{}^{18}O^- + CH_3O^\bullet \tag{68a}$$

$$ \xrightarrow{S_N2} 32\%\ (CH_3)_3C\overset{\overset{O}{\|}}{C}O^- + CH_3{}^{18}O^\bullet \tag{68b}$$

## C. Other Carbonyl Compounds

The reaction of the atomic oxygen radical anion with various acyl chlorides has been studied;[199] with most simple acyl chlorides, all products are proposed to result from nucleophilic attack at the carbonyl carbon. Isobutyryl chloride yields an additional product which was proposed to result from addition followed by intramolecular hydrogen-atom transfer; the authors suggested this pathway since intramolecular hydrogen transfer is well-established in various processes. Three diacyl chlorides have also been studied, all of which gave $Cl^-$ as the most intense ion. When the authors examined perfluorosuccinyl chloride and perfluoroglutaryl chloride, they found that these compounds gave essentially the same mass spectra whether $N_2O$, $N_2O$–$H_2$, or $N_2O$–$CH_4$ was used to generate the reactive anion. They concluded that the initial reaction in all these cases was the addition of $O^{\bullet -}$ to the perfluorodiacyl chlorides; that is, the chlorides competed successfully with $CH_4$ and $H_2$ for reaction with the atomic oxygen radical anion.

## D. Miscellaneous

We should mention, if only in passing, that while we did not explicitly look for reactions that produce the atomic oxygen radical anion as a product of a reaction, several reports turned up in our literature search. Refaey and Franklin[200] found that $I^-$ produces $O^{\bullet -}$ from $CO_2$ with a threshold of 7.1 eV and from $SO_2$ with a threshold of 6.0 eV. Kleyn and co-workers[201] reported on the cross sections for $O^{\bullet -}$ formation in Na, K, and Cs collisions with $O_2$ in the energy range from threshold up to 2 keV; the yield of $O^{\bullet -}$ was found to be at least a factor of 20 smaller than that for $O_2^-$. Mitsuke and co-workers have examined ion pair formation from photoexcitation of OCS ($O^{\bullet -} + CS^+$) and $CO_2$ ($O^{\bullet -} + CO^+$) using synchrotron radiation in the 15–25 eV photon energy range.[73]

There are a variety of $O^{\bullet -}$-transfer reactions known, in which "$O^{\bullet -}$" is transferred from one stable neutral to another. The energy dependence of several of these (e.g., eqs 69–73) have been examined by Albritton[202,203] and Lifshitz[204] and their co-workers. Note that in eqs

$$O_3^{\bullet -} + NO^\bullet \xrightarrow{2.2\times 10^{-12}} NO_2^- + O_2 \qquad \Delta H^\circ_{rxn} = -226\ kJ\ mol^{-1} \tag{69}$$

$$O_3^{\bullet -} + SO_2 \xrightarrow{1.7\times 10^{-9}} SO_3^{\bullet -} + O_2 \tag{70}$$

$$CO_3^{\bullet -} + NO^\bullet \xrightarrow{1.0\times 10^{-11}} NO_2^- + CO_2 \qquad \Delta H^\circ_{rxn} = -172\ kJ\ mol^{-1} \tag{71}$$

$$CO_3^{\bullet -} + SO_2 \xrightarrow{3.5\times 10^{-10}} SO_3^{\bullet -} + CO_2 \tag{72}$$

$$O_3^{\bullet -} + CO_2 \xrightarrow{5.5\times 10^{-10}} CO_3^{\bullet -} + O_2 \qquad \Delta H^\circ_{rxn} = -54\ kJ\ mol^{-1} \tag{73}$$

69–73, the thermally equilibrated rate coefficients, in units of $cm^3\ molecule^{-1}\ s^{-1}$, are shown above the arrows. For all these reactions, it was found that the dependence of the rate coefficient on the reactant center-of-mass kinetic energy was significant and that these reactions have a negligible vibrational or rotational energy dependence.

Another interesting reaction across which we came during our literature search was the collision-induced (He or $N_2$) charge-inversion reactions of $O^{\bullet -}$ (eq 74).[205] The workers found that when $O^{\bullet -}$ was generated from electron ionization of a $CH_4/N_2O$ mixture and He was used as the collision gas (M), the $O^{\bullet +}$ ion was formed in its ground state ($^4S$). When dinitrogen was used as the collision gas, the ion translational energy spectra indicated that although the $O^{\bullet +}$ ion was still formed in its ground state, the target molecule $N_2$ was excited to its first excited ($^3\Sigma$) state.

$$O^{\bullet -} + M \rightarrow O^{\bullet +} + M + 2e^- \tag{74}$$

# *VII. Condensed-Phase Reactivity*

## A. In Water

The atomic oxygen radical anion is the conjugate base of the hydroxyl radical, a primary species from the radiolytic decomposition of water; hence there have been a number of studies that address the reactivity of $O^{\bullet -}$ in water, especially compared to that of $HO^\bullet$. Generally considered, it appears that the reactivity of these two species are quite different, especially when the reaction under investigation involves electron transfer or addition to an unsaturated system. The differences between these reactive species are somewhat less, however, when one is comparing hydrogen abstraction rates; $O^{\bullet -}$ rates seem to be about two times slower than the corresponding values for $HO^\bullet$.[206] The reactivity of $O^{\bullet -}$ with aromatic derivatives of benzene, pyridine, and furan have been reviewed previously.[207] Several representative comparisons are discussed below; many additional topics have received experimental consideration.[208-223]

Neta et al., in 1972, reported that although the rate of addition of $O^{•-}$ to an aromatic ring or to a double bond is much slower than that of $HO^•$, the rates of H-atom abstraction are more nearly comparable.[224] In 1973, Simic and co-workers[225] found that whereas $HO^•$ reacts at nearly the diffusion-controlled rate with aromatic carboxylate anions in water, $O^{•-}$ reacts much more slowly, in accord with the 1972 study. From structure–reactivity studies, these authors conclude that $O^{•-}$, as compared to $HO^•$, is less electrophilic and displays an unfavorable interaction with the $\pi$-electron system of the aromatic nucleus.

In 1975, Neta and Schuler[226] reported a number of rate coefficients for the reaction of $O^{•-}$ with various organic substrates in aqueous solution. For H-atom abstraction reactions from saturated alcohols[208] and monocarboxylic acids, they found that the rate coefficients were ~50% of those for the analogous $HO^•$ reactions. Abstraction rates from allylic positions were 2–3 times larger than those for similar rates in saturated systems. Addition of $O^{•-}$ to double bonds and to aromatic systems was found to be quite slow compared to the abstraction processes. Simic and co-workers[227] found that $O^{•-}$ reacts with unsaturated aliphatic alcohols primarily by H-atom abstraction, and again, that hydroxyl radical reacts more rapidly (2–3 times) with the same compounds, albeit by a different process (they add to the carbon–carbon double bond). Savel'eva and co-workers also noted that the atomic oxygen radical anion is less reactive than the hydroxyl radical with several phenols in aqueous solution.[228]

Hickel and Sehested,[206] using pulse radiolysis in the temperature range 15–90 °C, determined the activation energies for $O^{•-}$ reacting with both $H_2$ and $D_2$ (the products are ultimately water and a hydrated electron) in aqueous solution. At room temperature, they found $k[O^{•-} + H_2] = 1.1 \times 10^8\ M^{-1}\ s^{-1}$ and $k[O^{•-} + D_2] = 2.5 \times 10^7\ M^{-1}\ s^{-1}$ and the corresponding activation energies to be 14 and 21 kJ $mol^{-1}$.

Wander et al.[223] have reported their observations on the reactions of $O^{•-}$ with methanol and ethanol in water; they found $k[O^{•-} + CH_3OH \text{ in water}] = (5.8 \pm 0.8) \times 10^8\ M^{-1}\ s^{-1}$ and $k[O^{•-} + CH_3CH_2OH \text{ in water}] = (11.3 \pm 1.7) \times 10^8\ M^{-1}\ s^{-1}$ at 25 °C. These authors write the products as the carbon-centered radical but do not explicitly mention how the product identities were obtained.

Christensen and co-workers[229] found that $O^{•-}$, in aqueous solution, reacts with toluene to form benzyl radicals via an H-atom transfer process from the methyl group and that this rate coefficient is $(2.1 \pm 0.3) \times 10^9\ M^{-1}\ s^{-1}$.

### B. In Liquid Argon

Bakale et al.[230] produced electrons in liquid argon by a short burst of X-rays; these electrons were allowed to react with dissolved $N_2O$ to give $O^{•-}$. The rate coefficients for the reaction of $O^{•-}$ with either $H_2$, CO, or $CH_4$ were obtained in this solvent and compared to the rate coefficients for the identical gas-phase reactions. In all cases, products were not directly detected but were assumed to be those observed for the gas-phase processes; however, all observations in liquid argon are consistent with the known gas-phase reactions.

### C. On Surfaces

There have been several reports[231] that show that the atomic oxygen radical anion plays a role in catalytic oxidations occurring on various oxide surfaces. For example, ESR has been used[232] to show that when $N_2O$ reacts with irradiated (UV) MgO, $O^{•-}$ is formed, which can further react with adsorbed oxygen, carbon monoxide or ethylene to give, respectively, $O_3^{•-}$, $CO_2^{•-}$ and $C_2H_4O^{•-}$. ESR studies over the temperature range 77 to 300 K of $O^{•-}$ adsorbed on $Mo/SiO_2$ reacting with ethylene were interpreted to indicate initial formation of $^•CH_2—CH_2—O^-$, followed by, at 150 K, dissociation into $H_2C{=}CH^•$ and $HO^-$.[231]

Sanche and Parenteau[78] have reported on the desorption of negative ions induced by low-energy (4–20 eV) electron impact on Pt surfaces on which $O_2$ and a hydrocarbon have been coabsorbed. These authors have interpreted their data to indicate formation of $O^{•-}$ by dissociative electron attachment to dioxygen; the atomic oxygen radical anions produced then react with the hydrocarbons by an H-atom abstraction process akin to that demonstrated for the pure gas-phase reaction. Other workers have reported that $O^{•-}$ reacts with methane at room temperature over various metal oxides[233-235] and that, in general, $O^{•-}$ is more reactive toward alkanes and alkenes than other ionic oxygen species on solid catalysts.[234,236-238] More recently, Iwamoto and co-workers have postulated that $O^{•-}$ is the active oxygen species which oxidizes benzene to phenol (70% selectivity at 10% conversion) on 3.3 wt % $V_2O_5/SiO_2$ at 823 K.[239] Others have discussed how $O^{•-}$ interacts with various molecular neighbors before leaving the solid.[77]

## *VIII. Conclusion*

The atomic oxygen radical anion is an important, intriguing, reactive species, not only in terms of gas-phase ion–molecule chemistry, but also in condensed-phase chemistry as well. While the mechanisms by which $O^{•-}$ reacts and the factors that control selectivity among these mechanisms are currently being aggressively examined, it is apparent from the diverse and unique observations to date that $O^{•-}$ has earned a niche as a valuable tool in gas-phase ion studies. Perhaps most importantly, the atomic oxygen radical anion is now indispensable as a means to prepare entire classes of anionic versions of the classical reactive intermediates of organic chemistry. As one example of many possible (with many more anticipated in the near future), consider vinylidene, $H_2C{=}C$. The anionic version of this reactive intermediate is readily prepared from the reaction of $O^{•-}$ with ethylene (section V.B.1); several groups have prepared $H_2C{=}C^{•-}$ in this fashion and then studied different aspects of its chemical and physical properties (e.g., its negative ion photoelectron spectrum,[240] its neutralization–ionization,[241] its chemical reactivity[6]). Didehydroaromatics and carbenes are two additional classes of reactive intermediates known to be accessible by the same approach; other classes (e.g., phosphinidenes from $RPH_2$ and silylenes from $R_2SiH_2$, among others) remain to be investigated, but hold great promise for similar studies. The interest in $O^{\bullet-}$ chemistry is wide ranging as represented by its role in our understanding of the chemistry of flames (both directly and indirectly)[79] as well as on surfaces; furthermore, it has been one of the species chosen to represent the active oxygen species of the ferryl compound in model calculations of the chemistry of cytochrome P-450.[242] The chemistry of $O^{\bullet-}$ in the liquid phase, especially water, has also been studied to some extent and appears to be closely related to that found in the gas phase.

Considering the number of techniques and approaches that have been utilized in the studies of $O^{\bullet-}$ and the varied disciplines used (ranging from atmospherically related studies to fundamental physical-organic investigations to analytical applications) we were pleasantly surprised to find that there is excellent agreement among the observations concerning the reactivity of the atomic oxygen radical anion. There *are* differences, more than a few of which remain unexplained, but these tend to be concerning precise details rather than more broadly applicable generalizations. Comparisons between data collected by different techniques must include which reaction channels are capable of being observed versus those that cannot be "seen" under the given experimental conditions (e.g., associative detachment channels). The role of competing reactions from contaminant ions or energetic neutrals present also needs to be considered when one is trying to account for apparent differences. Most importantly, due to their sensitivity to interaction energy, quantitative measurements on $O^{\bullet-}$ reactions must be carried out when the energy of the atomic oxygen radical anion is known, especially since it is most often formed with excess energy.

The opportunities for a detailed molecular-level understanding of $O^{\bullet-}$ reaction mechanisms are immense; considerable progress has already been made. Many of the areas reviewed in this document (e.g., the reaction of $O^{\bullet-} + CO_2$ or the role of excess interaction energy on the reaction of $O^{\bullet-}$ with $H_2C{=}CH_2$) deserve far more attention than they have received; in-depth consideration of these systems is left to another occasion. One can safely anticipate even greater efforts in the understanding and the utilization of $O^{\bullet-}$ reactions in the future.

## IX. Acknowledgments

We thank the National Science Foundation (Presidential Young Investigator Award CHE-8552742 and CHE-9196164) for financial support of this work. J.L. thanks the Department of Defense (National Defense Science and Engineering Graduate Fellowship in Chemistry P-28231-CH-NDF) for support.

## X. References

(1) Fehsenfeld, F. C.; Schmeltekopf, A. L.; Schiff, H. I.; Ferguson, E. E. *Planet. Space Sci.* **1967**, *15*, 373–379.
(2) Bohme, D. K. In *Interactions Between Ions and Molecules*; Ausloos, P., Ed.; Plenum Press: New York, 1975; p 489–504.
(3) (a) Feshenfeld, F. C.; Ferguson, E. E.; Schmeltekopf, A. L. *J. Chem. Phys.* **1966**, *45*, 1844–1845. (b) Ferguson, E. E.; Feshenfeld, F. C.; Schmeltekopf, A. L. *Adv. Chem. Ser.* **1969**, *80*, 83–91.
(4) Lifshitz, C.; Tassa, R. *Int. J. Mass Spectrom. Ion Phys.* **1973**, *12*, 433–437.
(5) Feshenfeld, F. C.; Howard, C. J.; Schmeltekopf, A. L. *J. Chem. Phys.* **1975**, *63*, 2835–2841.
(6) Guo, Y.; Grabowski, J. J. *Int. J. Mass Spectrom. Ion Processes* **1990**, *97*, 253–264.
(7) Guo, Y.; Grabowski, J. J. *J. Am. Chem. Soc.* **1991**, *113*, 5923–5931.
(8) Chou, P. K.; Kass, S. R. *J. Am. Chem. Soc.* **1991**, *113*, 697–698.
(9) Leopold, D. G.; Miller, A. E. S.; Lineberger, W. C. *J. Am. Chem. Soc.* **1986**, *108*, 1379–1384.
(10) Viggiano, A. A.; Paulson, J. F. In *Swarms of Ions and Electrons in Gases*; Lindinger, W., Märk, T. D., Howorka, F., Eds.; Springer-Verlag: New York, 1984; pp 218–240.
(11) Ferguson, E. E. *Acc. Chem. Res.* **1970**, *3*, 402–408.
(12) Tiernan, T. O. In *Interactions Between Ions and Molecules*; Ausloos, P., Ed.; Plenum Press: New York, 1975; pp 353–385.
(13) (a) Nibbering, N. M. M. *Recl. Trav. Chim. Pays-Bas* **1981**, *100*, 297–306. (b) Budzikiewicz, H. *Angew. Chem., Int. Ed. Engl.* **1981**, *20*, 624–637.
(14) Harrison, A. G. In *Chemical Ionization Mass Spectrometry*; CRC Press: Boca Raton, FL, 1983.
(15) Lias, S. G.; Bartmess, J. E.; Liebman, J. F.; Holmes, J. L.; Levin, R. D.; Mallard, W. G. *J. Phys. Chem. Ref. Data* **1988**, *17*, Supplement No. 1. These data, in a slightly updated form, are also available to us on a personal computer by way of *NIST Negative Ion Energetics Database* (Version 2.06, January 1990); NIST Standard Reference Database 19B.
(16) Su, T.; Bowers, M. T. *J. Am. Chem. Soc.* **1973**, *95*, 1370–1373.
(17) Su, T.; Bowers, M. T. *J. Chem. Phys.* **1973**, *58*, 3027–3037.
(18) Chesnavich, W. J.; Su, T.; Bowers, M. T. *J. Chem. Phys.* **1980**, *72*, 2641–2655.
(19) Su, T.; Chesnavich, W. J. *J. Chem. Phys.* **1982**, *76*, 5183–5185.
(20) Fehsenfeld, F. C.; Ferguson, E. E.; Schmeltekopf, A. L. *J. Chem. Phys.* **1966**, *44*, 3022–3024.
(21) Smith, D.; Adams, N. G. In *Gas-Phase Ion Chemistry*; Bowers, M. T., Ed.; Academic Press: New York, 1979; Vol. 1, Chapter 1.
(22) Graul, S. T.; Squires, R. R. *Mass Spectrom. Rev.* **1988**, *7*, 263–358.
(23) Beauchamp, J. L. *Annu. Rev. Phys. Chem.* **1971**, *22*, 527–561.
(24) Comisarow, M. B.; Marshall, A. G. *Chem. Phys. Lett.* **1974**, *25*, 282–283.
(25) Comisarow, M. B.; Marshall, A. G. *Chem. Phys. Lett.* **1974**, *26*, 489–490.
(26) Tal'roze, V. L.; Frakevich, E. L. *Russ. J. Phys. Chem.* **1960**, *34*, 1275–1279.
(27) Rol, P. V.; Entemann, E. A. *J. Chem. Phys.* **1968**, *49*, 1430–1431.
(28) McDaniel, E. W. *J. Chem. Phys.* **1970**, *52*, 3931–3935.
(29) Guo, Y.; Grabowski, J. J. *Int. J. Mass Spectrom. Ion Processes*, in press.
(30) Mazely, T. L.; Smith, M. A. *Chem. Phys. Lett.* **1988**, *144*, 563–569.
(31) Calculated from heats of formation obtained from ref 15.
(32) Kass, S. R. Personal communication.
(33) Ikezoe, Y.; Matsuoka, S.; Takebe, M.; Viggiano, A. A. In *Gas-Phase Ion-Molecule Reaction Rate Constants Through 1986*; Ion Reaction Research Group of The Mass Spectroscopy Society of Japan: Tokyo, 1986.
(34) Hotop, H.; Lineberger, W. C. *J. Phys. Chem. Ref. Data* **1985**, *14*, 731–750.
(35) (a) Neumark, D. M.; Lykke, K. R.; Andersen, T.; Lineberger, W. C. *Phys. Rev. A* **1985**, *32*, 1890–1892. (b) Schulz, P. A.; Meade, R. D.; Jones, P. L.; Lineberger, W. C. *J. Chem. Phys.* **1982**, *77*, 1153–1165.
(36) Cohen, D.; Basch, H.; Osman, R. *J. Chem. Phys.* **1984**, *80*, 5684–5686.
(37) Rabani, J.; Matheson, M. S. *J. Phys. Chem.* **1966**, *70*, 761–769.
(38) Weeks, J. L.; Rabani, J. *J. Phys. Chem.* **1966**, *70*, 2100–2106.
(39) Buxton, G. V. *Trans. Faraday Soc.* **1970**, *66*, 1656–1660.
(40) McFarland, M.; Albritton, D. L.; Fehsenfeld, F. C.; Ferguson, E. E.; Schmeltekopf, A. L. *J. Chem. Phys.* **1973**, *59*, 6610–6619.
(41) Moseley, J. T.; Cosby, P. C.; Peterson, J. R. *J. Chem. Phys.* **1976**, *64*, 4228–4229.
(42) Böhringer, H.; Fahey, D. W.; Lindinger, W.; Howorka, F.; Fehsenfeld, F. C.; Albritton, D. L. *Int. J. Mass Spectrom. Ion Processes* **1987**, *81*, 45–65.
(43) Snuggs, R. M.; Volz, D. J.; Schummers, J. H.; Martin, D. W.; McDaniel, E. W. *Phys. Rev. A* **1971**, *3*, 477–487.
(44) Matese, J. J. *Phys. Rev. A* **1974**, *10*, 454–457.
(45) Lin, S. L.; Bardsley, J. N.; Dotan, I.; Fehsenfeld, F. C.; Albritton, D. L. *Int. J. Mass Spectrom. Ion Phys.* **1980**, *34*, 113–124.
(46) Melton, C. E. *J. Chem. Phys.* **1972**, *57*, 4218–4225.
(47) Melton, C. E.; Neece, G. A. *J. Am. Chem. Soc.* **1971**, *93*, 6757–6759.
(48) See Table II in ref 46.
(49) Gupta, S. K.; Melton, C. E. *J. Phys. Chem.* **1973**, *77*, 2594–2598.
(50) Locht, R.; Momigny, J. *Int. J. Mass Spectrom. Ion Phys.* **1970**, *4*, 379–391.
(51) Hierl, P. M.; Franklin, J. L. *J. Chem. Phys.* **1967**, *47*, 3154–3161.
(52) Rapp, D.; Briglia, D. *J. Chem. Phys.* **1965**, *43*, 1480–1489.
(53) *CRC Handbook of Chemistry and Physics*; Weast, R. C., Ed.; Chemical Rubber Company: Boca Raton, FL, 1985.
(54) Chantry, P. J.; Schulz, G. J. *Phys. Rev.* **1967**, *156*, 134–141.
(55) Johlman, C. L.; Wilkins, C. L. *J. Am. Chem. Soc.* **1985**, *107*, 327–332.
(56) van der Wel, H.; Nibbering, N. M. M. *Int. J. Mass Spectrom. Ion Processes* **1986**, *72*, 145–153.

(57) Krishnakumar, E.; Srivastava, S. K. *Phys. Rev. A* **1990**, *41*, 2445–2452.
(58) Christophorou, L. G. *Radiat. Phys. Chem.* **1978**, *12*, 19.
(59) Itikawa, Y.; Ichimura, A.; Onda, K.; Sakimoto, K.; Takayanagi, K.; Hatano, Y.; Hayashi, M.; Nishimura, H.; Tsurubuchi, S. *J. Phys. Chem. Ref. Data* **1989**, *18*, 23–42.
(60) Moruzzi, J. L.; Harrison, L. *Int. J. Mass Spectrom. Ion Phys.* **1974**, *13*, 163–171.
(61) Chantry, P. J. *J. Chem. Phys.* **1969**, *51*, 3369–3379.
(62) Chantry, P. J. *J. Chem. Phys.* **1969**, *51*, 3380–3384.
(63) See for instance: Dotan, I.; Klein, F. S. *Int. J. Mass Spectrom. Ion Phys.* **1979**, *29*, 137–151.
(64) Parkes, D. A. *J. Chem. Soc., Faraday Trans. 1* **1972**, *68*, 2103–2120.
(65) Warman, J. M.; Fessenden, R. W. *J. Chem. Phys.* **1968**, *49*, 4718–4719.
(66) Warman, J. M.; Fessenden, R. W.; Bakale, G. *J. Chem. Phys.* **1972**, *57*, 2702–2711.
(67) Caledonia, G. E. *Chem. Rev.* **1975**, *75*, 333–351.
(68) Chantry, P. J. *J. Chem. Phys.* **1972**, *57*, 3180–3186.
(69) Orient, O. J.; Srivastava, S. K. *Chem. Phys. Lett.* **1983**, *96*, 681–684 and references therein.
(70) Dressler, R.; Allan, M. *Chem. Phys.* **1985**, *92*, 449–455 and references therein.
(71) Tronc, M.; Malegat, L.; Azria, R. *Chem. Phys. Lett.* **1982**, *92*, 551–555.
(72) Spence, D.; Schulz, G. J. *Phys. Rev.* **1969**, *188*, 280–287.
(73) Mitsuke, K.; Suzuki, S.; Imamura, T.; Koyano, I. *J. Chem. Phys.* **1990**, *93*, 1710–1719.
(74) Marx, R.; Mauclaire, G.; Fehsenfeld, F. C.; Dunkin, D. B.; Ferguson, E. E. *J. Chem. Phys.* **1973**, *58*, 3267–3273.
(75) Stockdale, J. A. D.; Compton, R. N.; Reinhardt, P. W. *Int. J. Mass Spectrom. Ion Phys.* **1970**, *4*, 401–414.
(76) Hacaloglu, J.; Gokmen, A.; Suzer, S. *J. Phys. Chem.* **1989**, *93*, 3418–3421.
(77) Azria, R.; Parenteau, L.; Sanche, L. *J. Chem. Phys.* **1988**, *88*, 5166–5170.
(78) Sanche, L.; Parenteau, L. *J. Chem. Phys.* **1990**, *93*, 7476–7482.
(79) See, for example: Hayhurst, A. N.; Jones, H. R. N. *J. Chem. Soc., Faraday Trans. 2* **1987**, *83*, 1–27.
(80) Acharya, P. K.; Kendall, R. A.; Simons, J. *J. Chem. Phys.* **1985**, *83*, 3888–3893.
(81) McFarland, M.; Albritton, D. L.; Fehsenfeld, F. C.; Ferguson, E. E.; Schmeltekopf, A. L. *J. Chem. Phys.* **1973**, *59*, 6629–6635.
(82) Viggiano, A. A.; Morris, R. A.; Deakyne, C. A.; Dale, F.; Paulson, J. F. *J. Phys. Chem.* **1991**, *95*, 3644–3647.
(83) (a) Huq, M. S.; Scott, D.; Champion, R. L.; Doverspike, L. D. *J. Chem. Phys.* **1985**, *82*, 3118–3122. (b) Hauffe, B. J. *Z. Phys. Chem.* **1973**, *85*, 175–190.
(84) Esaulov, V. A.; Champion, R. L.; Grouard, J. P.; Hall, R. I.; Montmagnon, J. L.; Penent, F. *J. Chem. Phys.* **1990**, *92*, 2305–2309.
(85) Johnson, S. G.; Kremer, L. N.; Metral, C. J.; Cross, R. J., Jr. *J. Chem. Phys.* **1978**, *68*, 1444–1447.
(86) Herbst, E.; Payne, L. G.; Champion, R. L.; Doverspike, L. D. *Chem. Phys.* **1979**, *42*, 413–421.
(87) de Koning, L. J.; Nibbering, N. M. M. *J. Am. Chem. Soc.* **1984**, *106*, 7971–7973.
(88) Bohme, D. K.; Fehsenfeld, F. C. *Can. J. Chem.* **1969**, *47*, 2717–2719.
(89) Lindinger, W.; Albritton, D. L.; Fehsenfeld, F. C.; Ferguson, E. E. *J. Chem. Phys.* **1975**, *63*, 3238–3242.
(90) Parkes, D. A. *J. Chem. Soc., Faraday Trans. 1* **1972**, *68*, 613–626.
(91) Holmes, J. L.; Lossing, F. P.; Maccoll, A. *J. Am. Chem. Soc.* **1988**, *110*, 7339–7342.
(92) Comer, J.; Schulz, G. J. *Phys. Rev. A* **1974**, *10*, 2100–2106.
(93) Viggiano, A. A.; Morris, R. A.; Paulson, J. F. *J. Chem. Phys.* **1988**, *89*, 4848–4852; corrected in Viggiano, A. A.; Morris, R. A.; Paulson, J. F. *J. Chem. Phys.* **1989**, *90*, 6811.
(94) Viggiano, A. A.; Morris, R. A.; Deakyne, C. A.; Dale, F.; Paulson, J. F. *J. Phys. Chem.* **1990**, *94*, 8193–8197.
(95) Bohme, D. K.; Fehsenfeld, F. C. *Can. J. Chem.* **1969**, *47*, 2715–2717.
(96) Fehsenfeld, F. C.; Ferguson, E. E. *J. Chem. Phys.* **1974**, *61*, 3181–3193.
(97) Van Doren, J. M.; Barlow, S. E.; DePuy, C. H.; Bierbaum, V. M. *J. Am. Chem. Soc.* **1987**, *109*, 4412–4414.
(98) Van Doren, J. M.; Barlow, S. E.; DePuy, C. H.; Bierbaum, V. M. *Int. J. Mass Spectrom. Ion Processes* **1991**, *109*, 305–325.
(99) van der Wel, H.; Nibbering, N. M. M. *Recl. Trav. Chim. Pays-Bas* **1988**, *107*, 479–490.
(100) Futrell, J. H.; Tiernan, T. O. In *Ion-Molecule Reactions*; Franklin, J. L., Ed.; Plenum Press: New York, 1972; Vol. 2, Chapter 11.
(101) Karnett, M. P.; Cross, R. J. *Chem. Phys. Lett.* **1981**, *82*, 277–280.
(102) Lifshitz, C. *J. Phys. Chem.* **1982**, *86*, 3634–3637.
(103) Hamilton, C. E.; Duncan, M. A.; Zwier, T. S.; Weisshaar, J. C.; Ellison, G. B.; Bierbaum, V. M.; Leone, S. R. *Chem. Phys. Lett.* **1983**, *94*, 4–9.
(104) Adams, N. G.; Bohme, D. K.; Dunkin, D. B.; Fehsenfeld, F. C.; Ferguson, E. E. *J. Chem. Phys.* **1970**, *52*, 3133–3140.
(105) Hopper, D. G.; Wahl, A. C.; Wu, R. L. C.; Tiernan, T. O. *J. Chem. Phys.* **1976**, *65*, 5474–5494.
(106) Rayment, S. W.; Moruzzi, J. L. *Int. J. Mass Spectrom. Ion Phys.* **1978**, *26*, 321–326.
(107) Compton, R. N.; Bailey, T. L. *J. Chem. Phys.* **1970**, *53*, 454–456.
(108) Parkes, D. A. *J. Chem. Soc., Faraday Trans. 1* **1972**, *68*, 627–640.
(109) Roche, A. E.; Goodyear, C. C. *J. Phys. B* **1969**, *2*, 191–200.
(110) Sanche, L.; Schulz, G. J. *J. Chem. Phys.* **1973**, *58*, 479–493.
(111) Moruzzi, J. L.; Phelps, A. V. *J. Chem. Phys.* **1966**, *45*, 4617–4627.
(112) Bierbaum, V. M.; Ellison, G. B.; Futrell, J. H.; Leone, S. R. *J. Chem. Phys.* **1977**, *67*, 2375–2376.
(113) Comer, J.; Schulz, G. J. *J. Phys. B* **1974**, *7*, L249–L253.
(114) Bardsley, J. N. *J. Chem. Phys.* **1969**, *51*, 3384–3389.
(115) Claydon, C. R.; Segal, G. A.; Taylor, H. S. *J. Chem. Phys.* **1970**, *52*, 3387–3398 and references therein.
(116) Pacansky, J.; Wahlgren, U.; Bagus, P. S. *J. Chem. Phys.* **1975**, *62*, 2740–2744.
(117) Hopper, D. G. *Chem. Phys.* **1980**, *53*, 85–94.
(118) Moruzzi, J. L.; Ekin, J. W., Jr.; Phelps, A. V. *J. Chem. Phys.* **1968**, *48*, 3070–3076.
(119) Mauer, J. L.; Schulz, G. J. *Phys. Rev. A* **1973**, *7*, 593–605.
(120) Ferguson, E. E.; Fehsenfeld, F. C.; Schmeltekopf, A. L. *J. Chem. Phys.* **1967**, *47*, 3085–3086.
(121) Morris, R. A.; Viggiano, A. A.; Paulson, J. F. *J. Phys. Chem.* **1990**, *94*, 1884–1886.
(122) Melton, C. E. *J. Phys. Chem.* **1972**, *76*, 3116–3120.
(123) Viggiano, A. A.; Paulson, J. F. *J. Chem. Phys.* **1983**, *79*, 2241–2245.
(124) Parkes, David A. *Trans. Faraday Soc.* **1971**, *67*, 711–729.
(125) Tiernan, T. O.; Hughes, B. M.; Lifshitz, C. *J. Chem. Phys.* **1971**, *55*, 5692–5703.
(126) Travers, M. J.; Cowles, E. C.; Ellison, G. B. *Chem. Phys. Lett.* **1989**, *164*, 449–455.
(127) Snuggs, R. M.; Volz, D. J.; Gatland, I. R.; Schummers, J. H.; Martin, D. W.; McDaniel, E. W. *Phys. Rev. A* **1971**, *3*, 487–493.
(128) Rebentrost, F. *Int. J. Mass Spectrom. Ion Phys.* **1973**, *11*, 475–481.
(129) Paulson, J. F. *J. Chem. Phys.* **1970**, *52*, 963–964.
(130) Fansler, T. D.; Colonna-Romano, L. M.; Varney, R. N. *J. Chem. Phys.* **1977**, *66*, 3246–3251.
(131) (a) Bohme, D. K.; Dunkin, D. B.; Fehsenfeld, F. C.; Ferguson, E. E. *J. Chem. Phys.* **1969**, *51*, 863–872. (b) Yang, X.; Castleman, A. W., Jr. *J. Am. Chem. Soc.* **1991**, *113*, 6766–6771.
(132) Dotan, I.; Karpas, Z.; Klein, F. S. *Int. J. Mass Spectrom. Ion Phys.* **1981**, *37*, 77–86.
(133) Vogt, D. *Int. J. Mass Spectrom. Ion Phys.* **1969**, *3*, 81–90.
(134) Stockdale, J. A. D.; Compton, R. N.; Reinhardt, P. W. *Phys. Rev.* **1969**, *184*, 81–93.
(135) Rutherford, J. A.; Turner, B. R. *J. Geophys. Res.* **1967**, *72*, 3795–3800.
(136) Rutherford, J. A.; Turner, B. R.; Vroom, D. A. *J. Chem. Phys.* **1973**, *58*, 5267–5271.
(137) Lifshitz, C.; Wu, R. L. C.; Haartz, J. C.; Tiernan, T. O. *J. Chem. Phys.* **1977**, *67*, 2381–2382.
(138) Dotan, I.; Albritton, D. L.; Fehsenfeld, F. C.; Streit, G. E.; Ferguson, E. E. *J. Chem. Phys.* **1978**, *68*, 5414–5416.
(139) Gilles, M. K.; Polak, M. L.; Lineberger, W. C. *J. Chem. Phys.*, in press.
(140) Dawson, J. H. J.; Noest, A. J.; Nibbering, N. M. M. *Int. J. Mass Spectrom. Ion Phys.* **1979**, *29*, 205–222.
(141) Streit, G. E. *J. Phys. Chem.* **1982**, *86*, 2321–2324.
(142) Babcock, L. M.; Streit, G. E. *J. Chem. Phys.* **1981**, *75*, 3864–3870.
(143) McDonald, R. N. *Tetrahedron* **1989**, *45*, 3993–4015.
(144) Dawson, J. H. J.; Jennings, K. R. *J. Chem. Soc., Faraday Trans. 2* **1976**, *72*, 700–706.
(145) Grabowski, J. J.; Melly, S. J. *Int. J. Mass Spectrom. Ion Processes* **1987**, *81*, 147–164.
(146) Yang, X.; Zhang, X.; Castleman, A. W., Jr. *J. Phys. Chem.* **1991**, *95*, 8520–8524.
(147) Bohme, D. K.; Young, L. B. *J. Am. Chem. Soc.* **1970**, *92*, 7354–7358.
(148) Tanaka, K.; Mackay, G. I.; Payzant, J. D.; Bohme, D. K. *Can. J. Chem.* **1976**, *54*, 1643–1659.
(149) Murray, K. K.; Leopold, D. G.; Miller, T. M.; Lineberger, W. C. *J. Chem. Phys.* **1988**, *89*, 5442–5453.
(150) Gilles, M. K.; Ervin, K. M.; Ho, J.; Lineberger, W. C. *J. Phys. Chem.* **1992**, *96*, 1130–1141.
(151) Dawson, J. H. J.; Nibbering, N. M. M. *Int. J. Mass Spectrom. Ion Phys.* **1980**, *33*, 3–19.
(152) Grabowski, J. J.; Roy, P. D.; Leone, R. *J. Chem. Soc., Perkin Trans. 2* **1988**, 1627–1632.
(153) Noest, A. J.; Nibbering, N. M. M. *Adv. Mass Spectrom.* **1980**, *8A*, 227–237.
(154) Jager, K.; Simic, M.; Henglein, A. *Z. Naturforsch.* **1967**, *22a*, 961–965.
(155) Dawson, J. H. J.; Nibbering, N. M. M. In *Ion Cyclotron Resonance Spectrometry*; Hartmann, H., Wanczek, K.-P, Eds.; Lecture Notes in Chemistry 7; Springer-Verlag: Berlin, 1978; pp 146–173.
(156) Bierbaum, V. M.; DePuy, C. H.; Shapiro, R. H.; Stewart, J. H. *J. Am. Chem. Soc.* **1976**, *98*, 4229–4235.
(157) Lin, T. H.; Grabowski, J. J. Unpublished data.
(158) McDonald, R. N.; Chowdhury, A. K. *J. Am. Chem. Soc.* **1980**, *102*, 5118–5119.

(159) McDonald, R. N.; Chowdhury, A. K. *J. Am. Chem. Soc.* **1981**, *103*, 674–676.
(160) McDonald, R. N.; Chowdhury, A. K. *J. Phys. Chem.* **1982**, *86*, 3641–3645.
(161) Drzaic, P. S.; Brauman, J. I. *J. Am. Chem. Soc.* **1984**, *106*, 3443–3446.
(162) Houriet, R.; Stahl, D.; Winkler, F. J. *Environ. Health Persp.* **1980**, *36*, 63–68.
(163) Boand, G.; Houriet, R.; Gäumann, T. *Adv. Mass. Spectrom.* **1980**, *8A*, 238–245.
(164) Cheng, X.; Grabowski, J. J. Unpublished results.
(165) Moran, S.; Ellison, G. B. *Int. J. Mass Spectrom. Ion Processes* **1987**, *80*, 83–98.
(166) Skell, P. S.; Fagone, F. A.; Klabunde, K. J. *J. Am. Chem. Soc.* **1972**, *94*, 7862–7866.
(167) Reiser, C.; Lussier, F. M.; Jensen, C. C.; Steinfeld, J. I. *J. Am. Chem. Soc.* **1979**, *101*, 350–357.
(168) Skell, P. S.; Villaume, J. E.; Fagone, F. A. *J. Am. Chem. Soc.* **1972**, *94*, 7866–7867.
(169) Reiser, C.; Steinfeld, J. I. *J. Phys. Chem.* **1980**, *84*, 680–681.
(170) Davison, P.; Frey, H. M.; Walsh, R. *Chem. Phys. Lett.* **1985**, *120*, 227–228.
(171) Ervin, K. M.; Ho, J.; Lineberger, W. C. *J. Chem. Phys.* **1989**, *91*, 5974–5992.
(172) Carrington, T., Jr.; Hubbard, H. M.; Schaefer, H. F., III; Miller, W. H. *J. Chem. Phys.* **1984**, *80*, 4347–4354 and references cited therein.
(173) Dykstra, C. E.; Parsons, C. A.; Oates, C. L. *J. Am. Chem. Soc.* **1979**, *101*, 1962–1965.
(174) Goode, G. C.; Jennings, K. R. *Adv. Mass. Spectrom.* **1974**, *6*, 797–803.
(175) Grabowski, J. J. In *Advances in Gas Phase Ion Chemistry*; Adams, N. G., Babcock, L. M., Eds.; JAI Press Inc.: Greenwich, in press.
(176) Rabasco, J. J.; Kass, S. R. *J. Am. Soc. Mass Spectrom.* **1992**, *3*, 91–98.
(177) Dawson, J. H. J.; Nibbering, N. M. M. *J. Am. Chem. Soc.* **1978**, *100*, 1928–1929.
(178) Burnett, S. M.; Stevens, A. E.; Feigerle, C. S.; Lineberger, W. C. *Chem. Phys. Lett.* **1983**, *100*, 124–128.
(179) Ervin, K. M.; Gronert, S.; Barlow, S. E.; Gilles, M. K.; Harrison, A. G.; Bierbaum, V. M.; DePuy, C. H.; Lineberger, W. C.; Ellison, G. B. *J. Am. Chem. Soc.* **1990**, *112*, 5750–5759.
(180) Schmitt, R. J. Ph.D. Thesis, University of Colorado at Boulder, 1979.
(181) Viggiano, A. A.; Morris, R. A.; Paulson, J. F.; Ferguson, E. E. *J. Phys. Chem.* **1990**, *94*, 7111–7113.
(182) Neuert, H.; Rackwitz, R.; Vogt, D. *Adv. Mass. Spectrom.* **1968**, *4*, 631.
(183) Bohme, D. K.; Mackay, G. I.; Schiff, H. I.; Hemsworth, R. S. *J. Chem. Phys.* **1974**, *61*, 2175–2179.
(184) Bohme, D. K.; Young, L. B. *J. Am. Chem. Soc.* **1970**, *92*, 3301–3309.
(185) Dawson, J. H. J.; Kaandorp, Th. A. M.; Nibbering, N. M. M. *Org. Mass Spectrom.* **1977**, *12*, 330–333.
(186) Stewart, J. H.; Shapiro, R. H.; DePuy, C. H.; Bierbaum, V. M. *J. Am. Chem. Soc.* **1977**, *99*, 7650–7653.
(187) Karnett, M. P.; Cross, R. J. *Chem. Phys. Lett.* **1981**, *84*, 501–503.
(188) Bruins, A. P.; Ferrer-Correia, A. J.; Harrison, A. G.; Jennings, K. R.; Mitchum, R. K. *Adv. Mass. Spectrom.* **1978**, *7*, 355–358.
(189) VanOrden, S. L.; Malcomson, M. E.; Buckner, S. W. *Anal. Chim. Acta* **1991**, *246*, 199–210. Note that the rate coefficient for $O^{\bullet -}$ with benzene cited in this paper has subsequently been remeasured by Prof. Buckner and colleagues; this new value is cited here.
(190) Matimba, H. E. K.; Crabbendam, A. M.; Ingemann, S.; Nibbering, N. M. M. *J. Chem. Soc., Chem. Commun.* **1991**, 644–645.
(191) Ingemann, S.; Nibbering, N. M. M.; Sullivan, S. A.; DePuy, C. H. *J. Am. Chem. Soc.* **1982**, *104*, 6520–6527.
(192) Harrison, A. G.; Jennings, K. R. *J. Chem. Soc., Faraday Trans. 1* **1976**, *72*, 1601–1608.
(193) Dawson, J. H. J.; Noest, A. J.; Nibbering, N. M. M. *Int. J. Mass Spectrom. Ion Phys.* **1979**, *30*, 189–191.
(194) Bohme, D. K.; Mackay, G. I.; Tanner, S. D. *J. Am. Chem. Soc.* **1980**, *102*, 407–409.
(195) Kleingeld, J. C.; Nibbering, N. M. M. *Tetrahedron* **1984**, *40*, 2789–2894.
(196) Marshall, A.; Tkaczyk, M.; Harrison, A. G. *J. Am. Soc. Mass Spectrom.* **1991**, *2*, 292–298.
(197) van der Wel, H.; Nibbering, N. M. M. In *Structure/Reactivity and Thermochemistry of Ions*; Ausloos, P., Lias, S. G., Eds.; D. Reidel Publishing Co.: Boston, 1987; p 406.
(198) Nibbering, N. M. M. In *Kinetics of Ion-Molecule Reactions*; Ausloos, P., Ed.; Plenum Press: New York, 1979; pp 165–197.
(199) Lloyd, J. R.; Agosta, W. C.; Field, F. H. *J. Org. Chem.* **1980**, *45*, 1614–1619.
(200) Refaey, K. M. A.; Franklin, J. L. *J. Chem. Phys.* **1974**, *61*, 733–734.
(201) Kleyn, A. W.; Hubers, M. M.; Los, J. *Chem. Phys.* **1978**, *34*, 55–63.
(202) Albritton, D. L.; Dotan, I.; Streit, G. E.; Fahey, D. W.; Fehsenfeld, F. C.; Ferguson, E. E. *J. Chem. Phys.* **1983**, *78*, 6614–6619.
(203) Dotan, I.; Davidson, J. A.; Streit, G. E.; Albritton, D. L.; Fehsenfeld, F. C. *J. Chem. Phys.* **1977**, *67*, 2874–2879.
(204) Lifshitz, C.; Wu, R. L. C.; Tiernan, T. O.; Terwilliger, D. T. *J. Chem. Phys.* **1978**, *68*, 247–260.
(205) Szulejko, J. E.; Howe, I.; Beynon, J. H. *Int. J. Mass Spectrom. Ion Phys.* **1981**, *37*, 27–34.
(206) Hickel, B.; Sehested, K. *J. Phys. Chem.* **1991**, *95*, 744–747.
(207) Vysotskaya, N. A. *Russ. Chem. Rev.* **1973**, *42* (10), 851–856.
(208) Zehavi, D.; Rabani, J. *J. Phys. Chem.* **1971**, *75*, 1738–1744.
(209) Christensen, H.; Sehested, K.; Corfitzen, H. *J. Phys. Chem.* **1982**, *86*, 1588–1590.
(210) Buxton, G. V.; Ellis, P. G.; McKillop, T. F. W. *J. Chem. Soc., Faraday Trans. 1* **1979**, *75*, 1050–1066.
(211) Clark, K. P.; Stonehill, H. I. *J. Chem. Soc., Faraday Trans. 1* **1977**, *73*, 722–33.
(212) Novais, H. M.; Steenken, S. *J. Phys. Chem.* **1987**, *91*, 426–433.
(213) Czapski, G.; Dorfman, L. M. *J. Phys. Chem.* **1964**, *68*, 1169–1177.
(214) Adams, G. E.; Boag, J. W.; Michael, B. D. *Nature (London)* **1965**, *205*, 898–899.
(215) Adams, G. E.; Boag, J. W.; Michael, B. D. *Proc. R. Soc. London Ser. A* **1966**, *289*, 321–341.
(216) Bielski, B. H. J.; Gebicki, J. M. *Adv. Radiat. Chem.* **1970**, *2*, 177–279.
(217) Sehested, K.; Holcman, J.; Bjergbakke, E.; Hart, E. J. *J. Phys. Chem.* **1982**, *86*, 2066–2069.
(218) Bühler, R. E.; Staehelin, J.; Hoigné, J. *J. Phys. Chem.* **1984**, *88*, 2560–2564.
(219) Bobrowski, K. *J. Chem. Soc., Faraday Trans. 1* **1984**, *80*, 1377–1389.
(220) McAskill, N. A. *Aust. J. Chem.* **1982**, 1927–1932.
(221) Karasawa, H.; Yugeta, R.; Yamaguchi, A.; Sato, S. *Bull. Chem. Soc. Jpn.* **1981**, *54*, 362–366.
(222) Bobrowski, K. *J. Phys. Chem.* **1981**, *85*, 382–388.
(223) Wander, R.; Gall, B. L.; Dorfman, L. M. *J. Phys. Chem.* **1970**, *74*, 1819–1821.
(224) Neta, P.; Hoffman, M. Z.; Simic, M. *J. Phys. Chem.* **1972**, *76*, 847–853.
(225) Simic, M.; Hoffman, M. Z.; Ebert, M. *J. Phys. Chem.* **1973**, *77*, 1117–1120.
(226) Neta, P.; Schuler, R. H. *J. Phys. Chem.* **1975**, *79*, 1–6.
(227) Simic, M.; Neta, P.; Hayon, E. *J. Phys. Chem.* **1973**, *77*, 2662–2667.
(228) Savel'eva, O. S.; Shevchuk, L. G.; Vysotskaya, N. A. *Zh. Org. Khim.* **1972**, *8*, 283–286.
(229) Christensen, H. C.; Sehested, K.; Hart, E. J. *J. Phys. Chem.* **1973**, *77*, 983–987.
(230) Bakale, G.; Sowada, U.; Schmidt, W. F. *Can. J. Chem.* **1977**, *55*, 2220–2224.
(231) Sapozhnikov, V. B.; Shvets, V. A.; Chuvylkin, N. D.; Kazansky, V. B. *Chem. Phys. Lett.* **1976**, *37*, 582–584 and references therein.
(232) Naccache, C. *Chem. Phys. Lett.* **1971**, *11*, 323–325.
(233) Aika, K.; Lunsford, J. H. *J. Phys. Chem.* **1977**, *81*, 1393–1398.
(234) Aika, K.; Lunsford, J. H. *J. Phys. Chem.* **1978**, *82*, 1794–1800.
(235) Kaliaguire, S. L.; Shelimov, B. N.; Kazansky, V. B. *J. Catal.* **1978**, *55*, 384–393.
(236) Takita, Y.; Lunsford, J. H. *J. Phys. Chem.* **1979**, *83*, 683–688.
(237) Takita, Y.; Iwamoto, M.; Lunsford, J. H. *J. Phys. Chem.* **1980**, *84*, 1710–1712.
(238) Iwamoto, M.; Lunsford, J. H. *J. Phys. Chem.* **1980**, *84*, 3079–3084.
(239) Iwamoto, M.; Hirata, J.; Matsukami, K.; Kagawa, S. *J. Phys. Chem.* **1983**, *87*, 903–905.
(240) Burnett, S. M.; Stevens, A. E.; Feigerle, C. S.; Lineberger, W. C. *Chem. Phys. Lett.* **1983**, *100*, 124–128.
(241) Sülzle, D.; Schwarz, H. *Chem. Phys. Lett.* **1989**, *156*, 397–400.
(242) Luke, B. T.; Collins, J. R.; Loew, G. H.; McLean, A. D. *J. Am. Chem. Soc.* **1990**, *112*, 8686–8691.

**Registry No.** $O^{\bullet -}$, 14337-01-0.